

4

Black Hole Binaries

Jeffrey E. McClintock

Harvard-Smithsonian Center for Astrophysics, 60 Garden St., Cambridge, MA 02138, USA

Ronald A. Remillard

Center for Space Research, MIT, Cambridge, MA 02139, USA

4.1 Introduction

4.1.1 Scope of this review

We focus on 18 black holes with measured masses that are located in X-ray binary systems. These black holes are the most visible representatives of an estimated 300 million stellar-mass black holes that are believed to exist in the Galaxy (van den Heuvel 1992; Brown & Bethe 1994; Tsinnes et al. 1996; Agolet al. 2002). Thus the mass of this particular form of dark matter, assuming $10M_{\odot}$ per black hole, is 4% of the total baryonic mass (i.e., stars plus gas) of the Galaxy (Bahcall 1986; Brown et al. 1988). Collectively this vast population of black holes outweighs the Galactic center black hole, SgrA*, by a factor of 1000. These stellar-mass black holes are important to astronomy in numerous ways. For example, they are one endpoint of stellar evolution for massive stars, and the collapse of their progenitor stars enriches the universe with heavy elements (Woolsey et al. 2002). Also, the measured mass distribution for even the small sample of 18 black holes featured here are used to constrain models of black hole formation and binary evolution (Brown et al. 2000a; Nelemans & van den Heuvel 2001; Fryer & Kalberla 2001). Lastly, some black hole binaries appear to be linked to the hypernovae believed to power gamma-ray bursts (Israeli et al. 1999; Brown et al. 2000b; Orosz et al. 2001).

This review is focused on the X-ray timing and spectral properties of these 18 black holes, plus a number of black hole candidates, with an eye to their importance to physics as potential sites for tests of general relativity (GR) in the strongest possible gravitational fields. There are now several current areas of research that probe phenomena in these systems that are believed to occur very near the event horizon. These X-ray phenomena include quasi-periodic oscillations (QPOs) at high frequency (40–450 Hz) observed from seven systems, relativistically broadened iron lines from the inner accretion disk, and thermal disk emission from near the innermost stable circular orbit allowed by GR. We also comment on evidence for the existence of the event horizon, which is based on a comparison of black-hole and neutron-star binaries and on models for advective accretion flows.

The black hole binaries featured here are mass-exchange binaries that contain an accreting black hole primary and a nondegenerate secondary star. They comprise about 10% of all bright X-ray binaries. For background on X-ray binaries, see Chapter 1, and references therein. For comprehensive reviews on black hole binaries, see

Tanaka & Lewin (1995; hereafter TL95) and Tanaka and Shibasaki (1996; hereafter TS96). In this review we emphasize the results of the past decade. Throughout we make extensive use of the extraordinary data base amassed by NASA's Rossi X-ray Timing Explorer since January 1996 (Swank 1998). Because of our page limit, several important topics are omitted such as X-ray reection studies (Done & Nayakshin 2001), the estimated number of black hole X-ray novae in the Galaxy, which is 1000 (van den Heuvel 1992; TS96; Romani 1998), and the present and projected rates of discovery of black hole binaries.

4.1.2 The 18 black hole binaries

The first black hole binary (BHB), Cygnus X-1, was established by Webster and Murdin (1972) and Bolton (1972); the second, LMC X-3, was found by Cowley et al. (1983). Both of these systems are persistently bright in X-rays; furthermore, they are classified as high-mass X-ray binaries (HMXBs) because their secondaries are massive O/B stars (White et al. 1995). The third BHB to be established, A 0620-00, is markedly different (McCormick & Remillard 1986). A 0620-00 was discovered as an X-ray nova in 1975 when it suddenly brightened to an intensity of 50 Crab to become the brightest nonsolar X-ray source ever observed (Evans et al. 1975). Then, over the course of a year, the source decayed back into quiescence to become a feeble (1 Crab) source (McCormick et al. 1995). Similarly, the optical counterpart faded from outburst maximum by $V = 7.1$ mag to $V = 18.3$ in quiescence, thereby revealing the optical spectrum of a K dwarf secondary.

During the past 20 years, black holes (BHBs) have been established in 15 additional X-ray binaries. Remarkably, nearly all these systems are X-ray novae like A 0620-00. Thus, in all there are now 18 confirmed BHBs. They are listed in Table 4.1 in order of right ascension. The coordinate name of each source is followed in the second column by its variable star name (or other name, such as Cyg X-1), which is useful for web-based literature searches. For X-ray novae, the third column gives the year of discovery and the number of outbursts that have been observed. As indicated in the table, among the confirmed BHBs, there are six recurrent X-ray novae and three persistent sources, Cyg X-1, LMC X-3 and LMC X-1. As indicated in the fourth column, these latter three sources are high-mass X-ray binaries and are the only truly persistent sources among the BHBs.

Two of the X-ray novae are peculiar: GRS 1915+105 has remained bright for more than a decade since its eruption in August 1992; GX 339-4 (1659-487), which was discovered by Markert et al. in 1973, undergoes frequent outbursts followed by very faint states, but it has never been observed to reach the quiescent state (Hynes et al. 2003). Columns 5 and 6 give the peak X-ray flux and a distance estimate for each source. The orbital period is given in the seventh column (a colon denotes an uncertain value) and the spectral type in the eighth. The first one or two references listed for each binary contain information on the orbital period and the spectral type. The remaining references support the distance estimates.

The data in Table 4.1 reveal considerable diversity among the BHBs. For example, these 18 binaries range in size from tiny XTE J1118+480 with $P_{\text{orb}} = 0.17$ days and

$1 \text{ Crab} = 2.6 \times 10^{-9} \text{ erg cm}^{-2} \text{ s}^{-1} \text{ keV}^{-1} = 1.06 \text{ mJy at } 5.2 \text{ keV}$ for a Crab-like spectrum with photon index = 2.1.

Table 4.1. Com m ed black hole binaries: primary properties

Source	Alternative name ^a	Year ^b	Type ^c	F _{rxm ax} (Jy ^d)	D (kpc)	P _{orb} (hr)	Spec.	References
0422+ 32	V 518 Per	1992/1	L,T	3000	2.6	0.7	M 2V	1,2
0538+641	LM C X 13	{	H,P	60	50	2.3	B 3V	3,4
0540+697	LM C X 11	{	H,P	30	50	2.3	O 7III	3,5,6
0620+003	V 616 Mon	1975/2	L,T	50000	1.2	0.1	K 4V	7,8,9,10
1009+45	MM Vel	1993/1	L,T	800	5.0	1.3	K 7/M 0V	11,12
1118+ 480	KV UMa	2000/1	L,T	40	1.8	0.5	K 5/M 0V	13,14
1124+684 ^e	GU Mus	1991/1	L,T	3000	5	1.3	K 3/K 5V	15,15a,16
1543+475	IL Lupi	1971/4	L,T	15000	7.5	0.5	A 2V	17,18
1550+564	V 381 Nor	1998/5	L,T	7000	5.3	2.3	G 8/K 8IV	19
1655+40	V 1033 Sco	1994/2	L,T	3900	3.2	0.2	F 3/F 5IV	20,21,22
1659+487 ^f	V 821 Ara	1972/ ^f	L,T	1100	4	42.1:	{	23,24
1705+250	V 2107 Oph	1977/1	L,T	3600	8	2	K 3/7V	7,25,26
1819.3+2525	V 4641 Sgr	1999/1	L,T	13000	7.4	{12.3	67.6	B 9III
1859+ 226	V 406 Vul	1999/1	L,T	1500		11	9.2:	{ 28,29
1915+ 105	V 1487 Aql	1992/1	L,T	3700	11	{12	804.0	K /M III
1956+ 350	Cyg X 1	{	H,P	2300	2.0	0.1	O 9.7Iab	34,35
2000+ 251	QZ Vul	1988/1	L,T	11000	2.7	0.7	K 3/K 7V	35a,7,36,37
2023+ 338	V 404 Cyg	1989/3	L,T	20000	2.2	{3.7	155.3	K 0III
								38,39,40

^a Name recognized by the SIMBAD Database and the Astrophysics Data System (ADS).

^b Year of discovery/number of outbursts observed (Chen et al. 1997; this work).

^c H' { HMXB, L' { LMXB, T' { transient, P' { persistent; Liu et al. 2000, 2001; this work.

^d 1 Jy = 10^{-29} ergs cm⁻² s⁻¹ Hz⁻¹ = 2.42 10^{-12} ergs cm⁻² s⁻¹ keV⁻¹ (2{11 keV).

^e Commonly known as Nova Muscae 1991.

^f Commonly known as GX 339-4; number of outbursts = 10 (Kong et al. 2002).

REFERENCES: ¹Esin et al. 1997; ²Filippenko et al. 1995a; ³Freedman et al. 2001; ⁴Cowley et al. 1983; ⁵Hutchings et al. 1987; ⁶Cowley et al. 1995; ⁷Barret et al. 1996b; ⁸Gelino et al. 2001b; ⁹Marsh et al. 1994; ¹⁰McCormick & Remillard 2000; ¹¹Barret et al. 2000; ¹²Filippenko et al. 1999; ¹³McCormick et al. 2001a; ¹⁴Wagnier et al. 2001; ¹⁵Orosz et al. 1996; ^{15a}Gelino et al. 2001a; ¹⁶Shahbaz et al. 1997; ¹⁷Orosz et al. 2002b; ¹⁸Orosz et al. 1998; ¹⁹Orosz et al. 2002a; ²⁰Hjellming & Rupen 1995; ²¹Orosz & Bailyn 1997; ²²Shahbaz et al. 1999; ²³Cowley et al. 1987; ²⁴Hynes et al. 2003; ²⁵Remillard et al. 1996; ²⁶Filippenko et al. 1997; ²⁷Orosz et al. 2001; ²⁸Zurita et al. 2002; ²⁹Filippenko & Chornock 2001; ³⁰Mirabel & Rodriguez 1994; ³¹Fender et al. 1999b; ³²Greiner et al. 2001a; ³³Greiner et al. 2001b; ³⁴Mirabel & Rodriguez 2003; ³⁵Gies & Bolton 1982; ^{35a}Harraldis et al. 1996; ³⁶Filippenko et al. 1995b; ³⁷Casares et al. 1995; ³⁸Shahbaz et al. 1994; ³⁹Casares & Charles 1994; ⁴⁰Casares et al. 1993.

a separation between the BH and its companion of a 2.8 R to GRS 1915+105 with $P_{orb} = 33.5$ days and a 95R. Only six of these 18 systems were established as BHs a decade ago (van Paradijs & McCormick 1995). As indicated in Table 4.1, all of the 15 X-ray novae are low-mass X-ray binaries (LMXBs), which typically contain a secondary with a mass of roughly 1 M_{sun} or less (White et al. 1995). The BHs 4U 1543+47 and SAX J1819.3+2525 have relatively massive secondaries: 2.7 1.0 M and 2.9 0.2 M, respectively (Orosz et al. 2002b). We classify them as LMXBs because their secondary masses are comparable to the mass of the secondary of Her X-1 (2.3 0.3 M; Reynolds et al. 1997), which is a well-known LMXB (Liu et al. 2001). Furthermore, a 2.3 M secondary is much less massive than the O/B secondaries (> 10 M) found in HMXB systems.

BHBs manifest themselves in five rather distinct spectral/temporal states defined in the 1-10 keV band (e.g., van der Klis 1994; TL95; TS96). The three most familiar are (1) the high/soft (HS) state, a high-intensity state dominated by thermal emission from an accretion disk; (2) the low/hard (LH) state, a low-intensity state dominated by power-law emission and rapid variability; and (3) the quiescent state an extraordinarily faint state also dominated by power-law emission. The remaining two states, (4) the very high (VH) state and (5) the intermediate (IM) state, are more complex; recently they have come to the fore, as they have now been observed in an appreciable number of sources. These five BH states and the transitions between them are the focus of §4.3, where they are reviewed and illustrated in detail.

Additional data specific to the BH primaries are contained in Table 4.2. Of special importance is the mass function, $f(M) = P_{\text{orb}} K_2^3 / 2G = M_1 \sin^3 i / (1 + q)^2$. The observables on the left side of the equation are the orbital period, P_{orb} , and the half-amplitude of the velocity curve of the secondary, K_2 . On the right, the quantity of most interest is the BH mass, M_1 ; the two additional parameters are the orbital inclination angle, i , and the mass ratio, $q = M_2/M_1$, where M_2 is the mass of the secondary. Thus a secure value of the mass function can be determined for a quiescent X-ray nova or an HMXB such as Cyg X-1 by simply measuring the radial velocity curve of the secondary star. The mass function, $f(M)$, and an estimate of the BH mass, M_1 , are given in the second and third columns of Table 4.2. An inspection of the equation for $f(M)$ shows that the value of the mass function is the absolute minimum mass of the compact primary. Thus, for 12 of the 18 BHBs, the very secure value of $f(M)$ alone is sufficient to show that the mass of the compact X-ray source is at least $3 M_{\odot}$ (Table 4.2), which is widely agreed to exceed the maximum stable mass of a neutron star (NS) in GR (Rhoades & Rutherford 1974; Kalogera & Baym 1996). For the remaining half-dozen systems, some additional data are required to make the case for a BH. The evidence for BHs in these 18 systems is generally very strong (see Ch. 5). Thus, assuming that GR is valid in the strong-field limit, we choose to refer to these compact primaries as BHs, rather than as BH candidates. We note, however, our reservations about three of the systems listed in Table 4.2: (1) The mass function of LMC X-1 (0540-697) is quite uncertain (Table 4.2); (2) the orbital period of XTE J1859+226 is not firmly established (Filippenko & Chornock 2001; Zurita et al. 2002); and (3) the dynamical data for GX 339-4 (1659-487) were determined in outburst by a novel technique, and neither the orbital period nor the velocity amplitude are securely determined (Hynes et al. 2003).

High frequency QPOs (HFQPOs) in the range 40-450 Hz are observed for the four systems with data given in the fourth column. Low-frequency QPOs (LFQPOs) are also observed from these systems and ten others, as indicated in column 5. Most of the systems were at one time or another detected as radio sources and at least five have exhibited resolved radio jets (column 6; see Mirabel & Rodriguez 1999). An X-ray jet (two-sided) has been observed from XTE J1550-564 (Corbel et al. 2002). As shown in column 7, power-law emission extending to 1 MeV has been observed for six sources. The references listed in the last column support the X-ray QPO, radio, and E_{max} data given in columns 4-7.

The dynamical evidence for massive ($M > 3 M_{\odot}$) collapsed stellar remnants is indisputable. However, this evidence alone can never establish the existence of

Table 4.2. Confirmed black hole binaries: X-ray and optical data

Source	$f(M^a)$ (M_\odot)	M^a_1 (M_\odot)	$f(HFQPO)$ (Hz)	$f(LFQPO)$ (Hz)	Radio ^b	E_{max}^c (MeV)	References
0422+32	1.19	0.02	3.2{13.2	{	0.035{32	P	0.8,1{2:1,2,3,4,5
0538+641	2.3	0.3	5.9{9.2	{	0.46	{	0.05 6,7
0540+697	0.14	0.05	4.0{10.0:	{	0.075	{	0.02 8,7
0620+003	2.72	0.06	8.7{12.9	{	{	P,J?	0.03: 9,10,11
1009+45	3.17	0.12	6.3{8.0	{	0.04{0.3	{ ^d	0.40, 1:12,4,13
1118+480	6.1	0.3	6.5{7.2	{	0.07{0.15	P	0.15 14,15,16,17
1124+684	3.01	0.15	6.5{8.2	{	3.0-8.4	P	0.50 18,19,20,21
1543+475	0.25	0.01	7.4{11.4 ^e	{	7	{ ^f	0.20 22,4
1550+564	6.86	0.71	8.4{10.8	92,184,276	0.1-10	P,J	0.20 23,24,25,26,27
1655+40	2.73	0.09	6.0{6.6	300,450	0.1{28	P,J	0.80 28,29,30,31,54
1659+487	> 2.0 ^g	{	{	{	0.09{7.4	P	0.45, 1:32,33,4,13
1705+250	4.86	0.13	5.6{8.3	{	{	{ ^d	0.1 34,35
1819.3+2525	3.13	0.13	6.8{7.4	{	{	P,J	0.02 36,37
1859+226	7.4	1.1	7.6{12:	190	0.5{10	P,J?	0.2 38,39,40,41
1915+105	9.5	3.0	10.0{18.0:41,67,113,168	0.001-10	P,J	0.5, 1: 42,43,44,4,13	
1956+350	0.244	0.005	6.9{13.2	{	0.035{12	P,J	2{5 45,46,47,48,49
2000+251	5.01	0.12	7.1{7.8	{	2.4{2.6	P	0.3 18,50,51
2023+338	6.08	0.06	10.1{13.4	{	{	P	0.4 52,53

^a Orosz et al. 2002b, except for 1659+487; colon denotes uncertain value.^b Radio properties: P - persistent over 10 or more days and/or inverted spectrum; J - relativistic jet detected.^c Maximum energy reported; colon denotes uncertain value.^d No observations made.^e Orosz, private communication.^f Very faint (e.g., see IAUC 7925).^g For preferred period, $P = 1.76$ days, $f(M) = 5.8 \pm 0.5 M_\odot$; Hynes et al. 2003.

REFERENCES: ¹van der Hooft et al. 1999; ²Vikhlinin et al. 1992; ³Shrader et al. 1994; ⁴Grove et al. 1998; ⁵van Dijk et al. 1995; ⁶Boyd et al. 2000; ⁷Nowak et al. 2001; ⁸Ebisawa et al. 1989; ⁹Owen et al. 1976; ¹⁰Kuulkers et al. 1999; ¹¹Coe et al. 1976; ¹²van der Hooft et al. 1996; ¹³Ling et al. 2000; ¹⁴Wood et al. 2000; ¹⁵Revnivtsev et al. 2000b; ¹⁶Fender et al. 2001; ¹⁷McCormick et al. 2001a; ¹⁸Rutledge et al. 1999; ¹⁹Bellon et al. 1997; ²⁰Balle et al. 1995; ²¹Sunyaev et al. 1992; ²²This work; ²³Remillard et al. 2002b; ²⁴Corbel et al. 2001; ²⁵Wu et al. 2002; ²⁶Corbel et al. 2003; ²⁷Sobczak et al. 2000b; ²⁸Remillard et al. 1999; ²⁹Strohmeier 2001a; ³⁰Hjelming & Rupen 1995; ³¹Hannikainen et al. 2000; ³²Revnivtsev et al. 2001; ³³Corbel et al. 2000; ³⁴Wilson & Rothschild 1983; ³⁵Cooke et al. 1984; ³⁶Hjelming et al. 2000; ³⁷Wijnands & van der Klis 2000; ³⁸Cui et al. 2000a; ³⁹Markwardt 2001; ⁴⁰Rockspott et al. 2002; ⁴¹Dai & Fiume et al. 1999; ⁴²Morgan et al. 1997; ⁴³Strohmeier 2001b; ⁴⁴Mirabel & Rodriguez 1994; ⁴⁵Vikhlinin et al. 1994; ⁴⁶Cui et al. 1997b; ⁴⁷Stirling et al. 2001; ⁴⁸Ling et al. 1987; ⁴⁹McCormick et al. 2002; ⁵⁰Hjelming et al. 1988; ⁵¹Sunyaev et al. 1988; ⁵²Han & Hjelming 1992; ⁵³Sunyaev et al. 1991b; ⁵⁴Tom sick et al. 1999.

BHs. At present, the argument for BHs depends on the assumption that GR is the correct theory of strong gravity. To make an airtight case that a compact object is a BH with an event horizon, we must make clean quantitative measurements of relativistic effects that occur in the near vicinity of the collapsed object. That is, we must measure phenomena that are predicted by GR to be unique to BHs. A possible route to this summit is to measure and interpret the effects of strong-field gravity that are believed to be imprinted on both high-frequency quasi-periodic oscillations

(HFQPOs; see x4.4.3) and on X-ray emission lines (x4.2.3). Another approach, which is discussed in x4.3.4, is based on sensing the qualitative differences between an event horizon and the material surface of a NS.

4.1.3 Black hole candidates

Certain characteristic X-ray properties of the 18 established BHs are often used to identify a candidate BH when the radial velocities of the secondary cannot be measured (e.g., because the secondary is too faint). These frequently observed characteristics of the established BHs, which are discussed in detail by TL95, include an ultrasoft X-ray spectrum ($1\text{-}10$ keV), a power-law spectral tail that extends beyond 20 keV, characteristic state transitions (x4.1.2; x4.3), and rapid temporal variability. However, none of these putative BH signatures has proved to be entirely reliable; each of them has been forged by one or more systems known to contain a NS primary (TL95). This is not surprising since the X-ray spectral/temporal properties originate in an accretion flow that is expected to be fairly similar whether the primary is a BH or a weakly magnetized NS. Another characteristic of all BHs is a complete absence of either periodic pulsations or type I X-ray bursts, which are the very common signatures of NS systems.

Nevertheless, despite the limitations of these spectral/temporal identifiers, they have served as useful guides and have allowed the identification of a number of probable BH primaries, which we refer to as BH candidates or BH Cs. In order to economize on acronyms, we also use BH C to refer to the binary system that hosts the BH candidate. A list of 22 BH Cs is given in Table 4.3. These systems are less well-known than the BHs listed in Table 4.1. Therefore, to aid in their identification we have included in most cases the prefix to the coordinate source name that identifies the discovery mission (e.g., EXO = EXOSAT). For the four sources with variable star names, the prefix is omitted. In columns 2{4, we give the best available coordinates and their uncertainties (if they exceed 10^0). These coordinates are also an excellent resource for interrogating ADS and SIMBAD.

In column 5 we list the characteristics that indicate the BH C classification, e.g., an observation of one or more of the canonical states of a BH. A source classified as "ultrasoft" in the older literature (e.g., White & Marshall 1984) is assumed here to have been observed in the HS state. Three BH Cs with resolved radio jets are also noted in column 5. Variability characteristics (x4.4) and broad Fe K α emission lines (x4.2.3) can also be important BH indicators, but these are not explicitly noted in Table 4.3. Selected references are cited in the last column. The coordinate data can be found in the first reference. The following few references support the BH characteristics given in column 5. For several sources, a few additional references provide limited information on optical/IR/radio counterparts, etc.

We have assigned a grade to each BH C that is based both on how thoroughly the candidate has been observed and on the BH characteristics it has displayed. In fact, this grade is qualitative and subjective and meant only as a guide. Our sense of the grade is as follows: We would be surprised if even one of the nine A-grade BH Cs contains a NS; on the other hand, we would not be surprised if one of the six C-grade BH Cs contains a NS. In compiling Table 4.3, we have been selective. For example, we did not include systems such as SAX J1805.5{2031 (Lowes et al. 2002)

Table 4.3. Candidate black hole binaries^a

Source	RA (2000)	DEC (2000)	r_x ^b	BH state ^c	Grade ^d	References
1354-645 (BW Cir)	13 58 09.74	-64 44 05.2		LH, HS	A	1,2,3,4
1524-617 (KY TrA)	15 28 16.7	-61 52 58		LH, HS	A	5,6,7
4U 1630-47	16 34 01.61	-47 23 34.8		LH, HS	A	8,9,10,11,83
XTE J1650-500	16 50 01.0	-49 57 45		LH, HS, VH	A	12,13,14,15,16
SAX J1711.6-3808	17 11 37.1	-38 07 06		LH, HS	B	17,18
GRS 1716-249 ^e	17 19 36.93	-25 01 03.4		LH	B	19,20,21
XTE J1720-318	17 19 59.06	-31 44 59.7		LH, HS	C	22,23,24
KS 1730-312	17 33 37.6	-31 13 12	30 ^{oo}	LH, HS	C	25,26
GRS 1737-31	17 40 09	-31 02 4	30 ^{oo}	LH	B	27,28,29
GRS 1739-278	17 42 40.03	-27 44 52.7		LH, HS, VH	A	30,31,32,33,34
1E 1740.7-2942	17 43 54.88	-29 44 42.5		LH, HS, J	A	35,36,37,38,39
H 1743-322	17 46 15.61	-32 14 00.6		HS, VH	A	40,41,42,80,81,82
A 1742-289	17 45 37.3	-29 01 05		HS:	C	43,44,45,46
SLX 1746-331	17 49 50.6	-33 11 55	35 ^{oo}	HS:	C	47,48,49
XTE J1748-288	17 48 05.06	-28 28 25.8		LH, HS, VH, J	A	50,51,52,53,54
XTE J1755-324	17 55 28.6	-32 28 39	1 ^o	LH, HS	B	55,56,57,58
1755-338 (V 4134 Sgr)	17 58 40.0	-33 48 27		HS	B	59,62,60,61,62
GRS 1758-258	18 01 12.67	-25 44 26.7		LH, HS, J	A	63,64,65,66
EXO 1846-031	18 49 16.9	-03 03 53	11 ^{oo} f	HS	C	67
XTE J1908+094	19 08 53.08	+09 23 04.9		LH, HS	B	68,69,70,71
1957+115 (V 1408 Aql)	19 59 24.0	+11 42 30		HS	B	72,73,74,75
XTE J2012+381	20 12 37.70	+38 11 01.2		LH, HS	B	76,77,78,79

^a For additional references and information, see TL95 and Liu et al. 2001.

^b Positional uncertainty given if $r_x > 10^{10}$.

^c LH' { low/hard state, HS' { high/soft state, VH' { very high state, J' { radio jet.

^d Qualitative grade indicating the likelihood that the candidate is in fact a BH.

^e GRS 1716-249 = GRO J1719-24 = X-ray Nova Oph 1993.

^f Alternative position also possible; see Parmar et al. 1993.

REFERENCES: ¹Kitamoto et al. 1990; ²Brockopp et al. 2001; ³Revnivtsev et al. 2000a;

⁴MccLintock et al. 2003b; ⁵Murdin et al. 1977; ⁶Kaluzienski et al. 1975; ⁷Barret et al. 1992;

⁸Hjellming et al. 1999; ⁹Tom sick & Kaaret 2000; ¹⁰Dietters et al. 2000; ¹¹Augsteijn et al. 2001;

¹²Groot et al. 2001; ¹³Kalemci et al. 2002; ¹⁴Homan et al. 2003a; ¹⁵Miller et al. 2002b;

¹⁶Sanchez-Fernandez et al. 2002; ¹⁷in't Zand et al. 2002a; ¹⁸Wijnands & Miller 2002; ¹⁹Mirabel et al. 1993; ²⁰van der Hooft et al. 1996; ²¹Revnivtsev et al. 1998b; ²²Rupen et al. 2003;

²³Remillard et al. 2003a; ²⁴Maryard & Swank 2003; ²⁵Borozdin et al. 1995; ²⁶Vargas et al.

1996; ²⁷Ueda et al. 1997; ²⁸Cui et al. 1997a; ²⁹Trudolyubov et al. 1999; ³⁰Marthi et al. 1997;

³¹Vargas et al. 1997; ³²Borozdin et al. 1998; ³³Wijnands et al. 2001; ³⁴Greiner et al. 1996; ³⁵Cui et al. 2001; ³⁶Churazov et al. 1993; ³⁷Smith et al. 1997; ³⁸Smith et al. 2002; ³⁹Marthi et al. 2000;

⁴⁰Gursky et al. 1978; ⁴¹Cooke et al. 1984; ⁴²White & Marshall 1984; ⁴³Davies et al. 1976;

⁴⁴Wilson et al. 1977; ⁴⁵Branduardi et al. 1976; ⁴⁶Kennea & Skinner 1996; ⁴⁷Skinner et al. 1990;

⁴⁸White & van Paradijs 1996; ⁴⁹Modt et al. 1998; ⁵⁰Hjellming et al. 1998b; ⁵¹Revnivtsev et al.

2000c; ⁵²Kotani et al. 2000; ⁵³Miller et al. 2001; ⁵⁴Rupen et al. 1998; ⁵⁵Remillard et al. 1997;

⁵⁶Ogle et al. 1997; ⁵⁷Revnivtsev et al. 1998a; ⁵⁸Goloni et al. 1999; ⁵⁹Bardt & McClelland

1983; ⁶⁰White et al. 1988; ⁶¹Pan et al. 1995; ⁶²Seon et al. 1995; ⁶³Rodriguez et al. 1992;

⁶⁴Sunyaev et al. 1991a; ⁶⁵Smith et al. 2001; ⁶⁶Rothstein et al. 2002; ⁶⁷Parmar et al. 1993;

⁶⁸Rupen et al. 2002; ⁶⁹in't Zand et al. 2002b; ⁷⁰Woods et al. 2002; ⁷¹Chaty et al. 2002;

⁷²Argon et al. 1978; ⁷³Wijnands et al. 2002; ⁷⁴Yaqoob et al. 1993; ⁷⁵Nowak & Williams 1999;

⁷⁶Hjellming et al. 1998a; ⁷⁷Campana et al. 2002; ⁷⁸Vasiliev et al. 2000; ⁷⁹Hynes et al. 1999;

⁸⁰Revnivtsev et al. 2003; ⁸¹Steeghs et al. 2003; ⁸²Homan et al. 2003b; ⁸³Remillard &

McClelland 1999.

and XTE J1856+053 (Barret et al. 1996a) primarily because we judged that the available information was too scanty. Thus the total number of binaries considered here (i.e., the systems listed in Tables 4.1–4.3 that contain either a BH or a BHC) is 40. For narrative discussions about many of the systems in Table 4.3, see TL95 and TS96. For additional data and as a supplement to the list of references given in Table 4.3, see Liu et al. (2001).

4.1.4 X-ray novae

If we include the X-ray novae observed during the past decade, then about 300 bright binary X-ray sources are known (van Paradijs 1995; Liu et al. 2000; Liu et al. 2001). More than half of them are LMXBs, and roughly half of each type (i.e., LMXB and HMXB) are classified as transient sources. The HMXB transients are neutron-star/Be-star binaries, which are not relevant to this review. The well-studied LMXB transients, on the other hand, include all of the X-ray novae that are listed in Tables 4.1–4.3. The principal hallmark of an X-ray nova include both the discovery of the source during a violent outburst and a very large ratio of maximum to minimum X-ray intensity. The behavior of A 0620+00, described in x4.1.2 provides a classic example of an X-ray nova. Indeed, it is the extreme faintness of the quiescent accretion disk in these systems that allows one to view the companion star, leading to secure dynamical measurements of the BH mass (x4.1.2, x4.3.4; Ch. 5).

Recurrent eruptions have been observed for several of the X-ray novae listed in Table 4.1; e.g., A 0620+00 in 1917 and 1975; H 1743+322 in 1977 and 2003; GS 2023+338 in 1938, 1956 and 1987; 4U 1543+47 in 1971, 1983, 1992 and 2002; and 4U 1630+472 and GX 339-4 at 1–2 year intervals. (Outbursts prior to 1970 are inferred from studies of optical plates *ex post facto*.) Most X-ray novae, however, have been observed to erupt only once. Nevertheless, all X-ray novae are thought to be recurrent, with cycle times for some possibly as long as several centuries or more. TS96 suggest an average cycle time of 10–50 years. The infrequent outbursts are due to a sudden surge in the mass accretion rate onto the BH. The generally accepted mechanism driving the outburst cycle is that described by the disk instability model, which was developed initially for dwarf novae (Smart 1971; Ostriker 1974; Cannizzo 1993; Lasota et al. 2001) and extended to X-ray novae (e.g., Dubus et al. 2001).

4.1.5 Accretion onto black holes

The desire to understand observations of BHs compels us to model the hydrodynamics and radiation processes of gas orbiting in the gravitational potential of a compact object (see Ch. 13 for a detailed review). The best-known such model is the thin accretion disk (Pringle & Rees 1972; Shakura & Sunyaev 1973; Novikov & Thorne 1973; Lynden-Bell & Pringle 1974). For nearly all of the systems included in Tables 4.1–4.3, the companion star lies its Roche equipotential lobe and a narrow stream of gas escapes the star through the inner Lagrangian (L_1) point. This gas has high specific angular momentum and cannot accrete directly onto the BH. It feeds into a thin disk of matter around the BH known as an accretion disk. Once entrained in the disk, the gas moves in Keplerian orbits with angular velocity $(GM/R^3)^{1/2}$. However, viscous dissipation slowly taps energy from the bulk orbital motion, and viscosity transports angular momentum outward. As a result, the gas

gets hotter as it sinks deeper into the gravitational potential well of the BH. Near the BH the disk term inates because there are no stable particle orbits possible in the extre me gravitational eld. The existence of an innermost stable circular orbit (ISCO) and other properties of BHs are discussed in many texts (e.g. Shapiro & Teukolsky 1983; Kato et al. 1998). In an astrophysical environment, a BH is completely speci ed by two numbers, its mass M , and its dimensionless spin parameter a , which has a value of between 0 for a Schwarzschild hole and 1 for a maximally rotating Kerr hole. The defining property of a BH is its event horizon, the immaterial surface that bounds the interior region of spacetime that cannot communicate with the external universe. The radius of the event horizon of a Schwarzschild BH is $R_s = 2GM/c^2 = 30$ km ($M = 10M_\odot$), the ISCO lies at $R_{\text{ISCO}} = 6R_s$, and the corresponding maximum orbital frequency is $\omega_{\text{ISCO}} = 220$ Hz ($M = 10M_\odot$)¹. For an extreme Kerr BH, the radii of both the event horizon and the minimum stable (prograde) orbit are identical, $R_K = R_{\text{ISCO}} = R_s$, and the maximum orbital frequency is $\omega_{\text{ISCO}} = 1615$ Hz ($M = 10M_\odot$)¹. For the Kerr BH, it is well known that the rotational energy can be tapped electromagnetically (Blandford & Znajek 1977). The gas flows driven by this process are both anisotropic and self-collimating (Blandford 2002, and references therein), and they may be the source of the relativistic jets seen from several BHs and BHs (Tables 4.2{4.3).

Even for XTE J1118+480, the smallest system in Table 4.1, the outer radius of the accretion disk is expected to be roughly one solar radius, $10^5 R_s$, vastly larger than the BH event horizon. Thus a gas element of mass that is destined to enter the BH starts far out with negligible binding energy. However, when it reaches the ISCO it will have radiated $0.057m c^2$ for a Schwarzschild BH or $0.42m c^2$ for an extreme Kerr BH. Moreover, 90% of this colossal binding energy is radiated within about $20R_s$ of the center. At all disk radii, the binding energy liberated by viscous dissipation is radiated locally and promptly and results in a gas temperature that increases radially inward reaching a maximum of $T = 10^7$ K near the BH. This picture is the basis of the standard thin accretion disk model (Shakura & Sunyaev 1973). A nonrelativistic approximation to this thin disk spectrum has been formulated conveniently as a multi-temperature blackbody (Mitsuda et al. 1984; Makishima et al. 1986). The total disk luminosity in a steady state is $L_{\text{disk}} = GM_- M_- / 2R_{\text{in}}$, where M_- is the mass accretion rate and R_{in} is the radius of the inner edge of the disk. This model, often referred to as the Multicolor Disk (MCD) model, is used to describe the thermal component that is dominant in the HS state and is also present in the VH state (x4.2.2; x4.3.5; x4.3.7). The MCD model has been available within XSPEC ("diskbb"; Amaud & Domman 2002) for many years and has been widely used. Despite the successes of the MCD model, it is important to note a significant limitation, namely, the neglect of a torque-free boundary condition at the ISCO (Gierlinski et al. 1999). In the MCD model, the temperature profile is simply $T(R) \propto R^{-3/4}$, which rises to a maximum at the ISCO, whereas a proper inner boundary condition produces null dissipation at the ISCO with the temperature peaking at $R > R_{\text{ISCO}}$ (Pringle 1981; Gierlinski et al. 1999). The current MCD model requires attention and improvement.

Efforts have also been made to include relativistic corrections to the MCD model (e.g., Ebisawa et al. 1991; Zhang et al. 1997a; Gierlinski et al. 2001). However, quan-

itative analyses (e.g., a spectroscopic measurement of the inner disk radius when the source distance and inclination angle is known) will require more sophisticated models. Accretion disk models are being developed to incorporate MHD effects in the context of GR (e.g., McKinney & Ramirez 2002), with additional considerations for radiation pressure and radiative transfer (Turner et al. 2002; Shimura & Takahara 1995). Early results show that magnetic fields may couple matter in the "plunging region" to matter at radii greater than the ISCO, and thereby extract energy from very near the horizon (Agol & Krolik 2000). In the case of a rapidly rotating Kerr hole, the spin/electromagnetic effects mentioned above may not only drive relativistic jets, but also may modify grossly the spectrum of the inner accretion disk (Wijmans et al. 2001b; Miller et al. 2002b).

At lower mass accretion rates corresponding to several percent of the Eddington luminosity, a BHB usually enters the LH (i.e., low/hard) state and at very low accretion rates it reaches the quiescent state, which may be just an extreme example of the LH state. In both of these states, the spectrum of a BHB is dominated by a hard, nonthermal power-law component (photon index 1.7; $\times 4.3.4$ & $\times 4.3.6$), which cannot be accounted for by a thermal accretion disk model; it is most plausibly explained as due to Comptonization of soft photons by a hot optically thin plasma. Early models for the spectrum of the quiescent state postulated that the disk does not extend all the way down to the ISCO (Narayan 1996; Narayan et al. 1996). The disk is truncated at some larger radius and the interior volume is filled with a hot ($T_e = 100$ keV) advection-dominated accretion flow or ADAF (Narayan & Yi 1994, 1995; Narayan et al. 1996; Quataert & Narayan 1999). In an ADAF, most of the energy released via viscous dissipation remains in the accreting gas rather than being radiated away (as in a thin disk). The bulk of the energy is advected with the flow. Only a small fraction of the energy is radiated by the optically thin gas before the gas reaches the center. Consequently, the radiative efficiency of an ADAF (which depends on the uncertain fraction of the viscous energy that is channeled to the electrons) is expected to be only 0.1(1%, whereas the radiative efficiency discussed above for disk accretion is definitely 5.7%. There is wide agreement that these radiatively inefficient flows have been observed in quiescent BHBs ($\times 4.3.4$) and from galactic nuclei (Bagano et al. 2001; Loewenstein et al. 2001). However, the theoretical picture has become complex with variant models involving winds (ADIOS; Blandford & Begelman 1999) and convection (CDAFs; Igumenshchev & Abramowicz 1999; Stone et al. 1999; Narayan et al. 2000; Quataert & Gruzinov 2000).

One attempt has been made to unify four of the five states of a BHB using both the MCD and ADAF models (Blin et al. 1997). This approach is illustrated in Figure 4.1, which shows how the geometry of the accretion flow changes as the mass accretion rate \dot{m} varies (\dot{m} is the mass accretion rate expressed in Eddington units). The scenario indicates how a BH system progresses through five distinct states of increasing \dot{m} , from the quiescent state to the VH state. In the three states at lower \dot{m} , the flow consists of two zones (disk and ADAF), as described above. For the two states of highest \dot{m} , the disk extends down to the ISCO. In all five states, the disk is bathed in a corona that is a seamless continuation of the ADAF. Apart from the VH state, the model treats consistently the dynamics of the accreting gas, the thermal balance of the ions and electrons in the ADAF and corona, and

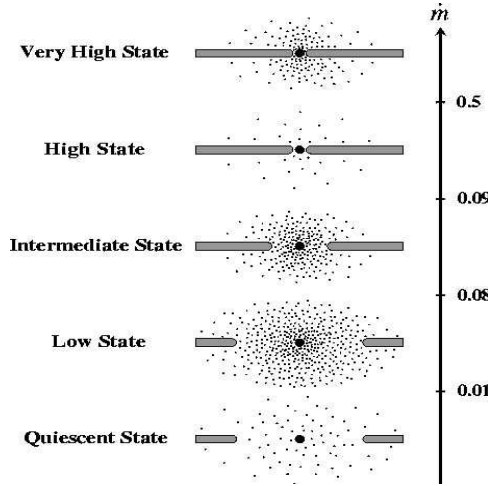


Fig. 4.1. Schematic sketch of the accretion flow in different spectral states as a function of the total Eddington-scaled mass accretion rate \dot{m} . The ADAF is represented by dots and the thin disk by the horizontal bars. The very high state is illustrated, but it is not included in the unification scheme (Esin et al. 1997).

the radiation processes. The model has had significant successes in describing the spectral evolution of several BHs (Esin et al. 1997; Esin et al. 1998). (For further discussion of the ADAF model, see x4.3.4.)

However, the multistate model of Esin et al. (1997) has important limitations. For example, it does not unify the most luminous state, the very high state, which is characterized by an unbroken power-law spectrum extending out to a few hundred keV or more (x4.3.7). Also, this simple ordering of the states by \dot{m} or luminosity is naive (x4.3). Moreover, the model does not account for the dynamical behavior of the corona, including strong flares and powerful low-frequency quasi-periodic oscillations (x4.4), nor does it account for the radio emission observed from most BHs (Table 4.2). Finally, the "evaporation" process by which the cold gas in a thin disk feeds into a hot ADAF is at best qualitatively understood, and there is no quantitative model relating the disk truncation radius to the accretion rate \dot{m} (Narayan 2002, and references therein).

There are alternative models of the X-ray states, and many of them invoke a dynamical accretion disk corona that is fed by MHD instabilities in the disk. For example, in the model of Merezhni & Fabian (2001a, 2001b) the hot corona that generates the power-law component is intimately connected with the thin accretion disk. Magnetic energy generated (presumably) by the sheared Keplerian disk creates magnetic flares that rise out of the disk because of the Parker instability. Within the framework of this model, Di Matteo et al. (1999) present a magnetic flare model for the two common states of GX 339-4. In the HS state, the flares occur near the disk and heat it. The disk reradiates the observed soft thermal component, whereas the faint hard component is produced by Comptonization of the soft flux. In the LH state, the flares occur far above the disk and the density of soft seed photons is greatly reduced. Thus, the system is photon-starved, and the resultant

Comptonized spectrum is hard. M erloni and Fabian (2002) also consider coronae as sources of powerful jets/out flows. They find that such out flows can render a source radiatively inefficient even if advection of energy into the BH is unimportant.

It is generally agreed that the temperatures of the corona are in the range 100–300 keV, with optical depths of 0.1–1 (e.g., M erloni & Fabian 2001b). There is little agreement, however, on the geometry and physical properties of the corona. Thus, a wide range of coronal models have been proposed (e.g., Haardt & Maraschi 1991; Dove et al. 1997a, 1997b; Meyer et al. 2000; Rozanska & Czerny 2000; Kawaguchi et al. 2000; Nowak et al. 2002; Liu et al. 2002). Liu et al. conclude that the primary difficulty in modeling the corona is the magnetic field that produces time variations and spatial inhomogeneities; in addition, one must consider complicated radiation/energy interactions between the disk and the corona. Because of the complexity of the problem, some students of the corona choose to apply their models to large quantities of X-ray (and radio) data, an approach that has proved fruitful (Zdziarski et al. 2002, 2003; Wardzinski et al. 2002).

Timing studies have been used to isolate the fast X-ray variability in BHs as primarily emanating from the corona rather than from the accretion disk (Churazov et al. 2001). Timing studies have also created requirements to explain X-ray QPOs, such as the strong low-frequency QPOs that are prevalent in the VH state. Many coronal models do not deal with fast variability or QPOs explicitly, although there are exceptions, such as the "Accretion/Ejection Instability" model (Tagger & Pellat 1999). In this model, magnetic spiral waves heat and accelerate material at those locations where the spiral waves and the disk are in corotation. During BH outbursts, it has become exceedingly clear that spectral and timing characteristics at both X-ray and radio frequencies may change dramatically and abruptly. Therefore, no single model can account for all of the complex behavior, and our goal in this review is to summarize what is known about each X-ray state and to then discuss physical models in the context of a given state.

In addition to the models discussed above (MCD, ADAF, and coronal), we mention briefly the jet model (e.g., Falcke & Biermann 1995). This model is motivated by the observations of resolved radio and X-ray jets (Tables 4.2–4.3), by observations of radio/X-ray correlations (e.g., Hannikainen et al. 2001; Corbel et al. 2000), and by successes in modeling the broadband spectra of some systems as synchrotron radiation.

4.1.6 Some consequences of an event horizon

The properties of BHs and BH accretion flows are discussed in many texts (e.g., Shapiro & Teukolsky 1983; Kato et al. 1998; Abramowicz 1998). As mentioned above, the defining feature of a BH is its event horizon. Since BHs lack a material surface, surface effects observed for NSs (e.g., type I thermal nuclear bursts) are absent for a BH. Similarly, a BH cannot sustain a magnetic field anchored within it; hence periodic X-ray pulsations, which are observed for many NSs, cannot be generated by a BH.

Both type I bursts and periodic pulsations are considered firm signatures of a NS (TL95). It is interesting to ask what fraction of catalogued, bright sources show either pulsations or type I bursts. We examined this question using the catalog of van

Paradijs (1995), selecting only the brighter sources ($F_x > 30$ Jy) that have been optically identified. We excluded the confirmed and candidate BH systems listed in Tables 4.1{4.3. For the 21 HM XB systems that met our selection criteria, we found that 18 out of 21 (86%) pulse. For 21 LM XB systems, we found that 12 burst and 2 pulse (67% burst or pulse). Thus a very high fraction of these sources manifest behavior that identifies them as NSs. It is also interesting to consider which systems have failed to produce detectable bursts or pulsations because they are either an unusual NS source or they contain a BH. The three non-pulsing HM XB sources are 1700{37, 1947+30 and Cyg X {3; the six corresponding LM XB sources are LM C X {2, 1543{62, Sco X {1, G X 349+2, G X 9+9 and 1822{00.

4.1.7 The Rossi X-ray Timing Explorer (RXTE): 1996.0 { present
 RXTE has been in continuous operation since its launch on 1995 December 30. Its prime objective is to investigate the fundamental properties of BHs, NSs and white dwarfs by making high time resolution observations of extremely hot material located near BH event horizons or stellar surfaces. It is the largest X-ray detector array ever built, and it provides energy coverage from 2{200 keV. It features high throughput (up to 150,000 counts s⁻¹) and 1 s time resolution. RXTE's year-round, wide-sky coverage and its fast response time has made it an important vehicle for the study of transient phenomena and for the support of multiwavelength science.

The observatory is comprised of two large area instruments (PCA and HEXTE) that act in concert, viewing the sky through a common 1° field of view. The third instrument is an All-Sky Monitor (ASM) that surveys about 80% of the sky each orbit. For descriptions of the instruments, see Levine et al. (1996), Swank (1998), Rothschild et al. (1998), and Bradt et al. (2001). The Proportional Counter Array (PCA), which has a total net area of 6250 cm², is the chief instrument. The PCA consists of five sealed proportional counter detectors. It is effective over the range 2{60 keV with 18% energy resolution at 6 keV. The High Energy Timing Experiment (HEXTE) covers the energy range 20{200 keV. It is comprised of eight NaI/CsI phosphor detectors with a combined net area of 1600 cm². The HEXTE has provided important spectral information beyond the reach of the PCA, but the modest count rates of the HEXTE (e.g., 289 counts s⁻¹ for the Crab) limit its use for timing studies. Indeed, it is the PCA (12,800 counts s⁻¹ for the Crab with 5 PCUs) that has achieved groundbreaking results in high-energy astrophysics.

The ASM is comprised of three wide-field proportional counters that are mounted on a rotating boom. On a daily basis, it surveys about 90% of the sky and obtains about 5{10 observations per source. It locates bright sources to a typical accuracy of 5°. In uncrowded regions it can monitor known sources down to about 35 mCrab (2⁻³) in one 90{s exposure or about 10 mCrab in one day. On many occasions, the ASM has proved indispensable in alerting PCA/HEXTE observers to targets of opportunity, such as the appearance of a new transient or a state{change in a cataloged source. Furthermore, the ASM public archive containing the continuous light curves of 400 X-ray sources (both Galactic and extragalactic) has been invaluable in studying the multiyear behavior of X-ray sources and in supplementing X-ray and multiwavelength (e.g., Chandra and HST) studies of individual sources. The data are also important to observers of AGN and gamma-ray bursts.

4.2 X-ray light curves, spectra and luminosity data

4.2.1 ASM light curves of BH binaries and BH candidates

To illustrate the diversity of behavior among BHs and BHCs, we show in Figure 4.2{4.5 the 1.5{12 keV ASM light curves and the (5{12 keV) / (3{5 keV) hardness ratio (HR2) for 20 of the systems listed in Tables 4.1{4.3 that were active during the past seven years. These light curves should be compared to the heterogeneous collection of 20 X-ray light curves collected by Chen et al. (1997). In making such comparisons, note that we use a linear intensity scale, whereas Chen et al. and most authors use a log scale. The light curves in Figures 4.2{4.5 are ordered by RA, although we discuss them roughly in order of increasing complexity. An intensity of 1 Crab corresponds to $75.5 \text{ A SM } \text{c s}^{-1}$. A hardness ratio (HR2) of 0.5 (1.5) generally corresponds to the HS state (LH state). All good data are included, although the time interval for binning the counts has been tailored to the source intensity. The hardness ratio is not plotted in the absence of a detectable 5-12 keV flux. References are cited sparingly in the narrative descriptions of the light curves given below; see Tables 4.1{4.3 for further references. In the following, the term "classic" light curve refers to an outburst profile that exhibits a fast rise and an exponential decay, like those observed for several pre{RXTE BH X-ray novae, including A 0620+00, GS/GRS 1124+68, GS 2000+25 and GRO J0422+32 (TL95; Chen et al. 1997). Such classic light curves often show a secondary maximum (roughly a doubling of intensity) that occurs during the decline phase about 40{100 days after the onset of the outburst (TL95; Chen et al. 1997).

4.2.1.1 Black hole binaries

Figure 4.2 shows the light curves of all six of the X-ray novae with short outburst cycles that were detected by the ASM (Tables 4.1{4.2). 4U 1543{47: An exceptionally clean example of a classic light curve with an e{folding decay time of 14 days. It lacks a secondary maximum, presumably because the outburst is so brief. For details and references on three prior outbursts of this source, see Chen et al. (1997). XTE J1859+226: A second example of a classic light curve that does show a secondary maximum (at about 75 days after discovery). Note the intense variability near the primary maximum. XTE J1118+480: One of five X-ray novae that remained in a hard state throughout the outburst and failed to reach the HS state. Note the prominent precursor peak.

Also shown in Figure 4.2 are the complex and similar light curves of two X-ray novae with long orbital periods, GRO J1655{40 and XTE J1550{564. GRO J1655{40: This source has undergone two outbursts since its discovery in 1994 July. Shown here is the full light curve of the second, 16{month outburst. The double-peaked profile is quite unlike the classic profile of 4U 1543{47. During the first maximum in 1996, the source exhibited strong flaring and intense nonthermal emission (VH state). In 1997 the source spectrum was soft and thermal except for a hard episode at the very end of the outburst (Sobczak et al. 1999). Note the several absorption dips in the light curve of this high inclination system (Kuulkers et al. 1998). XTE J1550{564: The complex profile includes two dominant peaks during 1998{99, followed several hundred days later by a smaller peak in 2000. Not shown here are three very small

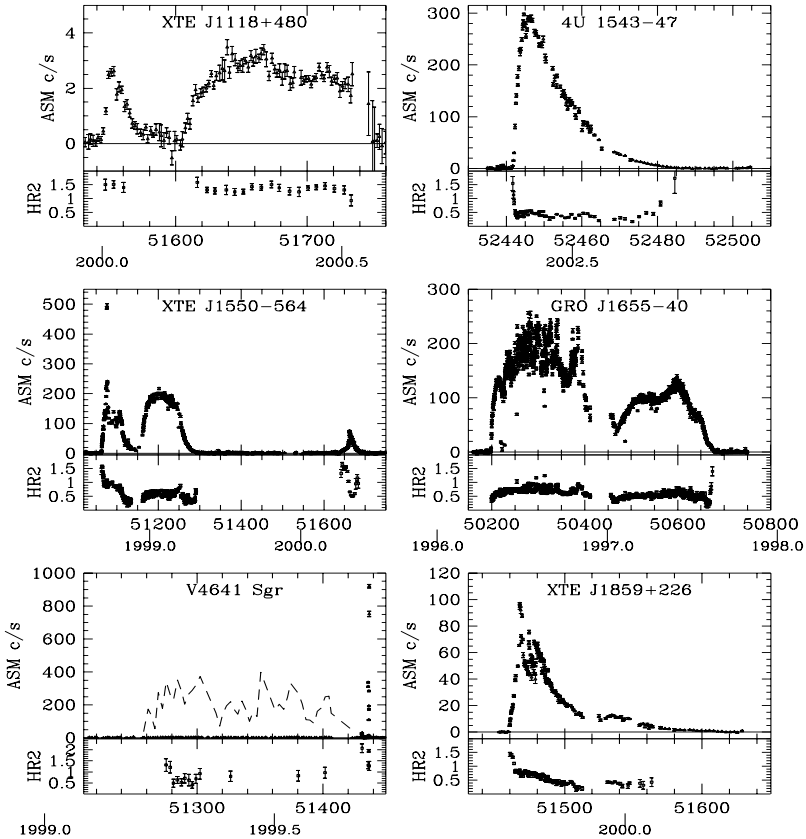


Fig. 4.2. Transient ASM light curves of six black hole binaries. For V 4641 Sgr, the dashed line shows intensity $\times 50$ in order to highlight the low-level activity that preceded the violent and short-lived outbursts.

outbursts (LH states) that have occurred subsequently. Some unusual characteristics include the slow 10-day rise following the source's discovery on 1998 September 6, followed by the dominant (6.8 Crab) X-ray outbursts and the abrupt 10-day decay timescale following each outburst. The source was predominantly in the VH or IM states during the first peak (1998), softening to the HS state during the second peak (1999). The spectral evolution through all of the X-ray states occurred much more rapidly during the small peak in 2000. SAX J1819.3-2525 = V 4641 Sgr: As this extraordinary light curve shows, the source became active at a low level in the spring of 1999 (dashed line shows intensity $\times 50$). Five months later it underwent a brief, violent outburst during which the 1.5-12 keV intensity increased very rapidly (within 7 hours) from 1.6 to 12.2 Crab. Within two hours thereafter, the intensity declined to less than 0.05 Crab (Wijnands & van der Klis 2000, and references therein).

Figure 4.3 shows the light curves of the two persistent BHs (LM C X-3 and Cyg X-1) and two other BHs that have been active throughout the RXTE era. LM C X-3: The light curve shows the large-amplitude cyclic modulation in the flux

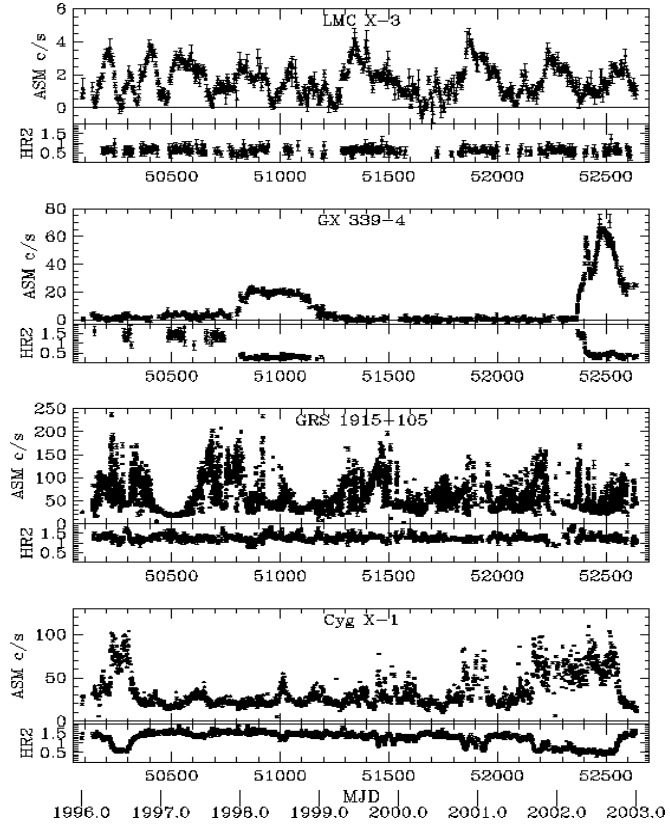


Fig. 4.3. Seven-year ASM light curves of four black hole binaries.

reported by Cowley et al. (1991); however, their 198-day cycle time is shorter than is indicated by these data. As the hardness ratio plot shows, the source remains in the HS state most of the time. However, at the local intensity minima, where there are gaps in the HR2 plot due to statistical limitations, the PCA observations show transitions to the LH state (Wijnands et al. 2001a). GX 339-4: As shown, the source underwent major eruptions into a soft spectral state (HR = 0.5) in 1998 and 2002. In the time between these two outbursts, the source was very faint (< 2 mCrab) compared to its customary hard-state intensity of 30 mCrab, which it enjoyed prior to its 1998 outburst. Remarkably, this transient BH has never been observed in a fully quiescent state (Hynes et al. 2003). GRS 1915+105: This source exhibits extraordinary variations in both the X-ray and radio bands. A astonishing and yet repetitive patterns are sometimes seen in the X-ray light curves (Muno et al. 1999; Belloni et al. 2000; Klein-Wolt et al. 2002). For a 1992 X-ray light curve showing the birth of this source, see Chen et al. (1997). Cyg X-1: Transitions between the LH and HS states were first observed in this archetypal BH source (x4.3.1). However, as this record shows, there are both gradual and rapid variations in the hardness ratio that blur the distinctions between the two states (see x4.3.9).

4.2.1.2 Black hole candidates

Figure 4.4 displays the light curves of six BHs with short outburst cycles. XTE J748-288: This short duration outburst that begins and ends in a hard spectral state is similar to the classic light curve of 4U 1543-47 (Fig. 4.2). The 1/e decay time is 16 days. This source is heavily absorbed, and the values of the hardness ratio are consequently increased. GRS 1739-278: A somewhat longer duration outburst with a nearly classic profile that is punctuated by a precursor peak, 40% variability near maximum, and undulations in intensity during the decay. Again, the source begins and ends its outburst with a hard spectrum. XTE J1755-324: This brief outburst, which follows an abrupt rise, provides yet another example of a classic light curve. The outburst appears to be locked in the HS state. XTE J2012+381: This unusual light curve combines a classic rise to maximum followed directly by a precipitous drop in intensity. Also unusual are a large secondary maximum occurring just 30 days after discovery plus an additional late maximum at 140 days. XTE J1650-500: A complex light curve. At the onset of the outburst there is a very rapid rise followed by a slow rise. This unusual behavior is accompanied by a remarkable, slow (15-day) transition from a hard spectral state to a soft one. 4U 1354-64: A slow rise followed by a rather rapid decline. During this outburst, the source remained in the LH state (Brockopp et al. 2001), whereas during its somewhat brighter outburst in 1987, the source reached the HS state (Kitamoto et al. 1990). This source may be identical to Cen X-2, which reached a peak intensity of 13 Crab in 1967 (Brockopp et al. 2001).

In Figure 4.5 we show the light curves of the BHB LMC X-1 and the light curves of three BHs. LMC X-1: The source is continually in a soft spectral state and maintains a relatively steady intensity. 4U 1630-47: The 600-day recurrence time has been known for 25 years (Jones et al. 1976). Here we see five, nearly equally-spaced outbursts. Note the very different profiles and sequences of the outbursts. Note also that the 1996 outburst starts distinctively with a soft spectrum. GRS 1758-258: This hard Galactic center source was discovered by GRANAT/SIGMA in 1991. Its spectrum extends to at least 300 keV (Sunyaev et al. 1991a). During 2001 it underwent a transition to an unusual soft state of very low intensity (Smith et al. 2001; Miller et al. 2002d); the low flux level during that event is evident in the ASM record shown here. 4U 1957+11: The source has long been considered a BH based on its "ultrasoft" spectrum (White & Marshall 1984), although Yaqoob et al. (1993) have argued that the primary is a NS. The source displays a consistent flaring behavior and a soft spectrum over the 7-year interval.

It is often said that the spectra of BH X-ray novae soften during the initial rise to maximum (i.e., their spectra transition from a hard spectral state to a soft one during the rise). For several sources, the data in Figures 4.2-4.5 support this view: 4U 1543-47, XTE J1550-564, XTE J1859+226, XTE J1650-500, GRS 1739-278, and XTE J2012+381. However, there are two clear counter-examples, sources whose spectra hardened during the initial rise: GRO J1655-40 (Fig. 4.2) and 4U 1630-47 (Fig. 4.5; first of 5 outbursts).

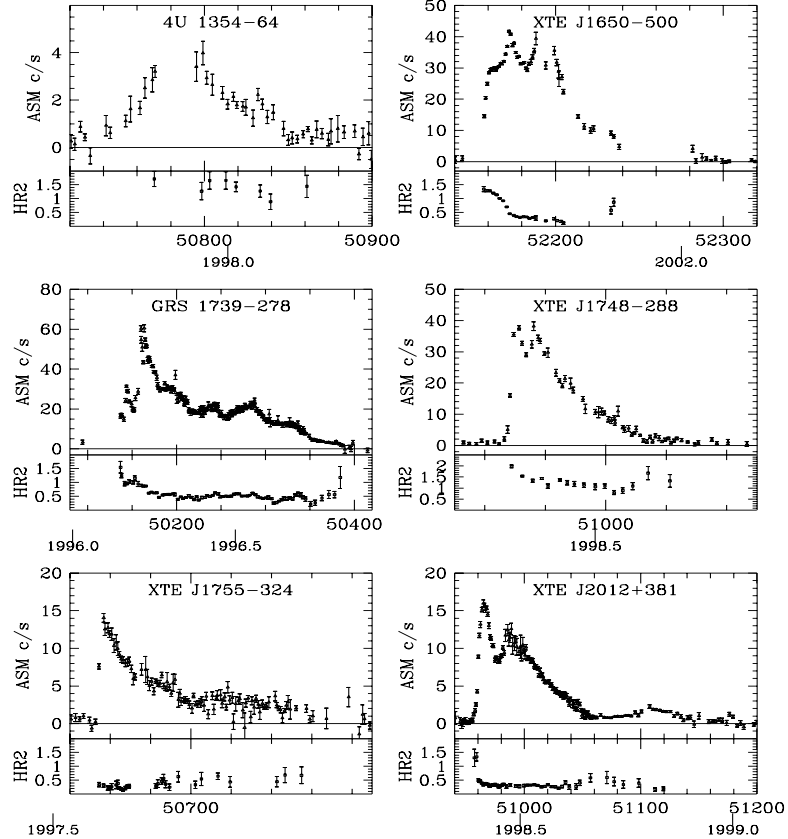


Fig. 4.4. Transient ASM light curves of six black hole candidates.

4.2.2 Synoptic studies of selected black hole binaries

It is important to follow the several-month spectral evolution of individual sources and to construct unified spectral models that can be used to represent the energy spectra of all BHBs. The necessary elements of such models can be deduced from a simple appraisal of the observational data: e.g., Cyg X-1 and other BHBs in the LH state show that the model must contain a nonthermal component, which can be well represented by a power-law function (TL95). On the other hand, the soft spectra observed from BHB X-ray novae in the HS state is most widely modeled as a multi-temperature blackbody, which approximates the emission from an optically-thick (relativistic) accretion disk. Many studies of BHB spectral evolution therefore choose a composite model comprised of disk blackbody and power-law components. Although this simple model has significant limitations, nevertheless it has proven to be widely applicable and quite effective in monitoring the spectra of BHBs, as we now discuss briefly by pointing to two examples.

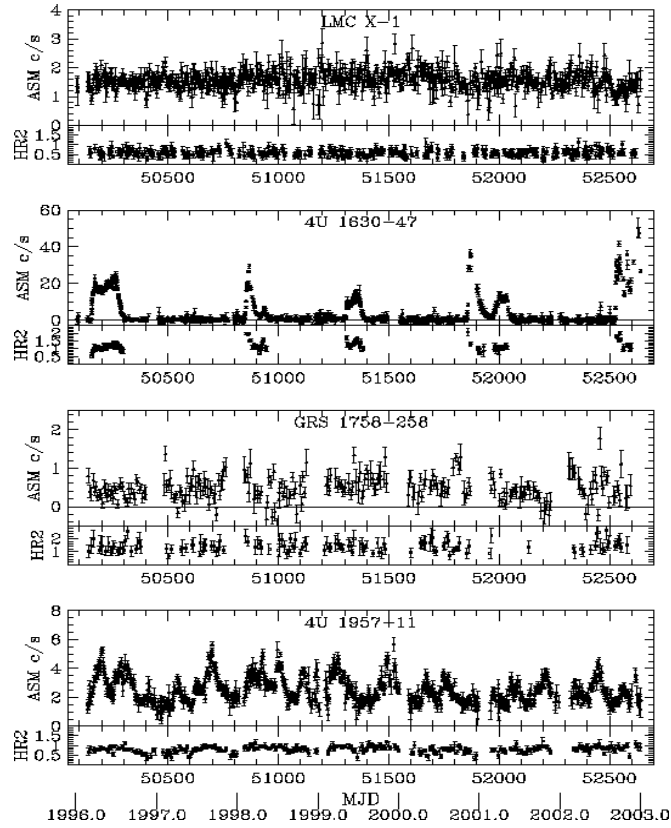


Fig. 4.5. Seven 7-year ASM light curves of three black hole candidates and the black hole binary LMC X-1.

Important studies of Ginga spectra using this model were made by Ebisawa et al. (1991, 1993, 1994). The authors added one refinement to the model, namely, a broad absorption feature above 7 keV. This feature is associated with the rection of X-rays by an optically thick accretion disk (Ebisawa et al. 1994). With this model a successful and quantitative comparison was made of the spectra of Cyg X-1, LMC X-3, GS 2000+25, LMC X-1, GX 339-4 and GS/GRS 1124-68 (Nova Mus 1991). This latter source, which exhibited a classic light curve, was observed 51 times in 1991 over a span of 235 days using the Ginga Large Area Counter (LAC). We direct the reader's attention to Figure 15 in Ebisawa et al. (1994) which shows the evolution over a full outburst cycle of the spectral parameters and fluxes for GS/GRS 1124-68. In their figure, it is evident that an important transition occurs 130 days into the outburst. For example, the photon spectral index suddenly decreases from 2.2(2.6 to a value near 1.6, the hard flux increases substantially and the soft disk flux decreases. This characteristic behavior, which has been observed for a number of BH X-ray novae, marks the transition from the HS (high/soft) state to the LH (low/hard) state.

We now compare the results obtained for GS/GRS 1124-68 to the results of an analogous study of the irregular BH X-ray nova XTE J1550-564, which was observed

extensively by RXTE during its 1997–1998 outburst (Sobczak et al. 2000b). A total of 209 pointed observations spanning the entire 255-day outburst were made using the PCA and HEXTE detectors. The 1998–1999 light curve of the source is complex and includes a slow (10 day) rise to maximum, an intense (6.8 Crab)

outburst that occurred early in the outburst, and a “double-peaked” profile that roughly separates the outburst into two halves of comparable intensity (Fig. 4.2). Sobczak et al. adopted very nearly the same spectral model and methodology as Ebisawa et al. (1994). We direct the reader’s attention to Figure 4 and the accompanying text in Sobczak et al. (2000b), which describes a complex course of evolution relative to that of GS/GRS 1124/68. Very briefly, Sobczak et al. show that during the first half of the outburst QPOs are ubiquitous and the spectrum is dominated by the power-law component, which are conditions that mark the very high/intermediate state. In contrast, during the second half of the outburst QPOs are scarce and the spectrum is dominated by emission from the accretion disk, which corresponds to the high/soft state. During this state, the inner disk radius ($\approx 4.1.5$) remained nearly constant for 4 months (Sobczak et al. 2000b). Very similar behavior has been observed for GS/GRS 1124/68 (Ebisawa et al. 1994) and for several other sources (TL95). The constancy of the disk inner radius is remarkable, given the accompanying, large variations in luminosity that are usually observed (TL95).

In overview, in both GS/GRS 1124/68 and XTE J1550/564, one sees time intervals where thermal emission from the disk dominates the spectrum, while at other times the disk spectrum is substantially modified and a power-law component may dominate at either high or low luminosity. In other sources, such as Cyg X-1, the nonthermal LH state may be stable for many months or years, but its soft-state spectrum does not resemble the thermal spectra seen from GS/GRS 1124/68 and XTE J1550/564. These results highlight the need to specify the physical properties of X-ray states while avoiding the confusing terminology that has developed during the past 30 years. Accordingly, in x4.3 we address this issue and seek clearer definitions of the X-ray states.

4.2.3 Relativistic iron emission lines

Strong evidence for accretion disks in active galactic nuclei has come from X-ray observations of broad iron K α lines. In particular, in some Seyfert galaxies the very asymmetric profile of the Fe K α line (e.g., its extended red wing) suggests strongly that the emission arises in the innermost region of a relativistic accretion disk (for reviews see Fabian et al. 2000, Reynolds & Nowak 2003). The good energy resolution of ASCA provided the first clear evidence for such a line profile (Tanaka et al. 1995). In some cases, the line profile indicates the presence of an accretion disk extending down to the ISCO (Walter et al. 2001). The broad Fe K α fluorescence line is thought to be generated through the irradiation of the cold (weakly ionized) disk by a source of hard X-rays (likely an optically thin, Comptonizing corona). Relativistic beaming and gravitational redshifts in the inner disk region can serve to create an asymmetric line profile.

In fact, the first broad Fe K α line observed for either a BHB or an AGN was reported in the spectrum of Cyg X-1 based on EXOSAT data (Barret et al. 1985). It was this result that inspired Fabian et al. (1989) to investigate the production of such

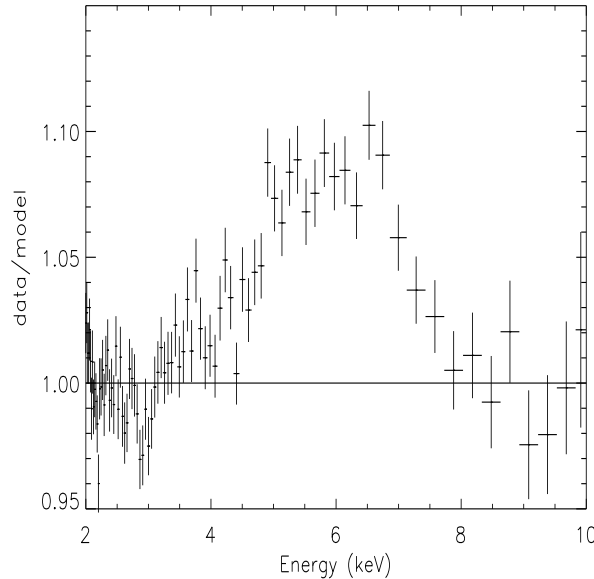


Fig. 4.6. Data/model ratio for XTE J1650-500. The model consists of multicolor disk blackbody and power law components (Miller et al. 2002b). Note the non-Gaussian shape and low-energy extent of the line profile.

a line in the near vicinity of a Schwarzschild BH, a result that was later generalized by Laor (1991) to include the Kerr metric. Other early studies of relativistically smeared Fe K lines from BHs were conducted by Done et al. (1992) and others. Their work was one part of a broader examination of the accretion geometry that is produced as hard X-rays from an overlying corona illuminate the optically-thick accretion disk. An Fe K line and a reflected continuum are always generated in this case (George & Fabian 1991; Matt et al. 1991). One example is a Ginga study of the reflected spectrum of V404 Cyg (Zycki et al. 1999a, 1999b). A limitation of this study is the use of proportional counter detectors (e.g., the Ginga LAC and RXTE PCA, which have an energy resolution of only FWHM = 1.2 keV at Fe K). Such iron K studies suffer both because the energy resolution is marginal and because the response matrices of the detectors are uncertain at the 1-2% level, while the Fe line profile in BHs is typically only 1-5% above the X-ray continuum. Consequently, the results from these instruments must be considered with caution. Some iron K sources that have been studied with RXTE include: GRO J1655-40 (Balucinska-Church & Church 2000); XTE J1748-288 (Miller et al. 2001); and GX 339-4 (Feng et al. 2001; Nowak et al. 2002).

More telling studies of the Fe K line have been achieved using the MECS and HPC/GSPC detectors aboard BeppoSAX, which have a resolution of 0.6 keV at Fe K. Broad line profiles (4-9 keV) have been observed for SAX J1711.6-3808 (in't Zand et al. 2002a) and XTE J1908+094 (in't Zand et al. 2002b); however, these profiles are rather symmetric and may be more a product of Compton scattering

than relativistic broadening. BeppoSAX studies have also revealed other systems with broad, asymmetric Fe K profiles that resemble the predictions of relativistic smearing: GRS 1915+105 (Maccacchia et al. 2002) and V4641 Sgr (Miller et al. 2002a). Interestingly, for both of these systems the inner disk radius deduced from the line profile is consistent with the radius of the ISCO for a Schwarzschild BH, suggesting that rapid spin is not required.

Spectral studies at higher resolution have been made recently with XMM (Newton and Chandra). Using the XMM EPIC (MOS1 detector, Miller et al. (2002b)) and for XTE J1650-500 a broad, skewed Fe K emission line (Fig. 4.6) which suggests the presence of an extreme Kerr BH and indicates a steep radial fall-off of disk emissivity with radius. An observation of Cyg X-1 with the HETG S grating and ACIS (S detector aboard Chandra) revealed a broad line centered at 5.82 keV with a FWHM of 1.9 keV (Miller et al. 2002c). Also present was a smeared Fe edge at 7.3 keV. The authors conclude that the line is predominantly shaped by Doppler/gravitational effects and to a lesser degree by Compton scattering due to refection.

4.2.4 Super-Eddington luminosities

Recently there has been considerable interest in ultraluminous X-ray sources (ULXs) in external galaxies with 0.5-10 keV luminosities in the range 10^{39} - $10^{40.5}$ erg s⁻¹ (Makishima et al. 2000; Fabbiano et al. 2001; Humphrey et al. 2003; Miller et al. 2003b; Ch. 12). The luminosities of ULXs greatly exceed the Eddington limit of a $1.4M_{\odot}$ NS: $L_{\text{Edd}} = 1.25 \times 10^{38} (M_{\odot}/M_{\text{NS}})$ erg s⁻¹. The most luminous systems also exceed by a factor of 20 the Eddington luminosity of a typical $10M_{\odot}$ BH. This fact has led to the suggestion that the most luminous ULXs are a new class of accreting BHs with masses $100M_{\odot}$ (Makishima et al. 2000; Fabbiano et al. 2001). Alternatively, it has been suggested that the ULXs are powered by conventional stellar-mass BHs that radiate anisotropically (King et al. 2001; Ch. 13). We examine this question by comparing as directly as possible the luminosities of the ULXs to the luminosities of the 18 BHs listed in Tables 4.1-4.2.

In terms of the maximum flux density of a BH B, $F_{\text{X, max}}$ (Table 4.1), the 2-11 keV luminosity is: $L_x = L_{\text{Edd}} \times 2.6 \times 10^{35} F_{\text{X, max}}$ (Jy) $\times (D/10 \text{ kpc})^2$ (Bradt & McClintock 1983). For a Crab-like spectrum (x4.1.2), the flux in the 0.5-10 keV (ULX) band is a factor of 1.9 greater (although this is somewhat of an overestimate compared to the use of a thermal spectrum). Including this factor and using the distances and peak fluxes in Table 4.1, we find that the three most luminous BHs are V4641 Sgr (6.2×10^{39} erg s⁻¹), 4U 1543-47 (4.2×10^{39} erg s⁻¹) and GRS 1915+105 (2.4×10^{39} erg s⁻¹). Thus, at peak luminosity these three BHs appear to be in the same league as many of the ULXs observed in external galaxies. Moreover, using the mass measurements from Table 4.2, it appears that all three BHs were super-Eddington at maximum ($0.5-10$ keV): $L_x = L_{\text{Edd}} = 7.0, 3.5$ and 1.4 for V4641 Sgr, 4U 1543-47 and GRS 1915+105, respectively.

This comparison of BHs and ULXs is problematic: First, the distances of the BHs are uncertain, and we have no direct measurements of their fluxes in the 0.5-2 keV band. Nevertheless, the results quoted above suggest that the peak luminosities of a few BHs approach the peak luminosities observed for ULXs to within a factor of 5 (e.g., Miller et al. 2003b). Second, the luminosity shortfall of BHs may

be ascribable to the small sample of 18 BHs compared to the very much larger sample of comparable systems that have likely been detected in surveys of external galaxies. Finally, some ULXs exhibit spectral properties unlike those of BHs. In particular, the cool disk spectra and the longevity at high luminosity of the most luminous ULXs may distinguish them from BHs in the Milky Way (Miller et al. 2003a; 2003b).

We conclude by noting that super-Eddington luminosities have plainly been observed for a few NS systems. The most clear-cut case is A 0535-668, the "LMC transient." This pulsating NS binary with a semi-major axis of $a = 50$ kpc (Freedman et al. 2001) achieved a peak luminosity of $L_x = 1.2 \times 10^{39}$ erg s⁻¹, assuming isotropic emission (Bradt & McClintock 1983, and references therein). This is 6.9 times the Eddington luminosity of a canonical 1.4 M_⊙ NS or 3.8 times the Eddington luminosity of a hypothetical 2.5 M_⊙ NS.

4.3 Emission states of black hole binaries

As discussed in x4.1 and x4.2, BHs exhibit thermal and nonthermal components of X-ray emission, both of which can vary widely in intensity. It has long been recognized that BHs undergo transitions between quasi-stable states in which one or the other of these components may dominate the X-ray luminosity. In the past, the study of BH emission states was based almost exclusively on X-ray spectral and timing studies. More recently, however, the results of X-ray studies have been supplemented with critical contributions by radio, optical and gamma-ray observers to give us a more physical and fruitful framework for regarding the emission states. In the following sections, we review the characteristic behavior that defines each of the principal X-ray states of BHs. We then describe the current picture of each state in terms of physical structures and the nature of the accretion flow. Finally, we discuss the prospects of using these states to deduce the properties of BHs.

4.3.1 Historical notes on X-ray states

In the spring of 1971, Tananbaum et al. (1972) observed a remarkable X-ray state change in Cyg X-1 during which the average soft flux (2-6 keV) decreased by a factor of 4 and the average hard flux increased by a factor of 2. Simultaneously, the radio counterpart of Cyg X-1 brightened. It was later found that luminous X-ray novae such as A 0620-00 exhibited similar spectral transitions, suggesting that common emission mechanisms were at work in both persistent and transient BHs (Coe et al. 1976). These early results suggested that such global spectral changes might signify important changes in accretion physics.

As the many light curves in x4.2 illustrate, the soft X-ray state is generally seen at higher luminosity, motivating frequent references to the high/soft (HS) state. In this state, the spectrum may also display a "hard tail" that contributes a small percentage of the total flux. As shown by the synoptic studies discussed in x4.2.2, the soft state is best explained as 1 keV thermal emission from a multi-temperature accretion disk (see x4.1.5), as foreseen in the standard theory for accretion in BHs (Shakura & Sunyaev 1973). However, it has been found that the soft state of Cyg X-1 is not consistent with a thermal interpretation (Zhang et al. 1997b), and this has caused considerable confusion as to the proper way to understand Cyg X-1 and/or describe

the HS state. In seeking a physical basis for describing X-ray states, it turns out that Cyg X-1 is not a good choice as a prototype, and further remarks about the states in Cyg X-1 are given in a separate section below (§4.3.9).

In the hard state the 2-10 keV intensity is comparatively low, prompting the use of the name low/hard (LH) state. The spectrum is nonthermal and conforms to a power-law with a typical photon index ~ 1.7 (2-20 keV). In this state, the disk is either not detected at 2-10 keV (e.g., Belloni et al. 1999), or it appears much cooler and larger than it does in the soft state (Wijnands et al. 1999; McClintock et al. 2001b).

An additional X-ray state of BHs was identified in the EXOSAT era. It is characterized by the appearance of QPOs in the presence of both disk and power-law components, each of which contributes substantial luminosity (e.g., $> 0.1L_{\text{Edd}}$; van der Klis 1995). In this state, which is referred to as the very high (VH) state, the power-law component is observed to be steep (~ 2.5). Initially, there were only two BHs (GX 339-4 and Nova Mus 1991) that displayed this behavior, but many additional examples have been seen in the RXTE era.

It was first thought that the two nonthermal states, i.e., the LH state and the VH state, could be distinguished through differences in their photon spectral indices, luminosities, and power density spectra. However, as shown below, with further study two of the distinctions have blurred; however, the value of the spectral index continues to be a valid discriminator. The importance of distinguishing between the LH and VH states was emphasized in a 40-500 keV study of seven BHs with the OSSE instrument aboard the Compton Gamma Ray Observatory (Grove et al. 1998). The gamma-ray spectra of these sources separate naturally into two distinct groups which were found to correspond to the LH state and VH state, respectively: (1) For the first group it was shown that the X-ray LH state corresponds with a "breaking gamma-ray state" in which the spectrum below 100 keV is harder than that of the VH state, but then suffers an exponential cutoff near 100 keV. (2) The second group exhibits a power-law gamma-ray spectrum with photon index $2.5 < \alpha < 3.0$ over the entire range of statistically significant measurements. This gamma-ray photon index is consistent with the X-ray photon index of the VH state. Furthermore, contemporaneous X-ray observations (e.g., with ASCA) confirmed that a luminous thermal component coexists with the power-law component, which is one characteristic of the VH state noted above.

4.3.2 X-ray states as different physical accretion systems

Several recent developments in the study of BHs has taken us beyond a largely phenomenological description of X-ray states to one based on physical elements (e.g., accretion disk, ADAF, jet, and corona). Although this work is still incomplete, the fundamental distinctions between the states are becoming clearer. For example, a key development in this regard is the recognition of a persistent radio jet associated with the LH state that switches off when the source returns to the HS state (§4.3.6; Ch. 9). Another example, revealed by gamma-ray observations, is the very different coronal structure that is responsible for the clear-cut distinction between the LH state and the VH state (§4.3.1). Arguably, each X-ray state can be

regarded as a different accretion system that can be used in unique ways to study accretion physics and the properties of accreting BHs.

In the sections below, we review each of the four canonical X-ray states of BHs, including the long-lived quiescent state. We illustrate the uniform X-ray properties of each of the three active states by showing X-ray spectra and power spectra for several BHs and BHCs observed by RXTE. We also examine a possible fifth X-ray state, the intermediate state, as part of our discussion of the VH state. While presenting this overview, we suggest an alternative set of state names that are motivated by the kinds of emergent physical pictures mentioned above. Although the new state names depend critically on multiwavelength results (i.e., radio to gamma-ray), we nevertheless attempt to define them on the basis of X-ray data. Furthermore, based on extensive observations of many sources with RXTE (e.g., see x4.2.2), we abandon luminosity as a criterion for defining the states of BHs (with the exception of the quiescent state).

4.3.3 Notes on X-ray spectral analyses

Many spectral models have been developed to describe one or more of the spectral states of BHs. Most models for the nonthermal continuum components invoke inverse Compton or synchrotron emission, but these mechanisms can be applied with many different assumptions and geometric details. Some models closely constrain the relationship between spectral components (e.g., thermal emission providing seed photons for Comptonization), while others allow the spectral components to vary independently. In presenting this review, we have adopted the following pragmatic and generic strategy. As discussed in x4.2.2, the spectra of BHs are well described by a model consisting of a multi-temperature accretion disk component and a power-law component (which may require an exponential cutoff at high energy). This model provides a robust, first-order description of BH spectra that covers all of the emission states, and we adopt it to help define the states and to compare the luminosities of the thermal and nonthermal components. We also include additional features in the model, such as Fe line emission and a disk reflection component, when the normalization parameter for such a feature is significant at the level of 5%. In the following discussions of each X-ray state, we comment on some physical interpretations and controversies related to the problem of determining the origin of the power-law component.

4.3.4 Quiescent state

A BH spends most of its life in a quiescent state that can be summarized as an extraordinarily faint state ($L_x = 10^{30.5} - 10^{33.5} \text{ erg s}^{-1}$), with a spectrum that is distinctly nonthermal and hard ($\gamma = 1.5 - 2.1$). The first short-period X-ray nova to be detected in quiescence was A 0620-00 ($P_{\text{orb}} = 7.8 \text{ hr}$); its X-ray luminosity was several times $10^{30} \text{ erg s}^{-1}$, which is only 10^{-8} of its outburst luminosity (McCullin et al. 1995; Narayan et al. 1996). The long-period systems, however, are significantly more luminous in quiescence because their mass transfer rates are driven by the nuclear evolution of their secondaries rather than by gravitational radiation (Menou et al. 1999). For example, the X-ray luminosity of V 404 Cyg

($P_{\text{orb}} = 155.3$ hr) is typically $L_x = 10^{33}$ erg s $^{-1}$ (Kong et al. 2002), but can vary by an order of magnitude in one day (Wagner et al. 1994).

It is now possible to make sensitive measurements in the quiescent state using *Chandra* and *XMM-Newton*. The minimum quiescent state luminosities (0.5–10 keV) of five BHs and stringent upper limits on two others have been reported by Garcia et al. (2001) and Narayan et al. (2002). Three additional BHs were observed in quiescence more recently (Sutaria et al. 2002; Hammani et al. 2003; McClintock et al. 2003a). Considering only the five short-period systems ($P_{\text{orb}} < 1$ day; see Narayan et al. 2002) that have been detected, one finds that four of them (XTE J1118+480, GRO J0422+32, GS 2000+25, and A 0620-00) have Eddington-scaled luminosities that are within a whisker of $10^{-8.5}$. GS 1124-68 is more luminous by about an order of magnitude. As Garcia et al. (2001) and Narayan et al. (2002) show, the Eddington-scaled luminosities of several ostensibly similar X-ray novae that contain NS primaries are about 100 times higher, a conclusion that is quite robust. In the context of the advection-dominated accretion flow model, these authors argue that the relative faintness of the BH X-ray novae provides strong evidence that they possess event horizons. For a thorough discussion of their model and several alternative models, see Narayan et al. (2002). Apart from any specific model, it appears quite reasonable to suppose that the established faintness of quiescent BHs is somehow connected with the existence of the event horizon.

The quiescent spectra of BHs from *Chandra* and *XMM-Newton* are well fitted by a single power-law plus interstellar absorption. The best-determined photon spectral indices for two systems with short orbital periods are consistent with the value -2 . Specifically, for A 0620-00 and XTE J1118+480, respectively, one has $\alpha = 2.07 \pm 0.28$; 0.19 (Kong et al. 2002) and $\alpha = 2.02 \pm 0.16$ (McClintock et al. 2003a). The spectra appear to be somewhat harder for three long-period systems: V 404 Cyg, XTE J1550-564, and GRO J1655-40 (Hammani et al. 2003; Kong et al. 2002). However, the evidence for harder spectra is weak because it relies on optically-determined values of the column density, which are systematically lower than the X-ray determined values (Kong et al. 2002). Only V 404 Cyg allows a relatively precise determination of both the column density and the photon index: $N_H = 6.98 \pm 0.76$ and $\alpha = 1.81 \pm 0.14$ (Kong et al. 2002), and this slope is consistent with that of the short-period systems.

A multiwavelength spectrum of XTE J1118+480 in quiescence is shown in Figure 4.7 (McClintock et al. 2003a). This shortest-period BH ($P_{\text{orb}} = 4.1$ hr) is located at $b = 62^\circ$, where the transmission of the ISM is very high (e.g., 70% at 0.3 keV). A very similar multiwavelength spectrum was observed earlier for A 0620-00 (McClintock & Remillard 2000), which implies that the spectrum shown in Figure 4.7 represents the canonical spectrum of a BH radiating at $10^{-8.5} L_{\text{Edd}}$. The spectrum is comprised of two apparently disjoint components: a hard X-ray spectrum with a photon index $\alpha = 2.02 \pm 0.16$, and an optical/UV continuum that resembles a 13,000 K disk blackbody spectrum punctuated by several strong emission lines.

The ADAF/disk model described in §4.1.5 accounts well for the following observations of BHs that have been made in the quiescent state: (1) The hard power-law spectra (Narayan et al. 1996; Narayan et al. 1997; Hammani et al. 1997; Quataert & Narayan 1999; McClintock et al. 2003a); (2) the faintness of BHs relative to NSs

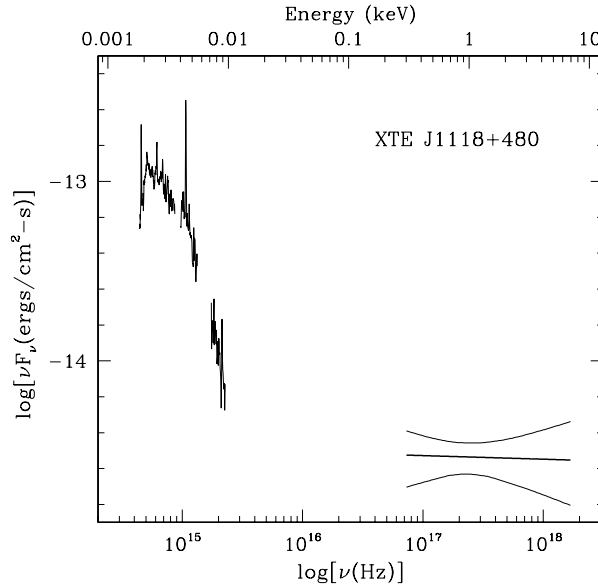


Fig. 4.7. Spectrum of XTE J1118+480 in the quiescent state based on simultaneous, multiwavelength observations. The optical spectrum of the mid-K dwarf secondary has been subtracted. Note the Planckian shape of the optical/UV continuum, which is punctuated by a dominant Mg II 2800Å line and a strong H line on the far left. The best-fit X-ray model is indicated by the heavy, horizontal line; the 90% error box is defined by the flanking curved lines.

(Narayan et al. 1997; Garcia et al. 2001; Narayan et al. 2002; (3) the several-day delay in the optical/UV light curve when X-ray novae go into outburst (Hammerly et al. 1997); and (4) the broadband spectrum shown in Figure 4.7 (McCormick et al. 2003a). Especially significant is the prediction, confirmed by observations, that the accretion disk is truncated at a large inner radius in both the quiescent and LH states (Narayan 1996; Esin et al. 1997; McCormick et al. 2001b; McCormick et al. 2003a).

4.3.5 Thermal dominant (TD) state or high/soft (HS) state

As discussed in x4.1.5, considerations of basic principles of physics predict that accreting BHs should radiate thermal emission from the inner accretion disk (Shakura & Sunyaev 1973). It was therefore readily accepted that the soft X-ray state of BHs represents thermal emission. Confirmations of this picture are largely based on the successful ability to describe the soft X-ray component using the simple multi-temperature accretion disk model (MCD model; x4.1.5). In Figures 4.8 & 4.9 we show the energy spectra and power spectra, respectively, of 10 BHs in the "thermal dominant" (TD) or high/soft (HS) X-ray state as observed by RXTE. The thermal component of the model, where it can be distinguished from the data, is shown as a solid line, and the power-law component is shown as a dashed line. Typically, below about 10 keV the thermal component is dominant. With a few exceptions, the temperature of this component falls in the range 0.7–1.5 keV (Table 4.4).

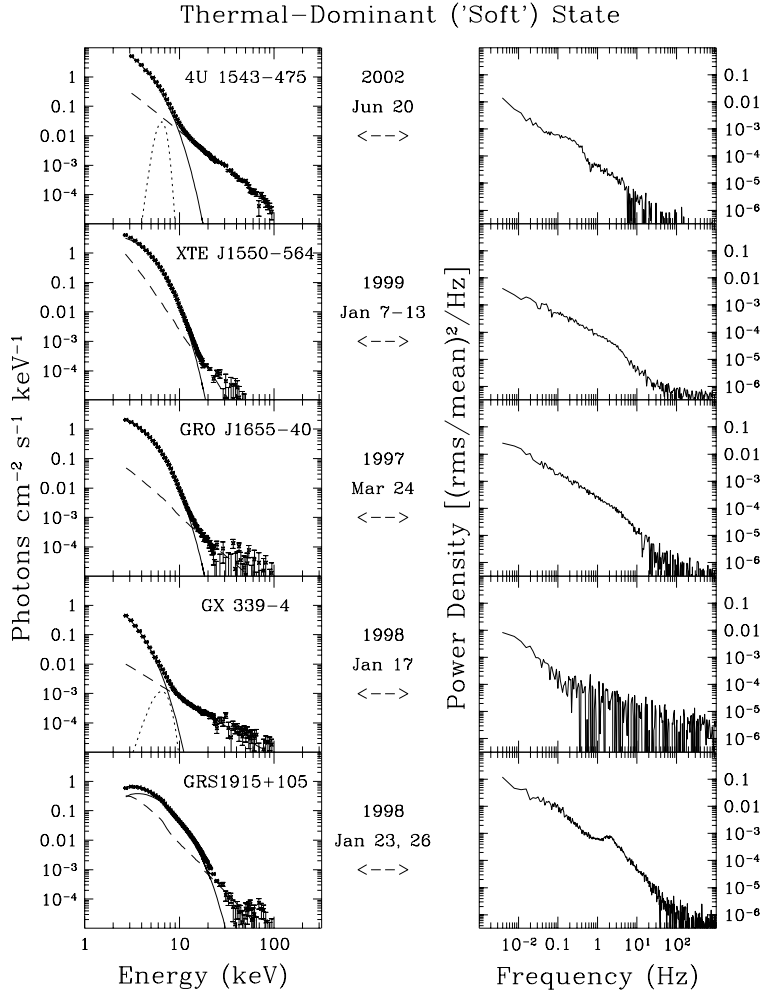


Fig. 4.8. Sample X-ray spectra of BHs in the X-ray state for which the dominant component is thermal emission from the accretion disk. The energy spectra (left) are decomposed into a thermal component, which dominates below 10 keV (solid line), and a faint power-law component (dashed line); GRS 1915+105 is modeled with a cutoff power-law (see text). For two of the BHs, an Fe line component is included in the model (dotted line). The corresponding power spectra are shown in the panels on the right.

The power-law component is steep ($\alpha = 2.1 - 4.8$) and faint. In GRS 1915+105 the power-law falls off even more steeply with an e-folding cutoff energy of 3.5 keV ; similar behavior has been reported for GRO J1655-40 (Sobczak et al. 1999).

In Figure 4.8 we feature data for BHs obtained during pointed observations with RXTE, while data for BHCs are shown in Figure 4.9. The spectra of four of the sources in the figures (4U 1543-47, GX 339-4, XTE J1755-324, and XTE J2012+381) correspond to the maximum luminosities observed during RXTE pointings (i.e., considering all possible states). The power density spectra (PDS) in Figures 4.8 & 4.9

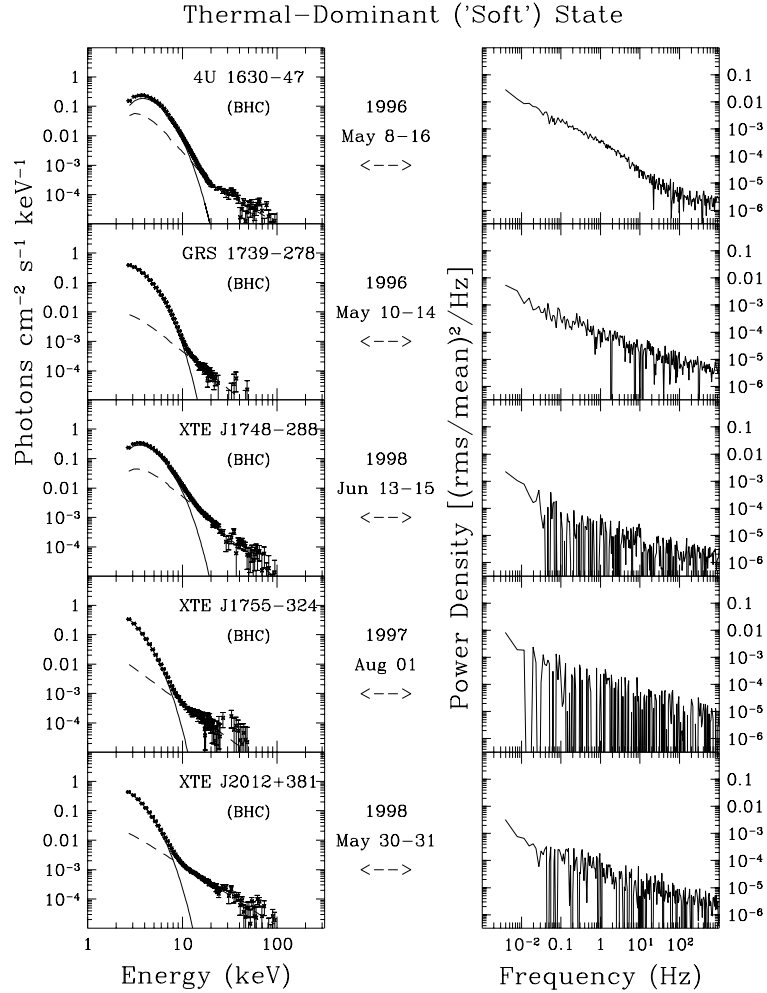


Fig. 4.9. Left panels: Sample X-ray spectra of BHs in the TD X-ray state. In the panels on the left, the energy spectra are shown deconvolved into a thermal component due to the accretion disk (solid line) and a power-law component (dashed line). The corresponding power spectra are shown in the right half of the figure.

show that the variability in the TD state is either weak or the power scales roughly as $\propto f^{-1}$, which is a characteristic of many physical processes including turbulence (Mandelbrot 1999). The total rms power (r) integrated over 0.1–10 Hz in these PDS is in the range $0.01 \leq r \leq 0.06$, which is significantly below that of the LH state. QPOs in the range 0.1–30 Hz are generally not seen in individual TD observations, but large groups of PDS in the TD state have yielded weak QPOs in two cases. A 0.3% (rms) QPO at 27 Hz was seen in a sum of 27 observations ('1997 soft state') of GRO J1655-40 (Remillard et al. 1999), and a similar (0.3%) QPO at 17 Hz was seen in 69 observations of XTE J1550-564 in the soft state during 1998–1999 (MJD 51160–51237; see Homan et al. 2001).

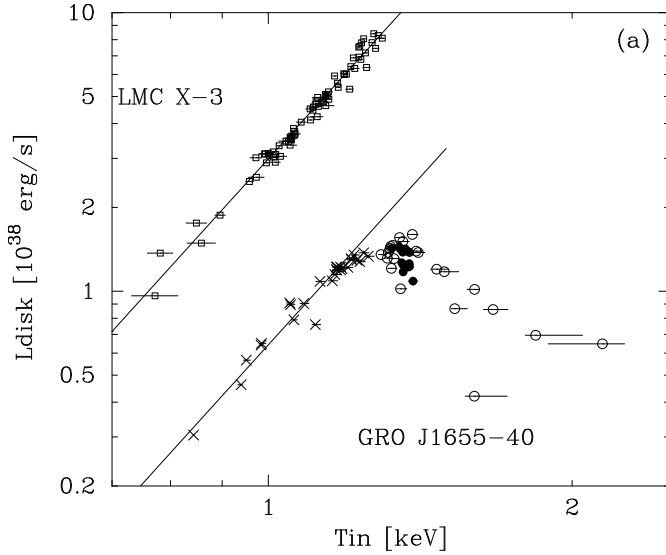


Fig. 4.10. The accretion disk luminosity vs temperature at the inner accretion disk (Kubota et al. 2001). For GRO J1655-40, the symbol type denotes the time periods: early outburst (filled circles), first phase (open circles), and second phase (crosses). The solid lines represent the $L_{\text{disk}} / T_{\text{in}}^4$ relation.

In the following section, we show that a transition to the LH state is followed by the appearance of a hard and dominant power-law spectrum, while the accretion disk, if visible, shows a substantial decrease in temperature. On the other hand, a transition to the VH state (§4.3.7) is marked by a steeper power-law spectrum accompanied by either a normal (~ 1 keV) disk or one that appears hot with a small inner radius. This latter transition is also accompanied by the presence of QPOs that appear when the disk contribution to the total, unabsorbed flux at 2-20 keV falls below the level of 0.75 (Sobczak et al. 2000a). We thus define the TD state as the set of conditions for which the disk flux fraction is above 75% (2-20 keV), the PDS shows no QPOs or very weak features ($\text{rms} < 1\%$), and the power continuum is also weak: $r < 0.06$ integrated over $0.1-10$ Hz.

As further support for a thermal interpretation of the soft X-ray component, many studies have found evidence for disk luminosity variations in which the inner disk radius (which scales as the square root of the MCD normalization constant) appears constant while the luminosity variations depend only on changes in temperature (§4.2.2). This effect is reported in a study of LMC X-3 (Kubota et al. 2001) and is illustrated in Figure 4.10. The measured disk flux and apparent temperature successfully track the relation L / T^4 (solid line) expected for a constant inner disk radius. The figure also shows gross deviations from this relation associated with the VH state of GRO J1655-40, a topic that is addressed below in §4.3.7.

Because of the successes of the simple MCD model, the inner disk radius has been used to provide a type of spectroscopic parallax. In principle, the inner disk radius can be deduced for those sources for which the distance and disk inclination are well constrained from the disk normalization parameter, $(R_{\text{in}} / D)^2 \cos i$, where R_{in} is the

inner disk radius in kilometers, D is the distance to the source in units of 10 kpc, and i is the inclination angle of the system (e.g., Amaud & Domman 2002). However, the MCD model is Newtonian, and the effects of GR and radiative transfer need to be considered. GR predicts a transition from azimuthal to radial accretion flow near R_{ISCO} , which depends only on mass and spin and ranges from $1 \sim 6R_g$ ($\times 4.1.5$). Therefore, for a system with a known distance and inclination, in principle it may be possible to estimate the spin parameter via an X-ray measurement of the inner radius and an optical determination of the mass. In lieu of a fully relativistic MHD model for the accretion disk, one could attempt to correct the MCD model parameters to account for the effects of radiative transfer through the disk atmosphere (Shimura & Takahara 1995) and modifications on the structure and emissivity of the inner disk due to GR (Zhang et al. 1997a). However, the accuracy of these corrections has been challenged (Meroni et al. 2000; Gierlinski et al. 1999), and at present the chief value of the MCD model is in monitoring the temperature and relative flux contribution of the accretion disk.

4.3.6 Low/hard (LH) X-ray state associated with a steady radio jet

As noted earlier (x4.3.1), Cyg X-1 and many transient sources have been observed to undergo transitions to a hard, nonthermal X-ray spectral state. This usually occurs at luminosities below that of the TD state, and the spectrum can be modeled (e.g., $1\{20 \text{ keV}$) as a power-law function with a photon index ~ 1.7 . In some sources, such as Cyg X-1 and GS 1354-64, this low/hard (LH) state is accompanied by a broad enhancement at $20\{100 \text{ keV}$ which is interpreted as re-emission of the power-law component from the surface of the inner accretion disk (Di Salvo et al. 2001). This component is discussed further at the end of this section.

In recent years there have been rapid advances in associating the X-ray LH state with the presence of a compact and quasi-steady radio jet (for a thorough review, see Ch. 9). This relationship, which constitutes one of the foundations of the 'disk : jet' connection, is based on at least three arguments. First, VLB I radio images have shown a spatially-resolved radio jet during episodes of quasi-steady radio and hard X-ray emission from GRS 1915+105 (Dhawan et al. 2000) and Cyg X-1 (Stirling et al. 2001). In both instances the radio spectrum was flat or inverted. Second, more generally (i.e., when VLB I images are not available), X-ray sources that remain in the LH state for prolonged periods (weeks to years) are highly likely to show correlated X-ray and radio intensities and a flat radio spectrum (Fender et al. 1999a; Fender 2001; Corbel et al. 2000; Klein-Wolt et al. 2002; Marti et al. 2002; Corbel et al. 2003). In one of these examples, GX 339-4, (Corbel et al. 2000), the jet interpretation is further supported by the detection of 2% linear radio polarization with a nearly constant position angle. Finally, it is now routine to witness the quenching of the persistent radio emission whenever an X-ray source exits the LH state and returns to the TD state (Fender et al. 1999b; Brockopp et al. 1999; Corbel et al. 2000).

In Figure 4.11, the five BHs shown in the LH state are the same sources shown earlier in the TD state (Figure 4.8). In the following cases, the data have been selected to coincide with specific radio observations: Flat-spectrum radio emission was reported for both XTE J1550-564 on 2000 June 1 during the decay of its second

Low-Hard State Associated with a Steady Radio Jet

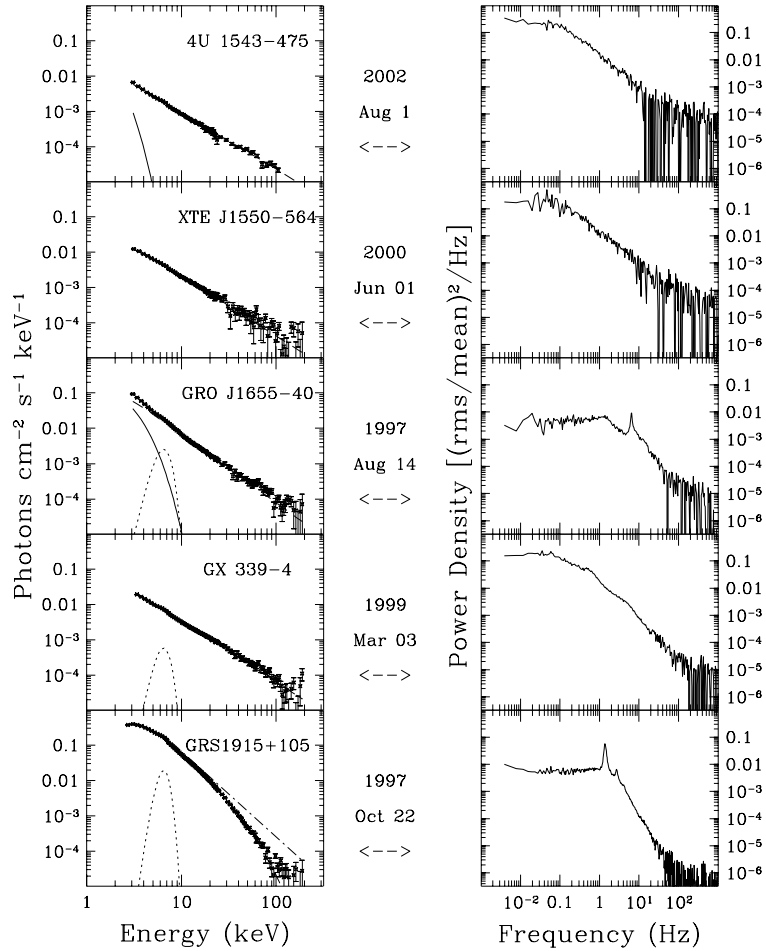


Fig. 4.11. Sample spectra of BHs in the LH state. The energy spectra are characterized by a relatively flat power-law component that dominates the spectrum above 1 keV. A second characteristic of the LH state is the elevated continuum power in the PDS. This state is associated with the presence of a steady type of radio jet (see text). The selected X-ray sources are the same BHs shown in Figure 4.8. The individual spectral components include the power-law (dashed line) and, if detected, the accretion disk (dotted line) and a re-lection component (long dashes).

outburst (Corbel et al. 2001) and for GX 339-4 on 1999 March 3 (Corbel et al. 2000). In addition, both the radio and X-ray emission of GRS 1915+105 are fairly steady on 1997 October 22, which coincides with one of the days in which the core radio image shows the extended structure of a nuclear jet (Dhawan et al. 2000).

A second sample of BHs and BHCs in the LH state is shown in Figure 4.12. The LH state for XTE J1748-288 occurred during decay from the HS state (Revnivtsev et al. 2000c). On the other hand, the data shown for XTE J1118+480 and GS 1354-

64 correspond with outburst maxima; these outbursts never reached the HS state (Revnivtsev et al. 2000a; Frontera et al. 2001b). Associated radio emission for these two sources was reported with jet interpretations by Fender et al. (2001) and Brocksopp et al. (2001), respectively. Finally, GRS 1758+258 and Cyg X-1 spend most of their time in the LH state, and their energy spectra are shown in the bottom two panels of Figure 4.12. These RXTE observations happened to coincide with radio observations that occurred at radio spectrum. In the case of GRS 1758+258, core radio emission (as distinct from the extended radio lobes observed for this source) was reported on 1998 August 3 and 5 by Marti et al. (2002), and a clear detection of Cyg X-1 during 1997 December 12(17 is evident in the public archive of the Greenbank Interferometer available on the NRAO web site.

The physical condition of the accretion disk in the LH state is a subject of great significance in the effort to build a detailed physical model for both the jet and the X-ray source. Observations with ASCA, which provided sensitivity in the range 0.5 to 9 keV, showed that the LH states of both GX 339-4 (Wells et al. 1999) and Cyg X-1 (Takahashi et al. 2001) exhibit power-law spectra with an additional soft X-ray excess that can be modeled as a large and cool (0.1-0.2 keV) accretion disk. The spectral decompositions illustrated in Figure 4.11 provide some evidence for a soft disk component in both GRO J1655+40 and GRS 1915+105, although RXTE is much less sensitive than ASCA to thermal spectra with temperatures well below 1 keV. By far, the best direct measurements of the temperature and inner radius of an accretion disk in the LH state have been made for XTE J1118+480, which has an extraordinarily small interstellar attenuation (e.g., only 30% at 0.3 keV). Based on simultaneous HST, EUVE and Chandra observations made in outburst, it was determined that the inner disk radius and temperature for the MCD model were $> 100 R_g$ and 0.024 keV, respectively (McLintock et al. 2001b). Some what higher temperatures (0.035-0.052 keV) have been inferred from observations using BeppoSAX (Frontera et al. 2003).

While it seems clear that the blackbody radiation appears truncated at a large radius ($100 R_g$) in the LH state, the physical state of the hot material within this large radius is still a matter of debate. Is the disk density truncated at this radius, as envisioned in the ADAF model (e.g., Esin et al. 2001), or is a substantial amount of matter present in a relativistic flow that is entrained by the magnetic field of a jet (e.g., Marko et al. 2001)? Or is the inner disk basically intact and either depleted of energy or veiled in some type of Compton corona? For the latter possibility, the properties of the corona would be strongly constrained by the absence of any normal (1 keV) thermal component in the LH state of XTE J1118+480 (Esin et al. 2001; Frontera et al. 2003).

Guidance in sorting out these options may eventually come from other types of investigations, such as the study of correlated optical/X-ray variability (Malzac et al. 2003). Also promising are spectral analyses that focus on broad Fe emission features (§4.2.3) or the X-ray re-emission component (Done & Nayakshin 2001). These spectral features depend on substantial density in the inner disk, while the Fe line additionally reveals the pattern of Keplerian flow modified by effects due to GR. Systematic studies of these features during different BHB states and transitions could help to determine the physical changes in the inner disk associated with the LH state. The

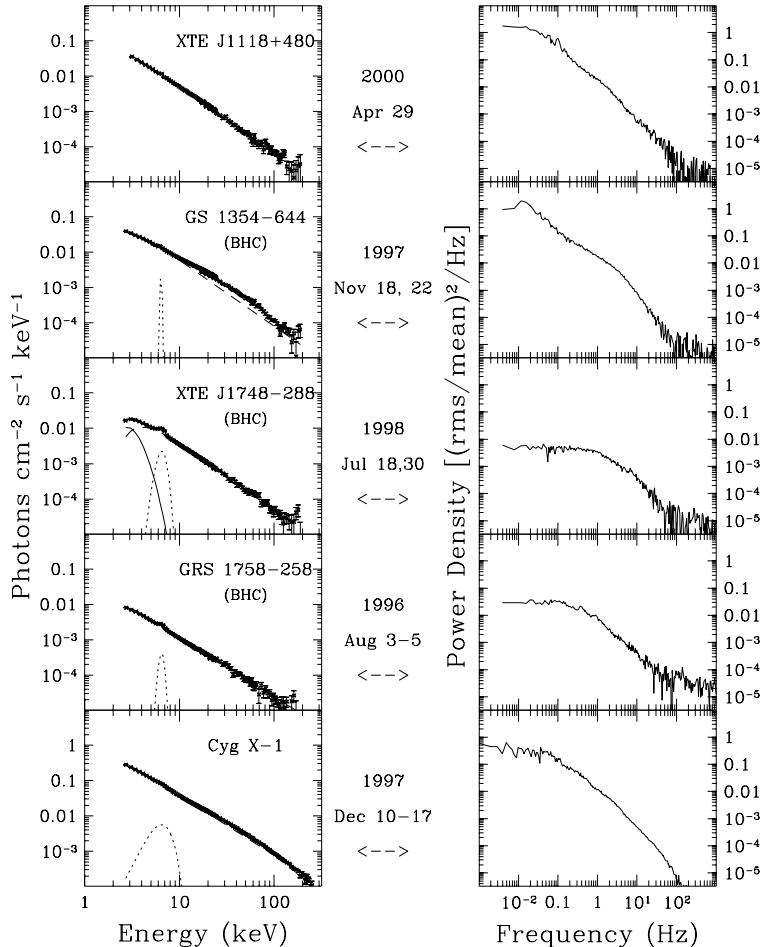


Fig. 4.12. A second sample of BHBs or BHCs seen in the LH state. The observations of XTE J1748{288 occurred during outburst decay, while XTE J1118+480 and GS 1354{64 are seen in the LH state at the peaks of their respective outbursts. GRS 1758{258 and Cyg X {1 spend most of their time in the LH state. There is radio coverage that confirms the presence of a flat radio spectrum for all the sources except XTE J1118+480. The line types denoting the spectral components follow the convention of Figure 4.11.

re-ejection component is most apparent when the disk is observed nearly face-on. One such system viewed at a low inclination angle is Cyg X-1, and a re-ejection analysis has been reported by Done & Zdziarski (1999). They find that the disk is physically truncated, but the transition radius (tens of R_g) is not as far from the event horizon as suggested by the value of R_{in} inferred from the disk spectrum in the LH state (Takahashi et al. 2001).

The origin of the X-ray power law is another aspect of the controversy concerning

the appropriate physical model for the LH state. As noted above, we regard the power-law fit as a general signature of nonthermal radiation; however, the observed spectrum can be produced by several different radiation mechanisms. This is well illustrated in the case of XTE J1118+480, where the X-ray spectrum has been fitted by an ADAF model (Esin et al. 2001), a synchrotron model (Marko et al. 2001) and a thermal Comptonization model (Frontera et al. 2001b). At the present time, we expect valuable inputs from INTEGRAL observations that will characterize the spectral shape and variability of the LH state beyond 100 keV.

Despite the large uncertainties that remain for physical models, it would appear that the association of the LH state with a steady radio jet is an important step forward. And it does remain possible to identify the LH state solely from X-ray spectral and temporal properties, as had been done in the past (TL95). Using Figures 4.11 & 4.12 and Table 4.4, we conclude that the LH state is well characterized by three conditions: the spectrum is dominated ($> 80\%$ at 2(20 keV) by a power-law spectrum, the spectral index is in the range $1.5 < \alpha < 2.1$, and the integrated power continuum (0.1{10 Hz) is strong and typically in the range $0.1 < r < 0.3$.

4.3.7 Steep power-law (SPL) state or very high (VH) state

There are times when BHBs become exceedingly bright ($L_x > 0.2L_{Edd}$), and the X-ray spectrum again displays substantial nonthermal radiation, which may constitute 40{90% of the total flux. In such cases the photon index is typically

2.5, which is steeper than the index (~ 1.7) seen in the LH state. The strength of this steep power-law component also coincides generally with the onset of X-ray quasi-periodic oscillations (QPOs) in the range 0.1{30 Hz. This suite of characteristics was initially seen in only two instances: during a bright outburst of GX 339{4 (Miyamoto & Kato 1991) and near the time of maximum flux in X-ray Nova Muscae 1991 (= GS/GRS 1124{68; Miyamoto et al. 1993). At the time, this very high (VH) state was interpreted as a signature of the highest rate of mass accretion in a BHB system (van der Klis 1995).

As mentioned previously (x4.3.1), the high-energy spectra of several BHCs observed with OSSE on CGRO (40{500 keV) reinforced the distinction between the X-ray LH and VH states, showing that the LH state spectra exhibit a steep cut-off near 100 keV (Grove et al. 1998). On the other hand, the VH state spectra showed no evidence for a high-energy cut-off, while the photon index in the X-ray and gamma-ray bands is the same ($\sim 2.5\{3.0$). The unbroken power-law spectra observed by OSSE for five sources suggested that these BHBs had been observed in the VH state, although most of the observations were not accompanied by X-ray observations that could assess the presence of QPOs.

The monitoring programs of RXTE have shown that the VH state is both more common and more complicated than originally envisioned. Some sources display both X-ray QPOs and a steep power-law component at luminosity levels that are well below the maximum seen even in their TD (HS) state (Remillard et al. 2002b; x4.5). This topic is considered further in x4.3.8 below. In response to these developments, we hereafter refer to this state as the "steep power-law" state, or the SPL state, rather than the VH state. We adopt this new name because the steep power-law

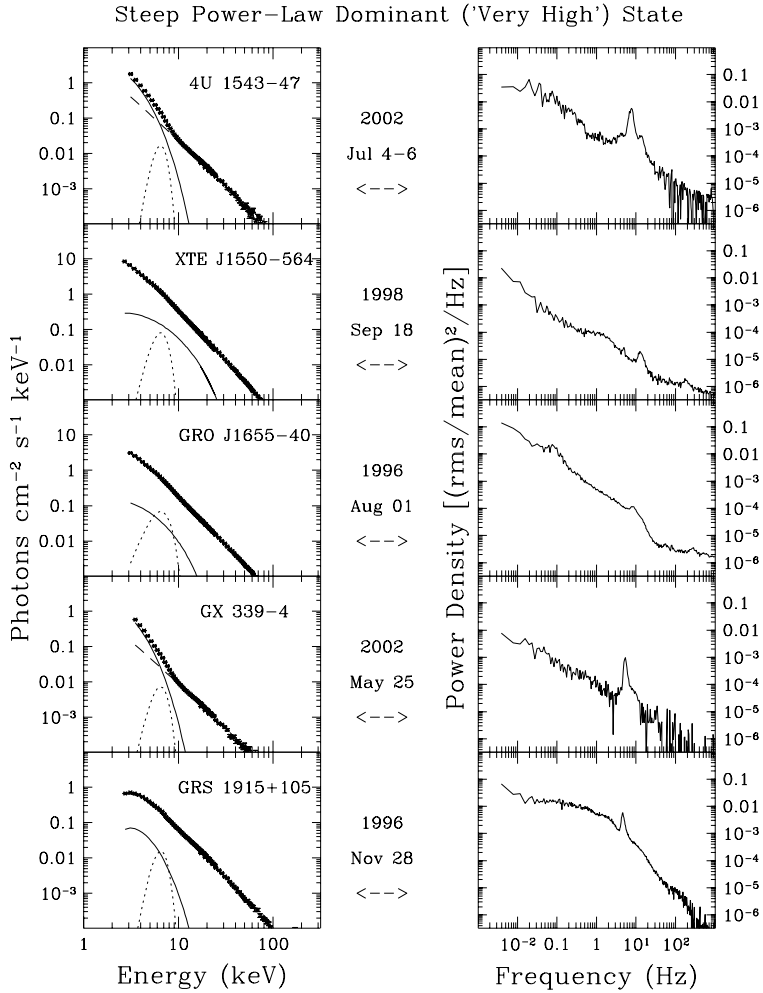


Fig. 4.13. X-ray spectra of BHs in the SPL state, which is characterized by a strong and steep power-law component in the energy spectrum, along with the presence of X-ray QPOs. The dashed and dotted lines follow the convention of earlier figures.

is a fundamental property of this state, whereas a very high luminosity is not. We view the presence of QPOs as a convincing property of the SPL state.

In Figure 4.13 we show examples of the SPL state for the same five BHs considered in Figures 4.8 & 4.11. The photon index of the steep power-law component covers the range $2.4 < \alpha < 3.0$ as shown in Table 4.4, and QPOs are present with central frequencies over the range 5–13 Hz. The spectra of XTE J1550-564 and GRO J1655-40 (Fig. 4.13) correspond to the highest luminosities that have been observed for these sources during pointed observations with RXTE (Sobczak et al. 2000b; Sobczak et al. 1999). Moreover, both observations revealed the presence of high-frequency QPOs, 186 Hz and 300 Hz, respectively (Remillard et al. 2002b).

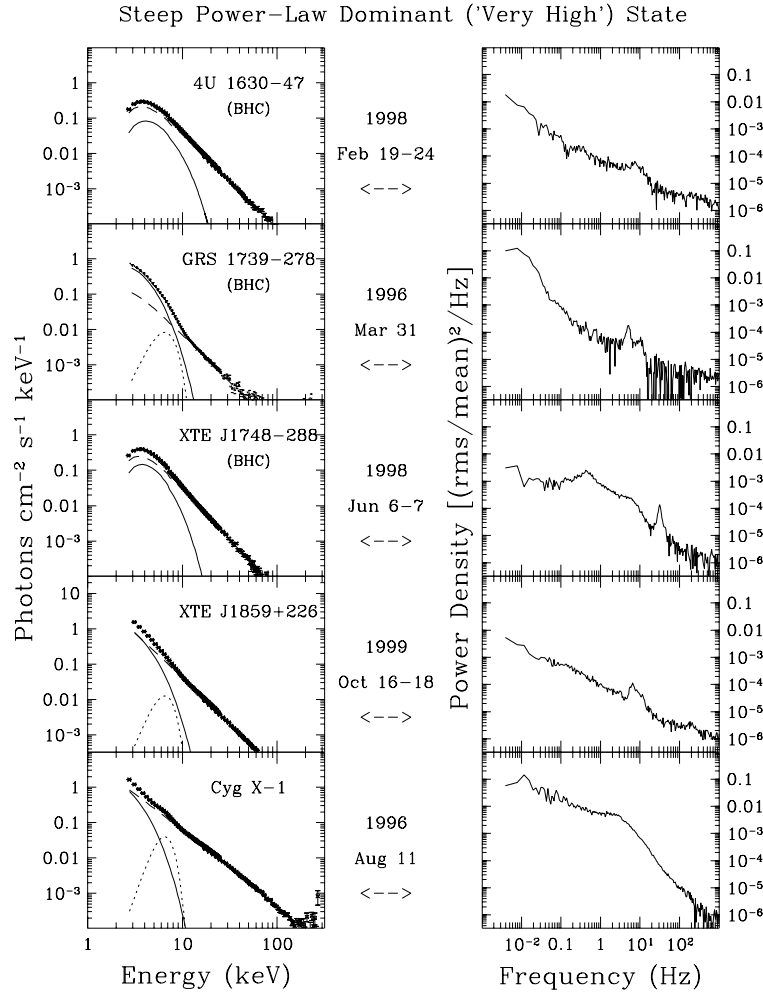


Fig. 4.14. Additional examples of sources in the SPL state. The observations were selected near the times of global or local maxima in the X-ray flux. Cyg X-1 is exceptional for its relatively low luminosity and for the absence of QPOs (see x4.3.9). The dashed and dotted lines follow the convention of earlier figures.

The relationship between the SPL state and high-frequency QPOs will be discussed further in x4.4.3.

In Figure 4.14 we show spectra of the SPL state for three BHCs and two additional BHs. For three of the sources we have selected observations near the time of maximum flux, as seen in RXTE pointed observations. For the two remaining sources we consider local maxima: the 1996 soft-state episode of Cyg X-1 and the second outburst of 4U 1630-47. X-ray QPOs are seen in the top four panels (5-8 Hz in three cases and 31 Hz in the case of XTE J1748-288). The power spectrum of Cyg X-1 contains broad continuum features but no X-ray QPOs, although the energy spectrum indicates that the source is in an SPL-like state.

We can encompass all of these SPL examples with the following criteria (see also Sobczak et al. 2000a). The SPL state is defined first by the presence of a power-law component in the X-ray spectrum with photon index $\gamma > 2.4$. Secondly, either there are X-ray QPOs present (0.1–30 Hz) while the power-law contributes more than 20% of the total (unabsorbed) flux at 2–20 keV, or the power-law contributes more than 50% of the total flux without detections of QPOs.

Transitions between the TD and LH states frequently pass through intervals of the SPL state, and this has led some authors to suggest that the SPL (or VH) state is itself an ‘intermediate state’ that lies between the TD and LH states (Rutledge et al. 1999; Homan et al. 2001). However, this appears to be a radical suggestion that gives inadequate weight to other SPL observations associated with (1) the episodes of highest absolute luminosity in many BHBs, (2) a distinct gamma-ray spectrum, and (3) occurrences of QPOs at both high and low frequency. We therefore conclude that the SPL state is a bona fide state of BHBs, and we note that nothing in our state definitions constrains the order in which state transitions should occur.

The radio properties of the SPL state are an important and complicated topic that calls for the heightened attention of observers. Here we highlight several salient results. The brightest days of GRO J1655+40 during its 1996–1997 outburst occurred in the SPL state (1996 August) when the source appeared radio-quiet (Tomsick et al. 1999). Similarly, Cyg X-1 becomes radio quiet whenever the spectrum switches from the LH state to the SPL state. On the other hand, the SPL state is also associated with the explosive formation of radio jets. For example, the giant X-ray flare in XTE J1550+564 (shown in Fig. 4.2 & 4.13) has been linked to a relativistic mass ejection seen as a superluminal separation of bipolar radio jets (Hannikainen et al. 2001). However, there is a distinct possibility that the X-ray are in the SPL state may have occurred after the moment of ejection, at a time when the radio properties of the core (i.e., the inner disk) are unknown. This conjecture is supported by radio observations of the same source during the 2000 outburst when a radio flare was observed to decay below detectable levels while the source remained in the SPL (VH) state (Corbel et al. 2001). We conclude that the best available evidence suggests that the SPL state is essentially radio quiet, while the instability that causes impulsive jets is somehow associated with the SPL state.

The physical origin of the SPL spectrum remains one of the outstanding problems in high-energy astrophysics. The SPL spectrum extends to 1 MeV in several sources: e.g., Cyg X-1, GRO J1655+40 and GRO J0422+32 (Table 4.2). The spectrum may extend to even higher energies, but present investigations are limited by photon statistics. At stake is our understanding of accretion physics at the extraordinary times of peak BHB luminosity. Equally important is our need to interpret the high-frequency X-ray QPOs associated with the SPL state. As discussed in §4.3, these fast QPOs may provide a constraint on the mass and spin of the accreting BH via an interpretation of the measured frequencies as effects of GR.

Most models for the SPL state invoke inverse Compton scattering as the operant radiation mechanism (see Zdziarski 2000). The broadband nature of the SPL spectrum has motivated proposals that the scattering occurs in a nonthermal corona, which may be a simple slab operating on seed photons from the underlying disk (Gierlinski et al. 1999; Zdziarski et al. 2001). Efforts to define the origin of the

Comptonizing electrons has led to more complicated geometric models with feedback mechanisms, such as are regions that erupt from magnetic instabilities in the accretion disk (Poutanen & Fabian 1999). One early model, which was applied to AGN, invokes a strongly magnetized disk and predicts power-law spectra extending to tens of MeV (Field & Rogers 1993). A recent model, which is based on extensive RXTE observations of GRO J1655-40 and XTE J1550-564, starts from the findings that as the power-law component becomes stronger and steeper, the disk luminosity and radius appear to decrease while maintaining a high temperature (see Figure 4.10). These results can be interpreted as an observational confirmation of strong Comptonization of disk photons in the SP L state (Kubota et al. 2001; Kubota & Makishima 2003).

There are a number of alternative models for the SP L state. For example, bulk motion Comptonization has been proposed in the context of a converging sub-Keplerian flow within $50 R_g$ of the BH. The authors have suggested pair production as a means of extending the photon spectrum beyond the 350 keV limit initially calculated for this model (see Turolla et al. 2002).

As noted above, Comptonization models are hard-pressed to explain the origin of the energetic electrons. As a further difficulty, a viable model must also account for the QPOs in the SP L state. This is important since strong QPOs (see Fig. 4.13 and Fig. 4.14) are common in this state. SP L models and X-ray QPOs are discussed further in §4.4 below.

4.3.8 Intermediate (IM) states

The four states described above capture the behavior observed for most BHs on many occasions. However, other forms of complex behavior are often seen, and these dispel the notion that every BH observation can be classified via these X-ray states. In the following three subsections, we consider the observational results that most directly challenge the four-state framework described above.

The LH state energy spectra displayed in Figures 4.11 & 4.12 show little or no spectral contribution from the accretion disk, while the PDS exhibit a "band-limited" power continuum (i.e., a flat power continuum that breaks to a steeper slope between 0.1 and 10 Hz). Such a band-limited power spectrum is sometimes seen in combination with a stronger contribution from the accretion disk. This condition of a BH has been interpreted as an intermediate (IM) state that lies between the LH and TD states (e.g., Mendez & van der Klis 1997). We agree that the spectra of GRO J1655-40 shown in Figure 4.11 does appear to represent a legitimate example of the IM state in the sense of a transition between the LH and TD states.

However, there are other cases that seem to display a different type of intermediate or hybrid emission state. For example, dozens of observations of XTE J1550-564 yielded energy spectra and QPOs that resemble the SP L state, but the PDS showed band-limited continuum power that is reminiscent of the IM state described above (Homan et al. 2001). In Figure 4.15 we show one example of this behavior for XTE J1550-564 and a very similar example for GRS 1915+105. It is problematic to interpret such observations of XTE J1550-564 as intermediate between the TD and LH states, since the energy spectra and QPOs resemble the SP L state (Sobczak et al. 2000b). It may seem more appropriate to describe the observations of XTE J1550-

564 and GRS 1915+105 in Figure 4.15 as SPL states with band-limited power continua." The significance of the band-limited power continuum is yet to be fully understood. This could suggest an IM state linking the LH and SPL states, a detail further supported by the fact that the disks in the two systems appear cooler and larger in these observations than they do in the respective TD states. However, such speculations may be ill-advised without considerations of sensitive radio measurements. We further note that the presence or absence of band-limited power observed in individual SPL state observations of XTE J1550{564 is closely coupled to the amplitudes and phase lags of the associated QPOs (of types A, B, and C; Remillard et al. 2002a). Finally, while the energy spectra of XTE J1550{564 and GRS 1915+105 in Figure 4.15 are distinctly steep, there is some ambiguity as to whether they are best modeled as a steep power-law or as a flatter power-law with an unusually low cut-off energy (~ 50 keV). In Table 4.4, we show the spectral parameters for the latter model, which is statistically preferred in the case of GRS 1915+105.

We conclude that it is inappropriate to refer to both the observations of XTE J1550{564 (Fig. 4.15) and the very different observations of GRO J1655{40 (Fig. 4.11) as representing a single BHB state, namely, the IM state. On the other hand, state transitions and hybrid emission properties are to be expected and X-ray spectra and PDS should be interpreted as IM states when necessary, while specifying which states can be combined to yield the observed X-ray properties. In summary, we describe the spectra of GRO J1655{40 (Fig. 4.11) as representing primarily an LH state or perhaps an IM state between LH and TD. On the other hand, the spectra and PDS of XTE J1550{564 and GRS 1915+105 considered here appear to show an IM state related to the SPL and LH states. Since transitions between these latter two states are not generally seen, this hybrid combination merits further scrutiny.

4.3.9 X-ray states of Cygnus X-1 and GRS 1915+105

In this section we briefly summarize the efforts to integrate the behavior of two uncommon BHBs within the framework of the TD, LH/radio jet, and SPL states. We first return to the issue of Cyg X-1 and the nature of its transitions to a soft state of high intensity, which is unlike the canonical TD (HS) state. As noted earlier (§4.2.1.1; §4.3.1), contrary to expectations the 1996 soft-state spectrum of Cyg X-1 revealed a power-law spectrum, rather than a TD spectrum (Zhang et al. 1997a; Frontera et al. 2001a; Fig. 4.14). Cyg X-1 has never been seen in the TD state, and the transition from a hard X-ray spectrum to a soft one must be seen as a transition from the LH state to the SPL state (Gierlinski et al. 1999; Zdziarski et al. 2001). However, this SPL-like state is unusual in two respects: the absence of QPOs and the relatively low temperature of the accretion disk (Table 4.4). Less surprising is the low luminosity of the SPL state (Zhang et al. 1997b), since this is also seen in other sources (e.g., XTE J1550{564; Remillard et al. 2002a). Whether the SPL state in Cyg X-1 requires a higher mass accretion rate than the LH state is a matter of controversy (Zhang et al. 1997b; Frontera et al. 2001a).

In the unique case of GRS 1915+105, the wildly varying X-ray light curves indicate an imposing number of instability modes (Belloni et al. 2000). Nevertheless, within this complexity it is often possible to identify the canonical states of a BHB (Muno et al. 1999; Belloni et al. 2000). About half of the observations of GRS 1915+105

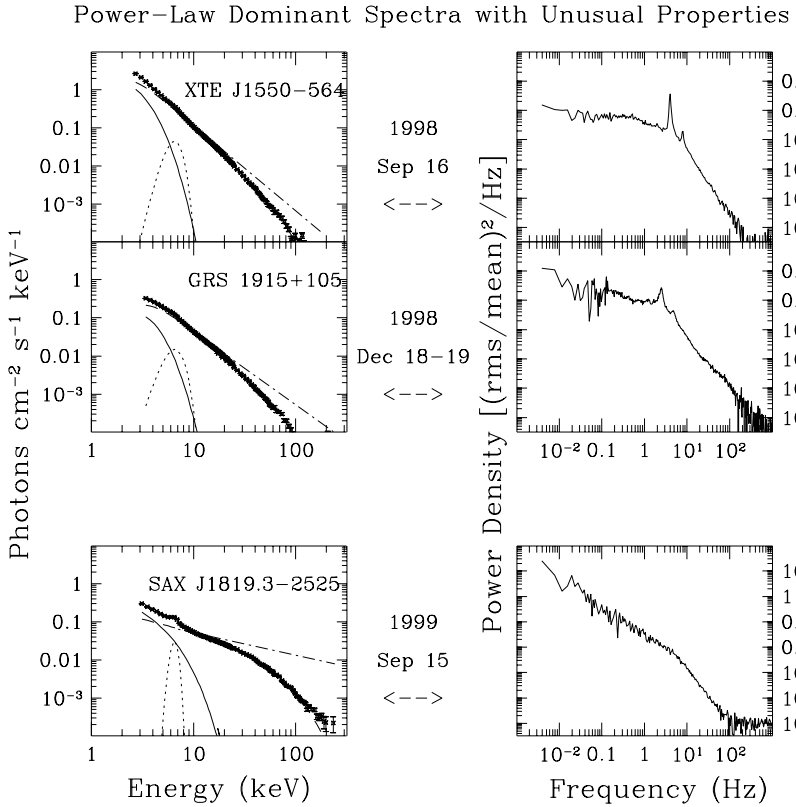


Fig. 4.15. Unusual spectra of three BHs. The observations of XTE J1550-564 and GRS 1915+105 show spectral properties of the SPL state, but the PDS show a band-limited power continuum that is customarily seen as a characteristic of the LH state. In the bottom panel, the ares and rapid fluctuations seen in SAX J1819.3-2525 (V4641 Sgr) do not coincide with any of the typical X-ray states of BH system s.

show fairly steady X-ray flux ($\text{rms} < 15\%$ in 1 s bins at $2\text{--}30\text{ keV}$), and most of these intervals yield spectra and PDS that resemble either the TD or LH states (Muno et al. 1999; Fender 2001; Klein-Wolt et al. 2002). There are, however, some noteworthy anomalies encountered while interpreting the behavior of GRS 1915+105 in terms of the canonical X-ray states. First, the condition of steady radio and X-ray emission extends to $L_x > 10^{38} \text{ erg s}^{-1}$, which is a factor 100 higher than is observed for other BHs in the LH state, compared to the LH states observed in other BHs. Secondly, the X-ray photon index (~ 2.2) is steeper than usual, although it remains flatter than the index seen in (see Table 4.4) in the SPL state (~ 2.6) or the hard tail of the TD state (~ 3.5). In short, the spectral index for GRS 1915+105 in the LH state appears shifted to somewhat high value compared to other BHs.

Overall, the spectral and temporal properties of Cyg X-1 and GRS 1915+105

are best integrated into the standard description of BH X-ray states if we relax the assumptions regarding the relative or absolute luminosity ranges that are appropriate for the various states. As we will see in x4.5.1, the spectral evolution of XTE J1550-564 motivates a similar conclusion, since the luminosity in the SPL state can lie well below that of the TD state. Undoubtedly, there is an overall correlation between spectral states and luminosity intervals in accreting BH B systems. However, the canonical X-ray states are most usefully defined in terms of the properties of the X-ray spectrum and PDS, rather than in terms of luminosity.

4.3.10 Anomalous behavior of SAX J1819.3-2525

Finally, we consider whether BHs exhibit characteristics that fall entirely outside the X-ray states considered thus far. The most challenging case may be the BH SAX J1819.3-2525 (V4641 Sgr; Fig. 4.2). The PCA observations of 1999 September 15.9 show the source in a unique flaring state (Wijnands & van der Klis 2000). The spectral hardness ratio remains remarkably constant throughout the brightest 500 s of this observation, despite the dramatic intensity fluctuations. The spectrum and PDS for this central time interval are shown in Figure 4.15. The spectral analysis yields a hot accretion disk and a broad Fe line, while the photon index is extraordinarily hard: $\Gamma = 0.60 \pm 0.03$ with a cut-off energy of 39 keV (Table 4.4). This source is also distinguished as a new prototype for a "fast X-ray nova" (Wijnands & van der Klis 2000) because it exhibited a 12-Crab flare that appeared and decayed in less than 1 day (Fig. 4.2). The multifrequency spectrum near X-ray maximum has been interpreted in terms of super-Eddington accretion with the binary immersed in an extended envelope (Revnivtsev et al. 2002).

4.4 Fast temporal variations: QPOs and broad power peaks

As shown in the preceding sections on X-ray states (x4.3.6-8), QPOs are prevalent in the SPL state, and they are sometimes seen in the LH state when thermal emission from the disk contributes some flux above 2 keV (e.g., GRO J1655-40 in Fig. 4.11). In this section we briefly consider the QPOs of BHs and BHCs in greater detail. For references on PDS computation, defining QPOs, and QPO characteristics of NS systems, see Chapter 2. We supplement this work by discussing X-ray timing results for BHs. Following van der Klis, we define QPOs as features (usually modeled as a Lorentzian function) in the PDS that have coherence parameter $Q = \omega_c/\omega_b > 2$ (FWHM). Features with significantly lower Q values are regarded as "broad power peaks" and are discussed separately.

4.4.1 Low frequency QPOs and accretion radiation mechanisms

The X-ray PDS of many BH transients display low frequency QPOs (LFQ-PQs) roughly in the range 0.1 to 30 Hz. The significance of these oscillations can be summarized as follows.

(1) LFQ-PQs are almost always seen during the SPL state. They can be exceedingly strong (see Figs. 4.13-4.15), with amplitudes (expressed as a fraction of the mean count rate) as high as $r > 0.15$ for sources such as GRS 1915+105 (Morgan et al. 1997) and XTE J1550-564 (Sobczak et al. 2000a). More generally, they are seen with $0.03 < r < 0.15$ whenever the steep power law contributes more than 20% of the

Table 4.4. SpectralFit Parameters

X-ray name	N_H (10^{22})	T_{DBB} (keV)	N_{DBB} (keV)	F_L	N_{PL}	Fe	N_{Fe}	χ^2	additional details
					F_{WM}				
TD State: Figs. 4.8 & 4.9									
4U 1543-475	0.3	1.01	0.02	7419.	165.	2.57	0.02	5.42	0.21 0.61 .0479 .0031 3.62 feature at 4.4 keV
XTE J1550-564	2.0	1.12	0.03	3289.	74.	4.76	0.04	152.	17. 0.98 sm edge at 9.2 keV
GRO J1655-40	0.9	1.16	0.03	1559.	21.	2.85	0.23	1.01	0.65 2.00 sm edge at 8.0 keV
GX 339-4	0.2	0.71	0.03	2520.	62.	2.02	0.04	0.08	0.01 1.05 .0032 .0003 1.45
GRS 1915+ 105	6.0	2.19	0.04	62.	5.	3.46	0.02	33.4	1.61 3.13 sm edge at 6.7 keV
4U 1630-47	11.0	1.33	0.03	315.	7.	3.75	0.03	17.4	1.40 1.06 break at 20.8 keV to = 1:9
GRS 1739-278	3.0	0.95	0.04	972.	23.	2.65	0.15	.210	0.008 1.11 .0068 .0008 1.42
XTE J1748-288	10.4	1.79	0.02	42.4	2.1	2.60	0.02	14.6	0.4 1.18
XTE J1755-324	0.2	0.75	0.08	1486.	133.	2.40	0.15	0.11	0.04 1.78
XTE J2012+ 381	0.8	0.85	0.05	1176.	56.	2.06	0.04	0.16	0.015 1.32
LH State: Figs. 4.11 & 4.12									
4U 1543-475	0.3	0.38	0.07	645.	1338.	1.67	0.02	0.041	0.001 1.57
XTE J1550-564	2.0	1.70	0.10	0.108	0.021 1.13
GRO J1655-40	0.9	0.77	0.02	228.	37.	1.93	0.02	0.571	0.021 1.00 .0065 .0006 1.83
GX 339-4	0.2	1.75	0.02	0.168	0.028	0.90 .0013 .0003 0.98 plus re ection
GRS 1915+ 105	6.0	2.11	0.02	0.231	0.043	0.91 .0458 .0003 2.39 plus re ection
XTE J1118+ 480	0.01	1.72	0.04	0.267	0.024 1.23
GS 1354-644	0.7	1.48	0.09	0.470	0.032	0.1 .0008 .0002 1.15 plus re ection
XTE J1748-288	10.4	0.48	0.05	5302.	479.	1.88	0.09	0.293	0.065 0.66 .0045 .0003 1.65
GRS 1758-258	1.0	1.67	0.07	0.053	0.010	0.36 .0004 .0001 1.84
Cyg X-1	0.5	1.68	0.07	0.446	0.025	1.44 .0206 .0018 3.40 plus re ection
SPL State: Fig. 4.13 & 4.14									
4U 1543-47	0.3	0.93	0.07	3137.	138.	2.47	0.02	6.85	0.21 0.82 .0347 .0034 1.90
XTE J1550-564	2.0	3.31	0.20	7.76	0.70	2.82	0.05	200.	1.5 1.30 .2136 .0314 2.16 sm edge at 8.5 keV
GRO J1655-40	0.9	2.22	0.20	9.89	1.6	2.65	0.05	75.3	1.1 1.32 .2321 .0157 4.45
GX 339-4	0.2	0.89	0.08	1917.	109.	2.42	0.02	2.34	0.08 0.97 .0178 .0017 1.39
GRS 1915+ 105	6.0	1.19	0.07	115.	31.	2.62	0.08	28.5	0.6 0.90 .0396 .0065 4.13
4U 1630-47	11.0	1.73	0.02	46.0	2.4	2.65	0.02	17.0	0.4 1.10
GRS 1739-278	3.0	1.01	0.06	1116.	38.	2.61	0.03	2.95	0.19 1.53 .0341 .0021 0.94
XTE J1748-288	10.4	1.36	0.02	210.	11.	2.92	0.02	26.2	1.2 0.96
XTE J1859+ 226	0.5	1.03	0.02	1164.	91.	2.55	0.08	14.5	0.31 1.33 .0426 .0060 1.36
Cyg X-1	0.5	0.49	0.03	55708.	2962.	2.68	0.03	7.65	0.37 0.73 .0270 .0016 1.78 breaks to = 1:83 above 12 keV
Unusual Spectra: Fig. 4.15									
XTE J1550-564	2.0	0.74	0.02	6932.	562.	2.24	0.02	23.0	0.87 1.03 .121 .008 1.34 p.l. cuto energy 51.7 keV
GRS 1915+ 105	6.0	0.88	0.03	775.	156.	1.91	0.02	4.51	0.18 1.28 .053 .004 1.45 p.l. cuto energy 50.0 keV
SAX J1819.3-2525	0.3	1.63	0.06	38.	6.	0.59	0.03	0.25	0.02 0.47 .038 .003 1.46 p.l. cuto energy 39.3 keV

flux at 2{20 keV (Sobczak et al. 2000a). LFQPOs have been observed at energies above 60 keV (Tom sick & Kaaret 2001).

(2) In several sources, the LFQPO frequency is correlated with the total disk flux (but not with temperature or inner disk radius; Sobczak et al. 2000a; Munoz et al. 1999; Trudolyubov et al. 1999). This behavior, in combination with the role of the steep power law mentioned directly above, suggests that LFQPOs may provide a vital clue to the mechanism that couples the thermal and SPL components.

(3) LFQPOs can be quasi-stable features that persist for days or weeks. In GRS 1915+105, QPOs at 2.0{4.5 Hz persisted for 6 months during late 1996 and early 1997 (Munoz et al. 2001).

(4) In a general sense, it can be argued that oscillations as distinct and strong as these QPOs (often with $Q > 10$), represent global requirements for an organized emitting region. For example, in the context of models in which thermal radiation originates from MHD instabilities, one cannot accept the common picture of numerous and independent magnetic cells distributed throughout the inner disk.

The effort to tie LFQPOs to the geometry and flow of accreting gas is complicated by the fact that LFQPO frequencies are much lower than the Keplerian frequencies for orbits in the inner accretion disk. For example, for a BH mass of $10 M_{\odot}$, an orbital frequency near 3 Hz coincides with a disk radius near $100 R_g$, while the expected radius for maximum X-ray emission lies in the range $1{10} R_g$ (depending on the value of the BH spin parameter). For the strongest QPOs in GRS 1915+105, the individual oscillations were tracked to determine the origin of frequency drifts and to measure the average 'QPO (folded" oscillation profile (Morgan et al. 1997). The results show a random walk in QPO phase and a nearly sinusoidal waveform. The ramifications of these results for QPO models remain uncertain.

There are now a large number of proposed LFQPO mechanisms in the literature, and we mention only a few examples here. The models are driven by the need to account for both the QPO frequency and also a mechanism to produce the allied power-law spectrum. The models include global disk oscillations (Titarchuk & Osherovich 2000), radial oscillations of accretion structures such as shock fronts (Chakrabarti & Manickam 2000), and oscillations in a transition layer between the disk and a hotter Comptonizing region (Nobili et al. 2000). Another alternative, known as the 'accretion-ejection instability model,' invokes spiral waves in a magnetized disk (Tagger & Pellat 1999) with a transfer of energy out to the radius where material corotates with the spiral wave. This model thereby combines magnetic instabilities with Keplerian motion to explain the observed QPO amplitudes and stability.

Further analyses have revealed phase lags associated with LFQPOs and their harmonics. The analysis technique uses Fourier cross spectra to measure both the phase lags and the coherence parameter (versus frequency) between different X-ray energy bands, e.g., 2{6 vs. 13{30 keV. Unexpectedly, both positive and negative phase lags were found (Wijnands et al. 1999; Cui et al. 2000b; Reig et al. 2000; Munoz et al. 2001), and efforts have been made to classify LFQPOs by phase lag properties. The expansion of LFQPO subtypes may not be widely viewed as a welcome complication. Nevertheless, it has been shown in the case of XTE J1550{564 that the properties of

the phase lags clarify how LFQPO parameters correlate with both the accretion disk and high-frequency QPO parameters (Remillard et al. 2002a).

4.4.2 Broad power peaks and comparisons of BH and NS systems

The study of broad features in the PDS has led recently to important developments. In many NS systems and in some of the thermal states of BHs, the PDS can be decomposed into a set of four or five broad power peaks (Nowak 2000; Belloni et al. 2002), generally with $0.5 < Q < 1.0$. The evolution of these features has been linked to major behavioral changes in Cyg X-1. For example, the disappearance of the third broad power peak occurred just at the time Cyg X-1 left the LH state and its steady radio jet was quenched (Pottschmidt et al. 2003).

Broad PDS features are also involved in renewed efforts to contrast accreting BHs and NS systems via their variability characteristics. It has been proposed that the observed frequency limit for the power continuum provides a means to distinguish accreting BH and NS systems (Sunyaev & Revnivtsev 2000), since only the latter exhibit intensity variations above 500 Hz.

Finally, some studies have used both QPOs and broad power peaks to examine the relationship between low- and high-frequency features and to make comparisons between different NS subclasses and BHs. There have been claims of a unified variability scheme that encompasses all X-ray binary types (Psaltis et al. 1999; Belloni et al. 2002). The bottom line of this scheme is that all of the oscillations must originate in the accretion disk. However, important aspects of this work remain controversial, particularly the handling of BH HFQPOs and their association with the lower kHz QPO observed for NSs (Remillard et al. 2002a).

4.4.3 High-frequency QPOs and general relativity

The topic of high-frequency QPOs (HFQPOs) in BHs (40–450 Hz) continues to evolve in the RXTE era. These transient QPOs have been detected in seven sources (4 BHs and 3 BHCs). HFQPOs have amplitudes that are generally 1–3% of the mean count rate in a given energy band. Remarkably, three sources exhibit pairs of QPOs that have commensurate frequencies in a 3:2 ratio (Remillard et al. 2002b; Remillard et al. 2003b; Table 4.2). As shown in Figure 4.16, GRO J1655-40 and XTE J1550-564 each exhibit a single such pair of frequencies. GRS 1915+105, on the other hand, shows two pairs of HFQPOs; the complete set of four QPO pairs is shown in Figure 4.16. In addition (see references in Tables 4.2 & 4.3), single-component HFQPOs have been observed in 4U 1630-47 (184 Hz), XTE J1859+226 (190 Hz), XTE J1650-500 (250 Hz), and H 1743-322 (240 Hz). Their profiles are similar to the 300 Hz QPO for GRO J1655-40 shown in the top left panel of Figure 4.16. HFQPOs occur in the SP/L state, except for the 67 Hz QPO in GRS 1915+105 (see Fig. 4.16) which appears in the TD state, especially when $L_x > 10^{38}$ erg s⁻¹.

The preponderance of evidence indicates that HFQPOs do not shift freely in frequency in response to luminosity changes, as do the kHz QPOs in NS systems (see Ch. 2). Instead, they appear to exhibit an "X-ray voiceprint". That is, the QPOs occur in harmonics of an unseen fundamental frequency which has a unique value for each BH. For the three cases that show 3:2 frequency pairs, the relationship between the HFQPO frequencies vs. BH mass scales as M_1^{-1} . This relationship is shown in

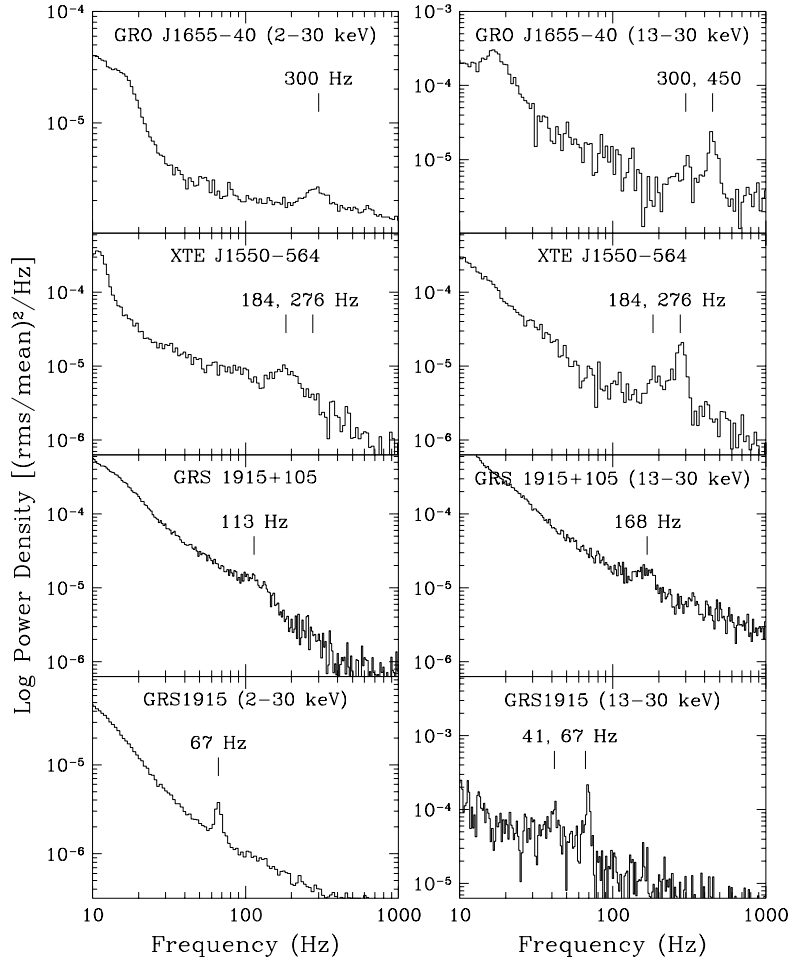


Fig. 4.16. Four pairs of HFQPOs observed in three black hole binary systems. The energy band is 6–30 keV unless otherwise indicated. These usually subtle oscillations are only visible during a fraction of the observations for each source.

Figure 4.17, where we have plotted the frequency of the stronger feature (i.e. $2\omega_0$), since the fundamental is generally not seen. These results offer strong encouragement for seeking interpretations of BH HFQPOs via GR theory, since each type of GR disk oscillation under strong gravity varies as M_1^{-1} , assuming the sampled BHs have similar values of the dimensionless spin parameter (a).

These commensurate frequencies can be seen as strong support for the idea that HFQPOs may represent some type of resonance phenomenon involving oscillations describable by GR, as originally proposed by Abramowicz & Kluźniak (2001). Resonances in some form may be applicable to both BH and NS systems (Abramowicz

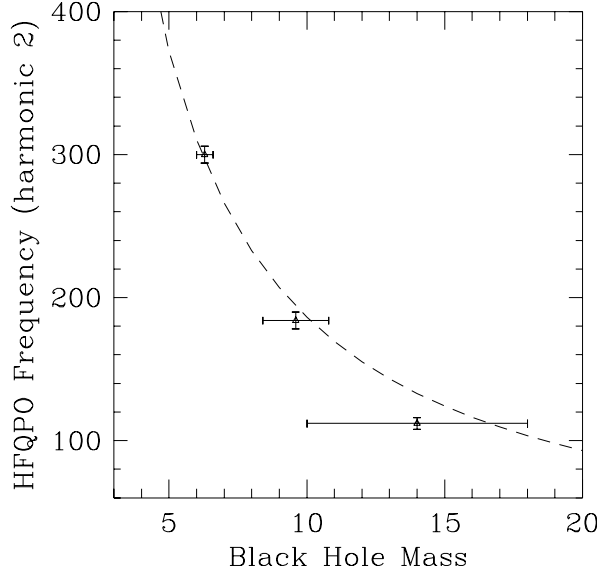


Fig. 4.17. Relationship between HFQPO frequency and BH mass for XTE J1550{564, GRO J1655{40, and GRS 1915+105. These three systems display a pair of HFQPOs with a 3:2 frequency ratio. The frequencies are plotted for the stronger QPO that represents 2₀. The fundamental is generally not seen in the power spectra. The dashed line shows a relation, $\omega_0 = 931M^{-1}$, that fits these data.

et al. 2003). We note that the 3:2 harmonic pattern cannot be attributed to a distorted sine wave with harmonic content because the individual detections (in a given energy band, on a given day) generally appear as a single peak in the PDS, and the presence of a pair of commensurate frequencies is recognized only when the ensemble of results is examined.

Coordinate frequencies and their differences (i.e., beat frequencies) in GR were proposed earlier to explain some of the X-ray QPOs from both NSs and BHs (Stella et al. 1999); however, this work did not treat the commensurate frequencies that are of interest here. In the resonance hypothesis (Abramowicz & Kluźniak 2001), these harmonic frequencies are discussed in terms of accretion blobs following perturbed orbits in the inner accretion disk. Unlike Newtonian gravity, GR predicts independent oscillation frequencies for each spatial coordinate for orbits around a rotating compact object, as seen from the rest frame of a distant observer. At the radii in the accretion disk where X-rays originate, the GR coordinate frequencies were expected to have varying, non-integral ratios. Therefore, the discovery of HFQPOs with commensurate frequencies can be seen to suggest enhanced emissivity at a particular radius where a pair of coordinate frequencies are in some type of resonance. Unlike the azimuthal and polar coordinate frequencies, the radial coordinate frequency reaches a maximum value and then falls to zero as the radius decreases toward R_{ISCO} (Kato 2001; Mervin et al. 2001). This ensures the possibility of commensurate coordinate frequencies somewhere in the inner disk. For example, there is

a wide range in the dimensionless spin parameter, a , where one can find a particular radius that corresponds to a 2:1, 3:1, or 3:2 ratio in the orbital and radial coordinate frequencies. A resonance between the polar and radial coordinate frequencies is also possible. In the resonance scenario, linear perturbations may grow at these radii, ultimately producing X-ray oscillations that represent some combination of the individual resonance frequencies, their sum, or their difference. However, there remain serious uncertainties as to whether such structures could overcome the severe damping forces and emit X-rays with sufficient amplitude and coherence to produce the observed HFQPOs (Markovic & Lamb 1998).

Models for "diskoseismic" oscillations adopt a more global view of the inner disk as a GR resonance cavity (Kato & Fukue 1980; Waggoner 1999). This paradigm has certain attractions for explaining HFQPOs, but integral harmonics are not predicted for the three types of diskoseismic modes derived for adiabatic perturbations in a thin accretion disk. Clearly, there is a need to investigate further the possibility of resonances within the paradigm of diskoseismology.

It has been argued by Strohmayer (2001a) that HFQPO frequencies are sufficiently high that they require substantial BH spin. For example, in the case of GRO 1655{40 the 450 Hz frequency exceeds the maximum orbital frequency (ω) at the ISCO around a Schwarzschild BH (i.e., $a = 0$; $x4.1.5$) of mass $M_1 = 6.3 \times 10^5 M_\odot$ (Greene et al. 2001). If the maximum Keplerian frequency is the highest frequency at which a QPO can be seen, then the results for GRO J1655{40 require a Kerr BH with prograde spin, for example, $a > 0.15$. However, the conclusion that spin is required may not be valid if the QPO represents the sum of two beating frequencies. On the other hand, even higher values of the spin parameter may be required if the QPO represents either resonant coordinate frequencies ($a > 0.3$; Remillard et al. 2002b) or diskoseismic oscillations ($a > 0.9$; Waggoner et al. 2001).

Accurate and sensitive measurements of X-ray HFQPO frequencies may lead to a determination of the GR mechanism that is responsible for these oscillations, and ultimately to secure measurements of the spin parameter a for a number of BHs. These spin measurements would be very valuable in assessing the role of BH rotation in the production of jets (Blandford & Znajek 1977). This is especially true since the three systems with paired frequencies have a history of relativistic mass ejections during some (but not all) of their outbursts.

4.5 Energetics and key variables determining BH B radiation

4.5.1 Division of spectral energy: disk and power-law components

A revealing view of the behavior of a BHB over the course of its entire outburst cycle can be obtained by plotting the flux in the power-law component vs. the flux from the accretion disk. Four such plots are shown in Figure 4.18, where the various plotting symbols identify the emission states described in x4.3. The figure shows the flux diagrams for 3 BHBs, while considering two of the outbursts of XTE J1550{564 (Muno et al. 1999; Remillard et al. 2001; Remillard et al. 2002b). It has been shown that the emerging patterns in these flux diagrams are largely unaffected by the choice of integration limits, e.g., whether the energy measurements

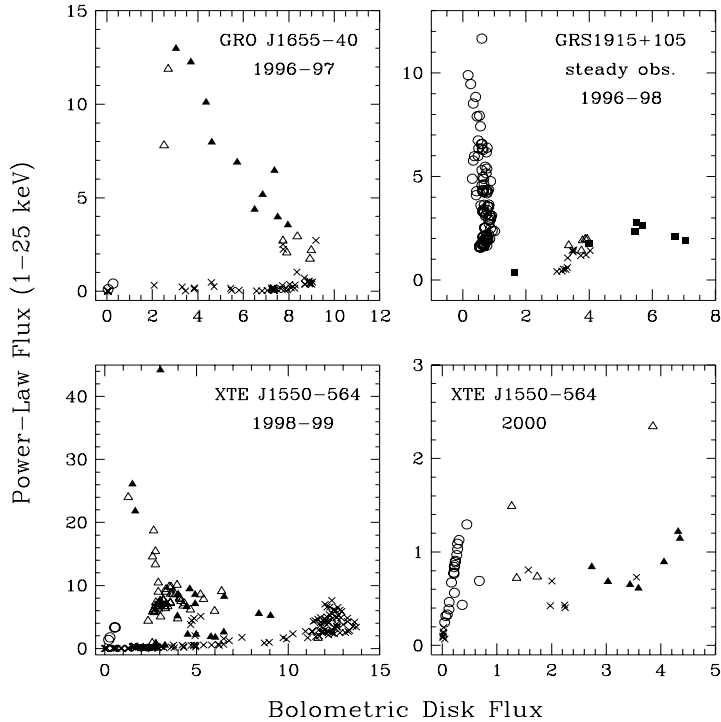


Fig. 4.18. Radiation energy division between the accretion disk and the power-law component. The symbol types denote the X-ray state as TD (x), LH (○), or SPL (△). Furthermore, in the SPL state, an open triangle is used when there is only an LFQPO, while a filled triangle denotes the additional presence of an HFQPO. Finally, the TD-like observations that show 67 Hz QPOs in GRS 1915+105 are shown with a filled square. All fluxes are in units of 10^{-8} erg cm $^{-2}$ s $^{-1}$ and corrected for absorption.

are computed in terms of bolometric flux or the integrated flux within the 2-25 keV PCA bandpass (Remillard et al. 2002a).

The TD points ("x" symbol; Fig. 4.18) for GRO J1655-40 and XTE J1550-564 (1998-99) appear well-organized; they can be described as horizontal tracks in which accretion energy is freely converted to thermal radiation from the accretion disk. These tracks correspond to the standard accretion disk model (Shakura & Sunyaev 1973), and they may also convey moderate Comptonization effects expected from MHD turbulence (e.g., Hawley & Krolik 2001) as these tracks curve upward at high luminosity. The TD points at the highest flux levels correspond to Eddington luminosities of 0.2 for GRO J1655-40, 0.6 for XTE J1550-564 (1998-99), and 0.4 for GRS 1915+105, using the values for mass and distance given in Tables 4.1 & 4.2.

Observations in the LH state (i.e., a dominant power-law component with $1.4 < \alpha < 2.2$) are plotted as circles in Figure 4.18. These points form vertical tracks with only minor flux contributions from the disk. The LH-state points coincide with fairly

steady radio emission for GRS 1915+105 (Muno et al. 2001) and XTE J1550{564 in 2000 (Corbel et al. 2001), as expected for this state.

Observations in the SPL state (defined by a power-law index $\gamma > 2.4$ and by QPOs) are plotted as triangles in Figure 4.18; a solid symbol is used when there is an additional detection of an HFQPO above 100 Hz. The wide diversity in the relative contributions from the disk and power-law components within the SPL state are especially apparent for XTE J1550{564. It is these results, combined with the wide range in the luminosities of the TD and LH tracks shown in Figure 4.18, that have caused us to abandon the luminosity requirements in defining the X-ray states of BHBs (x4.3). Finally, detections of the 67 Hz QPO in GRS 1915+105 are shown as filled squares. They appear to extend the TD branch out to 0.6 L_{Edd} .

4.5.2 Key variables determining BHB radiation

Prior to the RXTE era, it was thought that the X-ray states primarily represent a simple progression in luminosity, and that the emission properties depend only on the accretion rate and the BH mass (e.g., Tanaka & Lewin 1995). The behavioral complexity of sources such as XTE J1550{564 (Fig. 4.18) have challenged this viewpoint (Homan et al. 2001; Remillard et al. 2002b) because it now appears that any of the three active states of accretion may occur at a given luminosity.

Finally, what other parameters must also be considered in the theory of BH accretion? It is clear that BH spin and the angle between this spin axis and the disk axis must also be considered in a complete theory of BH accretion, but these would not help to explain the types of rapid state transitions seen in many systems. As noted in several previous sections, MHD instabilities are widely invoked to explain nonthermal radiation, and magnetic fields are additionally expected to play a leading role in the formation and collimation of jets. It then seems relevant to question whether a parameter of magnetism, such as the ratio of magnetic to gas pressure, must be considered as a dependent variable of accretion physics. The continued development of 3D MHD simulations are expected to be very fruitful in gaining a deeper understanding of the radiation emitted by black hole binaries.

4.6 Concluding remarks

As reviewed in x4.4.3, high frequency QPOs at 40{450 Hz have been observed with RXTE for four BHBs and three BHCs. Furthermore, three of these sources show harmonic (3:2) pairs of frequencies that scale as M_{BH}^{-1} . The models for these QPOs (e.g., orbital resonance and diskoseismic oscillations) invoke strong-field GR effects in the inner accretion disk, and they depend on both the mass and spin of the BH. On the other hand, studies of broadened Fe K α emission lines (x4.2.3), which can also reveal the conditions in the very inner accretion disk, may prove as revealing as timing studies. The line photons that reach a distant observer are gravitationally redshifted and Doppler and transverse(Doppler shifted. Encoded in the line profile are the mass and spin of the BH. The most provocative result has been obtained for the BH C XTE J1650{500 (x4.2.3), where the line profile suggests the presence of an extreme Kerr BH.

Our hunch is that the compact objects we now pursue are the result of the complete gravitational collapse of matter. That is, that these objects possess an event horizon

and are the BHs described by GR. Our challenge is to prove that this paradigm is correct by making clean quantitative measurements of relativistic effects in the strong gravitational fields near these objects. At present, no one can say which future mission can best help us meet this challenge: LISA, MAXIM, Constellation-X, or an X-ray Timing Observatory (XTO). Perhaps all of the approaches will be required. In any case, an XTO with effective area and telemetry ten times that of RXTE and with improved energy resolution, would be a powerful probe of physics near the event horizon. Consider that RXTE with just 1.6 times the effective area of Ginga, broke through to discover kHz QPOs in NSs, a discovery that led quickly to hard constraints on dense matter.

Acknowledgments

We thank Jon Miller, Mike Munro, David Smith, Jean Swank, John Tompkins, and Rudy Vijnhands for their help in assembling the catalogue of candidate BHs presented in Table 4.3, and Keith Maud, George Field, Mike Garcia, Ayako Kubota, Kazuo Makishima, and Mike Revnivtsev for valuable comments. We are indebted to Andy Fabian, Jon Miller, Ramesh Narayan, Jerry Orosz and Andrej Zdziarski for a careful reading of portions of the manuscript and their valuable comments. We are especially grateful to Jeroen Homan and John Tompkins for their detailed comments on a near-final draft of the manuscript. We thank Ann Esin for supplying Figure 4.1, Jon Miller for supplying Figure 4.6, John Tompkins and Emrah Kalemci for the use of unpublished data on 4U 1543-47, John Huchra for advice on the distance to the LMC, and Suresh Kumar for his assistance in typesetting the manuscript. This work was supported in part by NASA under Grants NAG 5-10813 and by the NASA contract to M.I.T. for support of RXTE.

References

Abramowicz, M. A. (1998) in *Theory of Black Hole Accretion Discs*, eds. M. A. Abramowicz, G. Björnsson and J. E. Pringle (Cambridge University Press, Cambridge), 50-60

Abramowicz, M. A., Karas, V. and Kłuzniak, W., et al. (2003), *PA SJ* 55, 467-471

Abramowicz, M. A. and Kłuzniak, W. (2001), *A & A* 374, L19-L20

Agol, E. and Krolík, J.H. (2000), *ApJ* 528, 161-170

Agol, E., Kamionkowski, M., Koopmans, L.V.E. and Landford, R.D. (2002), *ApJ* 576, L131-L135

Amundsen, K. and Domman, B. (2002), XSPEC (An X-ray Spectral Fitting Package), version 11.2x (NASA/GSFC/HEASARC, Greenbelt)

Augusteijn, T., Kuulkers, E. and van der Eijk, M. H. (2001), *ApJ* 375, 447-454

Bagano, F. K., Bautz, M. W., Brandt, W. N., et al. (2001), *Nature* 413, 45-48

Bahcall, J. N. (1986), *ARA & A* 24, 577-611

Ball, L., Estevez, M. J., Campbellbell, D., et al. (1995), *MNRAS* 273, 722-730

Balucinska-Church, M. and Church, M. J. (2000), *MNRAS* 312, L55-L59

Barr, P., White, N. E. and Page, C. G. (1985), *MNRAS* 216, 65P-70P

Barret, D., Grindlay, J. E., Bloser, P. F., et al. (1996a), *IAU Circ.* 6519

Barret, D., McClelland, J. E. and Grindlay, J. E. (1996b), *ApJ* 473, 963-973

Barret, D., O'live, J. F. and Boirin, L. (2000), *ApJ* 533, 329-351

Barret, D., Roques, J. P., Mandrou, P., et al. (1992), *ApJ* 392, L19-L22

Belloni, T., Klein-Wolt, M., Mandez, M., et al. (2000), *A & A* 355, 271-290

Belloni, T., Mandez, M., van der Klis, M., et al. (1999), *ApJ* 519, L159-L163

Belloni, T., Psaltis, D. and van der Klis, M. (2002), *ApJ*, 572, 392{406

Belloni, T., van der Klis, M., Lewin, W.H.G., et al. (1997), *A&A* 322, 857{867

Blandford, R.D. (2002), to appear in *Lighthouses of the Universe*, eds. M.G. Gilfanov, R. Sunyaev, et al. (Springer, Berlin), (astro-ph 0202265)

Blandford, R.D. and Begelman, M.C. (1999), *MNRAS* 303, L1{L5

Blandford, R.D. and Znajek, R.L. (1977), *MNRAS* 179, 433{456

Bolton, C.T. (1972), *Nature* 240, 124{126

Borozdin, K.N., Alekseevich, N.L., Aref'ev, V.A., et al. (1995), *ASTL* 21, 212{216

Borozdin, K.N., Revnivtsev, M.G., Trudolyubov, S.P., et al. (1998), *ASTL* 24, 435{444

Boyd, P.T., Smale, A.P., Homann, J., et al. (2000), *ApJ* 542, L127{L130

Bradt, H., Levine, A.M., Remillard, R.A. and Smith, D.A. (2001), *MmSAI* 73, 256{271

Bradt, H.V.D. and McClintock, J.E. (1983), *ARA&A* 21, 13{66

Branduardi, G., Ives, J.C., Sanford, P.W., et al. (1976), *MNRAS* 175, 47P{56P

Briggs, C., Fender, R.P., Larionov, V., et al. (1999), *MNRAS* 309, 1063{1073

Briggs, C., Fender, R.P., McClough, M., et al. (2002), *MNRAS* 331, 765{775

Briggs, C., Jonker, P.G., Fender, R.P., et al. (2001), *MNRAS* 323, 517{528

Bronfman, L., Cohen, R.S., Alvarez, H., et al. (1988), *ApJ* 324, 248{266

Brown, G.E. and Bethe, H.A. (1994), *ApJ* 423, 659{664

Brown, G.E., Lee, C.-H., Wijers, R.A.M.J. and Bethe, H.A. (2000a), *Phys. Rep.* 333{334, 471{504

Brown, G.E., Lee, C.-H., Wijers, R.A.M., et al. (2000b), *NewA* 5, 191{210

Campana, S., Stella, L., Belloni, T., et al. (2002), *A&A* 384, 163{170

Cannizzo, J.K. (1993), *ApJ* 419, 318{336

Casares, J., Charles, P.A. and Marsh, T.R. (1995), *MNRAS* 277, L45{L50

Casares, J. and Charles, P.A. (1994), *MNRAS* 271, L5{L9

Casares, J., Charles, P.A., Naylors, T. and Pavlenko, E.P. (1993), *MNRAS* 265, 834{852

Chakrabarti, S.K. and Manickam, S.G. (2000), *ApJ* 531, L41{L44

Chaty, S., Mignani, R.P. and Israel, G.L. (2002), *MNRAS* 337, L23{L26

Chen, W., Shrader, C.R. and Livio, M. (1997), *ApJ* 491, 312{338

Churazov, E., Gilfanov, M. and Revnivtsev, M. (2001), *MNRAS* 321, 759

Churazov, E., Gilfanov, M., Sunyaev, R., et al. (1993), *ApJ* 407, 752{757

Coe, M.J., Engel, A.R. and Quenby, J.J. (1976), *Nature* 259, 544{545

Cooke, B.A., Levine, A.M., Lang, F.L., et al. (1984), *ApJ* 285, 258{263

Corbel, S., Fender, R.P., Tzioumis, A.K., et al. (2000), *A&A* 359, 251{268

Corbel, S., Fender, R.P., Tzioumis, A.K., et al. (2002), *Science* 298, 196{199

Corbel, S., Kaastra, J., Jain, R.K., et al. (2001), *ApJ* 554, 43{48

Corbel, S., Nowak, M.A., Fender, R.P., et al. (2003), *A&A*, 400, 1007{1012

Cowley, A.P., Crampton, D. and Hutchings, J.B. (1987), *AJ* 92, 195{199

Cowley, A.P., Crampton, D., Hutchings, J.B., et al. (1983), *ApJ* 272, 118{122

Cowley, A.P., Schmidtko, P.C., Anderson, A.L. and McGrath, T.K. (1995), *PA SP* 107, 145{147

Cowley, A.P., Schmidtko, P.C., Ebisawa, K., et al. (1991), *ApJ* 381, 526{533

Cui, W., Heindl, W.A., Swank, J.H., et al. (1997a), *ApJ* 487, L73{L76

Cui, W., Schulz, N.S., Bagano, F.K., et al. (2001), *ApJ* 548, 394{400

Cui, W., Shrader, C.R., Haswell, C.A. and Hynes, R.I. (2000a), *ApJ* 535, L123{L127

Cui, W., Zhang, S.N. and Chen, W. (2000b), *ApJ* 531, L45{L48

Cui, W., Zhang, S.N., Focke, W. and Swank, J.H. (1997b), *ApJ* 484, 383{393

Dal Fiume, D., Frontera, F., Orlanini, M., et al. (1999), *IAU Circ.* 7291

Davies, R.D., Walsh, D. and Brown, I.W.A., et al. (1976), *Nature* 261, 476{478

Dhawan, V., M irabel, I.F. and Rodriguez, L.F. (2000), *ApJ* 543, 373{385

Dieters, S.W., Belloni, T., Kuulkers, E., et al. (2000), *ApJ* 538, 307{314

Dimatteo, T., Celotti, A. and Fabian, A.C. (1999), *MNRAS* 304, 809{820

Di Salvo, T., Done, C., Zyczyk, P.T., et al. (2001), *ApJ* 547, 1024{1033

Done, C. and Nayakshin, S. (2001), *MNRAS* 328, 616{622

Done, C., M ulchaey, J.S., M ushotzky, R.F. and Amaud, K.A. (1992), *ApJ* 395, 275{288

Done, C. and Zyczyk, P.T. (1999), *MNRAS* 305, 457{468

Dove, J.B., W ilms, J. and Begelman, M.C. (1997a), *ApJ* 487, 747{758

Dove, J.B., W ilms, J., Maisack, M. and Begelman, M.C. (1997b), *ApJ* 487, 759{768

Dubus, G., Ham eury, J.-M. and Lasota, J.-P. (2001), *A&A* 373, 251{271

Ebisawa, K., Makino, F., Mitsuda, K., et al. (1993), *ApJ* 403, 684{689

Ebisawa, K., Mitsuda, K. and Inoue, H. (1989), *PA SJ* 41, 519{530

Ebisawa, K., Mitsuda, K. and Tomoyuki, H. (1991), *ApJ* 367, 213{220

Ebisawa, K., Ogawa, M., Aoki, T., et al. (1994), *PA SJ* 46, 375{394

Ebisawa, K., Page, C.G., Pounds, K.A., et al. (1975), *Nature* 257, 656{657

Esin, A.A., McClymont, J.E. and Narayan, R. (1997), *ApJ* 489, 865{889

Esin, A.A., McClymont, J.E., Drake, J.J., et al. (2001), *ApJ* 555, 483{488

Esin, A.A., Narayan, R., Cui, W., et al. (1998), *ApJ* 505, 854{868

Fabbiano, G., Zezas, A. and Murray, S.S. (2001), *ApJ* 554, 1035{1043

Fabian, A.C., Iwasawa, K., Reynolds, C.S. and Young, A.J. (2000), *PA SP* 112, 1145{1161

Fabian, A.C., Rees, M.J., Stella, L. and White, N.E. (1989), *MNRAS* 238, 729{736

Falcke, H. and Biermann, P.L. (1995), *A&A* 293, 665{682

Fender, R.P. (2001), *MNRAS*, 322, 31{42

Fender, R., Corbel, S., Tzioumis, T., et al. (1999a), *ApJ* 519, L165{L168

Fender, R.P., Garrington, S.T., McCray, D.J., et al. (1999b), *MNRAS* 304, 865{876

Fender, R.P., Hjellming, R.M., Tibanus, R.P.J., et al. (2001), *MNRAS* 322, L23{L27

Feng, Y.X., Zhang, S.N., Sun, X., et al. (2001), *ApJ* 553, 394{398

Field, G.B. and Rogers, R.D. (1993), *ApJ* 403, 94{109

Filippenko, A.V., Matheson, T. and Ho, L.C. (1995a), *ApJ* 455, 614{622

Filippenko, A.V. and Chornock, R. (2001), *IAU Circ.* 7644

Filippenko, A.V., Leonard, D.C., Matheson, T., et al. (1999), *PA SP* 111, 969{979

Filippenko, A.V., Matheson, T. and Barth, A.J. (1995b), *ApJ* 455, L139{L142

Filippenko, A.V., Matheson, T., Leonard, D.C., et al. (1997), *PA SP* 109, 461{467

Freedman, W.L., Madore, B.F., Gibson, B.K., et al. (2001), *ApJ* 553, 47{72

Frontera, F., Amati, L., Zdziarski, A.A., et al. (2003), *ApJ* 592, 1110-1118

Frontera, F., Palazzi, E., Zdziarski, A.A., et al. (2001a), *ApJ* 546, 1027{1037

Frontera, F., Zdziarski, A.A., Amati, L., et al. (2001b), *ApJ* 561, 1006{1015

Fryer, C. and Kalogera, V. (2001), *ApJ* 554, 548{560

Garcia, M.R., McClymont, J.E., Narayan, R., et al. (2001), *ApJ* 553, L47{L50

Gelino, D.M., Harrison, T.E. and McDonald, B.J. (2001a), *AJ* 122, 971{978

Gelino, D.M., Harrison, T.E. and Orosz, J.A. (2001b), *AJ* 122, 2668{2678

George, I.M. and Fabian, A.C. (1991), *MNRAS* 249, 352{367

Gierlinski, M., Maciolek, Niedzwiecki, A. and Ebisawa, K. (2001), *MNRAS* 325, 1253{1265

Gierlinski, M., Zdziarski, A.A., Poutanen, J., et al. (1999), *MNRAS* 309, 496{512

Gies, D.R. and Bolton, C.T. (1982), *ApJ* 260, 240{248

Goldoni, P., Vargas, M., Goldwurm, A., et al. (1999), *ApJ* 511, 847{851

Greene, J., Bailyn, C.D. and Orosz, J.A. (2001), *ApJ* 554, 1290{1297

Greiner, J., Cuby, J.G. and McCaughrean, M.J. (2001a), *Nature* 414, 522{525

Greiner, J., Cuby, J.G., McCaughrean, M.J., et al. (2001b), *A&A* 373, L37{L40

Greiner, J., Dennerl, K. and Predehl, P. (1996), *A&A* 314, L21{L24

Grout, P., Tingay, S., Udralski, A. and Miller, J. (2001), *IAU Circ.* 7708

Grove, J.E., Johnson, W.N., Kroeger, R.A., et al. (1998), *ApJ* 500, 899{908

Gursky, H., Bradt, H., Doxsey, R., et al. (1978), *ApJ* 223, 973{978

Haaardt, F. and Maraschi, L. (1991), *ApJ* 380, L51{L54

Hameury, J.-M., Barret, D., Lasota, J.-P., et al. (2003), *A&A* 399, 631{637

Hameury, J.-M., Lasota, J.-P., McClymont, J.E. and Narayan, R. (1997), *ApJ* 489, 234{243

Han, X. and Hjellming, R.M. (1992), *ApJ* 400, 304{314

Hannikainen, D., Campbellbell, W., Unstead, R., et al. (2001), *ApSSS* 276, 45{48

Hannikainen, D.C., Unstead, R.W., Campbellbell, W., et al. (2000), *ApJ* 540, 521{534

Haraftis, E.T., Horne, K. and Filippenko, A.V. (1996), *PA SP* 108, 762{771

Hawley, J.F. and Krolk, J.H. (2001), *ApJ* 548, 348{367

Hjellming, R.M. and Rupen, M.P. (1995), *Nature* 375, 464{468

Hjellming, R.M., Calovini, T.A. and Han, X.H. (1988), *ApJ* 335, L75{L78

Hjellming, R.M., Rupen, M.P. and Mioduszewski, A.J. (1998a), *IAU Circ.* 6924

Hjellming, R.M., Rupen, M.P. and Mioduszewski, A.J. (1998b), *IAU Circ.* 6934

Hjellming, R.M., Rupen, M.P., Unstead, R.W., et al. (2000), *ApJ* 544, 977{992

Hjellming, R.M., Rupen, M.P., Mioduszewski, A.J., et al. (1999), *ApJ* 514, 383{387

Homan, J., Klein-Wolt, M., Rossi, S., et al. (2003a), *ApJ* 586, 1262{1267

Homan, J., Miller, J.M., Wijnands, R., et al. (2003b), *ATEL* 162

Homan, J., Wijnands, R., van der Klis, M., et al. (2001), *ApJS* 132, 377{402

Humphrey, P.J., Fabbiano, G., Elvis, M., et al. (2003), *MNRAS*, in press (astro-ph/0305345)

Hutchings, J.B., Crompton, D., Cowley, A.P., et al. (1987), *AJ* 94, 340{344

Hynes, R.I., Roche, P., Charles, P.A. and Coe, M.J. (1999), *MNRAS* 305, L49{L53

Hynes, R.I., Steeghs, D., Casares, J., et al. (2003), *ApJ* 583, L95{L98

Igumenshchev, I.V. and Abramowicz, M.A. (1999), *MNRAS* 303, 309{320

in't Zand, J.J.M., Markwardt, C.B., Bazzano, A., et al. (2002a), *A&A* 390, 597{609

in't Zand, J.J.M., Miller, J.M., Oosterbroek, T. and Parmar, A.N. (2002b), *A&A* 394, 553{560

Israelian, G., Rebolo, R., Basri, G. (1999), *Nature* 401, 142{144

Jones, C., Forman, W., Tananbaum, H. and Turner, M.J.L. (1976), *ApJ* 210, L9{L11

Kalemci, E., Tomsick, J.A., Rothschild, R.E., et al. (2002) *ApJ* 586, 419{426

Kalogera, V. and Baym, G. (1996), *ApJ* 470, L61{L64

Kaluzienski, L.J., Holt, S.S., Boldt, E.A., et al. (1975), *ApJ* 201, L121{L124

Kato, S. (2001), *PA SJ* 53, 1{24

Kato, S. and Fukue, J. (1980), *PA SJ* 32, 377{388

Kato, S., Fukue, J. and Mineshige, S. (1998), *Black Hole Accretion Disks* (Kyoto University Press, Japan)

Kawaguchi, T., Shimura, T. and Mineshige, S. (2000), *NewAR* 44, 443{445

Kennea, J.A. and Skinner, G.K. (1996), *PA SJ* 48, L117{L117

King, A.R., Davies, M.B., Ward, M.J., et al. (2001), *ApJ* 552, L109{L112

Kitamoto, S., Tsubomi, H., Pedersen, H., et al. (1990), *ApJ* 361, 590{595

Klein-Wolt, M., Fender, R.P., Pooley, G.G., et al. (2002), *MNRAS* 331, 745{764

Kong, A.K.H., Charles, P.A., Kuulkers, E. and Kitamoto, S. (2002), *MNRAS* 329, 588{596

Kong, A.K.H., McClelland, J.E., Garcia, M.R., et al. (2002), *ApJ* 570, 277{286

Kotani, T., Kawai, N., Nagase, F., et al. (2000), *ApJ* 543, L133{L136

Kubota, A. and Makishima, K. 2003, *ApJ*, submitted

Kubota, A., Makishima, K. and Ebisawa, K. (2001), *ApJ* 560, L147{L150

Kuulkers, E., Fender, R.P., Spencer, R.E., et al. (1999), *MNRAS* 306, 919{925

Kuulkers, E., Wijnands, R., Belloni, T., et al. (1998), *ApJ* 494, 753{758

Laor, A. (1991), *ApJ* 376, 90{94

Lasota, J.-P. (2001), *NewAR* 45, 449{508

Levine, A.M., Bradt, H., Cui, W., et al. (1996), *ApJ* 469, 33{36

Ling, J.C., Mahoney, W.A., Heaton, Wm A. and Jacobson, A.S. (1987), *ApJ* 321, L117{L122

Ling, J.C., Heaton, Wm A., Wallin, P., et al. (2000), *ApJS* 127, 79{124

Liu, B.F., Mineshige, S. and Shibata, K. (2002), *ApJ* 572, L173{L176

Liu, Q.Z., van Paradijs, J. and van den Heuvel, E.P.J. (2001), *A&A* 368, 1021{1054

Liu, Q.Z., van Paradijs, J. and van den Heuvel, E.P.J. (2000), *A&A* 347, 25{49

Loewenstein, M., Moshotsky, R.F., Angelini, L., et al. (2001), *ApJ* 555, L21{L24

Lowes, P., in't Zand, J.J.M., Heise, J., et al. (2002), *IAU Circ.* 7843

Lynden-Bell, D. and Pringle, J.E. (1974), *MNRAS* 168, 603{637

Makishima, K., Kubota, A., Mizuno, T., et al. (2000), *ApJ* 535, 632{643

Makishima, K., Maejima, Y., Mitsuhashi, K., et al. (1986), *ApJ* 308, 635{643

Malzac, J., Belloni, T., Spruit, H.C. and Kanbach, G. (2003), *A&A*, in press, (astro-ph/0306256)

Mandelbrot, B.B. (1999), *Multifractals and 1/f Noise: Wild Self-Affinity in Physics* (Springer-Verlag: Heidelberg)

Marion, B., Thorstensen, J.R. and Bowyer, S. (1978), *ApJ* 221, 907{911

Markert, T.H., Canizares, C.R., Clark, G.W., et al. (1973), *ApJ* 184, L67{L70

Markoff, S., Falcke, H. and Fender, R. (2001), *A&A* 372, L25{L28

Markovic, D. and Lamb, F.K. (1998), *ApJ* 507, 316{326

Markwardt, C. (2001), *ApSS* 276, 209{212

Markwardt, C.B. and Swank, J.H. (2003), *IAU Circ.* 8056

Marsh, T.R., Robinson, E.J. and Wood, J.H. (1994), *MNRAS* 266, 137{154

Marti, J., Mirel, I.F., Chaty, S. and Rodriguez, L.F. (2000), *A&A* 363, 184{187

Marti, J., Mirel, I.F., Duc, P.-A. and Rodriguez, L.F. (1997), *A&A* 323, 158{162

Marti, J., Mirel, I.F., Rodriguez, L.F. and Smith, I.A. (2002), *A&A* 386, 571{575

Martocchia, A., Matt, G., Karas, G., et al. (2002), *A&A* 387, 215{221

Matt, G., Perola, G.C. and Piro, L. (1991), *A & A* 247, 25{34

Mendez, M. and van der Klis, M. (1997), *ApJ* 479, 926{932

McCormick, J.E., Garcia, M.R., Caldwell, N., et al. (2001a), *ApJ* 551, L147{L150

McCormick, J.E., Haswell, C.A., Garcia, M.R., et al. (2001b), *ApJ* 555, 477{482

McCormick, J.E., Home, K. and Remillard, R.A. (1995), *ApJ* 442, 358{365

McCormick, J.E., Narayan, R., Garcia, M.R., et al. (2003a), *ApJ*, in press (astro-ph/0304535)

McCormick, J.E. and Remillard, R.A. (1986), *ApJ* 308, 110{122

McCormick, J.E. and Remillard, R.A. (2000), *ApJ* 531, 956{962

McConnell, M.L., Zdziarski, A.A., Bennett, K., et al. (2002), *ApJ* 572, 984{995

McKinney, J.C. and Gammie, C.F. (2002), *ApJ* 573, 728{737

Menou, K., Esin, A.A., Narayan, R., et al. (1999), *ApJ* 520, 276{291

Mendez, M. and van der Klis, M. (1997), *ApJ* 479, 926{932

Merloni, A. and Fabian, A.C. (2001a), *MNRAS* 321, 549{552

Merloni, A. and Fabian, A.C. (2001b), *MNRAS* 328, 958{968

Merloni, A. and Fabian, A.C. (2002), *MNRAS* 332, 165{175

Merloni, A., Fabian, A.C. and Ross, R.R. (2000), *MNRAS* 313, 193{197

Merloni, A., Vietri, M., Stella, L. and Bini, D. (2001), *MNRAS* 304, 155{159

Meyer, F., Liu, B.F. and Meyer-Hofmeister, E. (2000), *A & A* 361, 175{188

Miller, J.M., Fabbiano, G., Miller, M.C., and Fabian, A.C. (2003a), *ApJ* 585, L37{L40

Miller, J.M., Fabian, A.C., 't Zand, J.J.M., et al. (2002a), *ApJ* 577, L15{L18

Miller, J.M., Fabian, A.C., Wijnands, R., et al. (2002b), *ApJ* 570, L69{L73

Miller, J.M., Fabian, A.C., Wijnands, R., et al. (2002c), *ApJ* 578, 348{356

Miller, J.M., Fox, D.W., D'Imatteo, T., et al. (2001), *ApJ* 546, 1055{1067

Miller, J.M., Wijnands, R., Rodriguez-Pascual, P.M., et al. (2002d), *ApJ* 566, 358{364

Miller, J.M., Zezas, A., Fabbiano, G. and Schweizer, F. (2003b), *ApJ*, submitted (astro-ph/0302535)

Mirabel, I.F. and Rodriguez, L.F. (1994), *Nature* 371, 46{48

Mirabel, I.F. and Rodriguez, L.F. (1999), *ARA & A* 37, 409{443

Mirabel, I.F. and Rodriguez, L.F. (2003), *Science* 300, 1119{1120

Mirabel, I.F., Rodriguez, L.F. and Cordier, B. (1993), *IAU Circ.* 5876

Mitsuda, K., Inoue, H., Koyama, K., et al. (1984), *PA SJ* 36, 741{759

Miyamoto, S., Iga, S., Kitamoto, S. and Kamado, Y. (1993), *ApJ* 403, L39{L42

Miyamoto, S. and Kitamoto, S. (1991), *ApJ* 374, 741{743

Morgan, E.H., Remillard, R.A. and Greiner, J. (1997), *ApJ* 482, 993{1010

Motch, C., Guillout, P., Haberl, F., et al. (1998), *A & A* 32, 341{359

Muno, M.P., Morgan, E.H. and Remillard, R.A. (1999), *ApJ* 527, 321{340

Muno, M.P., Morgan, E.H., Remillard, R.A., et al. (2001), *ApJ*, 556, 515{532

Murdin, P., Griffiths, R.E., Pounds, K.A., et al. (1977), *MNRAS* 178, 27P{32P

Narayan, R. (1996), *ApJ* 462, 136{141

Narayan, R. (2002), to appear in *Lighthouses of the Universe*, eds. M. Gilfanov, R. Sunyaev, et al. (Springer, Berlin)

Narayan, R., Garcia, M.R. and McCormick, J.E. (1997), *ApJ* 478, L79{L82

Narayan, R., Garcia, M.R. and McCormick, J.E. (2002), in *Proc. Ninth Marcel Grossmann Meeting*, eds. V.G. Gurzadyan et al. (World Scientific, Singapore), 405{425

Narayan, R. and Inoue, Y. (1994), *ApJ* 428, L13{L16

Narayan, R. and Inoue, Y. (1995), *ApJ* 444, 231{243

Narayan, R., Igumenshchev, I.V. and Abramowicz, M.A. (2000), *ApJ* 539, 798{808

Narayan, R., McCormick, J.E. and Yi, I. (1996), *ApJ* 457, 821{833

Nelemans, G. and van den Heuvel, E.P.J. (2001), *A & A* 376, 950{954

Nobili, L., Turolla, R., Zampieri, L. and Belloni, T. (2000), *ApJ* 538, L137{L140

Novikov, I.D. and Thorne, K.S. (1973), in *Black Holes*, eds. C.D. Dewitt and B. DeWitt, (Gordon & Breach, NY)

Nowak, M.A. (2000), *MNRAS* 318, 361{367

Nowak, M.A. and Wilms, J. (1999), *ApJ* 522, 476{486

Nowak, M.A., Wilms, J. and Dove, J.B. (2002), *MNRAS* 332, 856{878

Nowak, M.A., Wilms, J., Heindl, W.A., et al. (2001), *MNRAS* 320, 316{326

Ogle, R.N., Ash, T.D.C. and Fender, R.P. (1997), *IAU Circ.* 6726

Orosz, J.A. and Bailyn, C.D. (1997), *ApJ* 477, 876{896

Orosz, J.A., Bailyn, C.D., McClelland, J.E. and Remillard, R.A. (1996), *ApJ* 468, 380{390

Orosz, J.A., Groot, P.J., van der Klis, M., et al. (2002a), *ApJ* 568, 845{861

Orosz, J.A., Jain, R.K., Bailyn, C.D., et al. (1998), *ApJ* 499, 375{384

Orosz, J.A., Kuulkers, E., van der Klis, M., et al. (2001), *ApJ* 555, 489{503

Orosz, J.A., Polisensky, E.J., Bailyn, C.D., et al. (2002b), *BAAS* 201, 1511

Ostriker, Y. (1974), *PA SJ* 26, 429{436

Owen, F.N., Balonek, T.J., Dickie, J., et al. (1976), *ApJ* 203, L15{L16

Pan, H.C., Skinner, G.K., Sunyaev, R.A. and Borozdin, K.N. (1995), *MNRAS* 274, L15{L18

Parmar, A.N., Angelini, L., Roche, P. and White, N.E. (1993), *A&A* 279, 179{187

Pottschmidt, K., Wilms, J., Nowak, M.A., et al. (2003), submitted to *A&A* (astro-ph/0202258)

Poutanen, J. and Fabian, A.C. (1999), *MNRAS* 306, L31{L37

Pringle, J.E. (1981), *Ann. Rev. Astron. Astrophys.* 19, 137{162

Pringle, J.E. and Rees, M.J. (1972), *A&A* 21, 1{9

Psaltis, D., Belloni, T. and van der Klis, M. (1999), *ApJ* 520, 262{270

Quataert, E. and Gruzinov, A. (2000), *ApJ* 539, 809{814

Quataert, E. and Narayan, R. (1999), *ApJ* 520, 298{315

Reig, P., Belloni, T., van der Klis, M., et al. (2000), *ApJ* 541, 883{888

Remillard, R., Levine, A., Swank, J. and Strohmayer, T. (1997), *IAU Circ.* 6710

Remillard, R.A., Levine, A.M., Morgan, E.H., et al. (2003a), *IAU Circ.* 8050

Remillard, R.A. and Morgan, E.H. (1999), *Bull. AAS* 31, 1421

Remillard, R.A., Morgan, E.H., McClelland, J.E., et al. (1999), *ApJ* 522, 397{412

Remillard, R.A., Morgan, E.H. and Munro, M. (2001), in *Proc. Ninth Marcel Grossmann Meeting*, eds. V.G. Gurzadyan et al. (World Scientific, Singapore), 2220{2223

Remillard, R.A., Munro, M.P., McClelland, J.E. and Orosz, J.A. (2002a), *ApJ* 580, 1030{1042

Remillard, R.A., Munro, M.P., McClelland, J.E. and Orosz, J.A. (2003b), *BAAS* 35, 648

Remillard, R.A., Orosz, J.A., McClelland, J.E. and Bailyn, C.D. (1996), *ApJ* 459, 226{235

Remillard, R.A., Sobczak, G.J., Munro, M.P. and McClelland, J.E. (2002b), *ApJ* 564, 962{973

Revnivtsev, M., Borozdin, K.N., Priedhorsky, W.C. and Vikhlinin, A. (2000a), *ApJ* 530, 955{965

Revnivtsev, M., Gilfanov, M. and Churazov, E. (1998a), *A&A* 339, 483{488

Revnivtsev, M., Gilfanov, M. and Churazov, E. (2001), *A&A* 380, 520{525

Revnivtsev, M., Gilfanov, M., Churazov, E., et al. (1998b), *A&A* 331, 557{563

Revnivtsev, M., Gilfanov, M., Churazov, E. and Sunyaev, R. (2002), *A&A* 391, 1013{1022

Revnivtsev, M., Sunyaev, R. and Borozdin, K. (2000b), *A&A* 361 L37{L39

Revnivtsev, M., Trudolyubov, S.P. and Borozdin, K.N. (2000c), *MNRAS* 312, 151{158

Revnivtsev, M., Chemvakova, M., Capitanio, F., et al. (2003), *ATEL* 132

Reynolds, C.S. and Nowak, M.A. (2003), *Phys.Rept.* 377, 389{466

Reynolds, A.P., Quaintrell, H., Still, M.D., et al. (1997), *MNRAS* 288, 43{52

Rhoades, C.E. and Rubin, R. (1974), *Phys.Rev.Lett.* 32, 324{

Rodriguez, L.F., Mirabel, I.F. and Marti, J. (1992), *ApJ* 401, L15{L18

Romani, R.W. (1998), *A&A* 333, 583{590

Rothschild, R.E., Blanck, P.R., Gruber, D.E., et al. (1998), *ApJ* 496, 538{549

Rothstein, D.M., Eikenberry, S.S., Chatterjee, S., et al. (2002), *ApJ* 580, L61{L63

Rozanska, A. and Czemy, B. (2000), *A&A* 360, 1170{1186

Rupen, M.P., Bracke, C., Mioduszewski, A.J., et al. (2003), *IAU Circ.* 8054

Rupen, M.P., Dahan, V. and Mioduszewski, A.J. (2002), *IAU Circ.* 7874

Rupen, M.P., Hellming, R.M. and Mioduszewski, A.J. (1998), *IAU Circ.* 6938

Rutledge, R.E., Lewin, W.H.G., van der Klis, M., et al. (1999), *ApJS* 124, 265{283

Sanchez-Fernandez, C., Zurita, C., Casares, J., et al. (2002), *IAU Circ.* 7989

Seon, K., Min, K., Kenji, Y., et al. (1995), *ApJ* 454, 463{471

Shahbaz, T., Naylor, T. and Charles, P.A. (1997), *MNRAS* 285, 607{612

Shahbaz, T., Ringwald, F.A., Bunn, J.C., et al. (1994), *MNRAS* 271, L10{L14

Shahbaz, T., van der Hooft, F., Casares, J., et al. (1999), *MNRAS* 306, 89{94

Shakura, N.I. and Sunyaev, R.A. (1973), *A&A* 24, 337{366

Shapiro, S.L. and Teukolsky, S.A. (1983), *Black Holes, White Dwarfs and Neutron Stars: The Physics of Compact Objects* (Wiley, New York)

Shimura, T. and Takahara, F. (1995), *ApJ* 445, 780{788

Shrader, C.R., Wagner, R.M., Hellings, R.M., et al. (1994), *ApJ* 434, 698{706

Skinner, G.K., Foster, A.J., Willmore, A.P. and Eyles, C.J. (1990), *MNRAS* 243, 72{77

Smak, J. (1971), *Acta Astron.* 21, 15{21

Smith, D.M., Heindl, W.A. and Swank, J. (2002), *ApJ* 578, L129{L132

Smith, D.M., Heindl, W.A., Markwardt, C.B. and Swank, J.H. (2001), *ApJ* 554, L41{L44

Smith, D.M., Heindl, W.A., Swank, J., et al. (1997), *ApJ* 489, L51{L54

Sobczak, G.J., McClelland, J.E., Remillard, R.A., et al. (1999), *ApJ* 520, 776{787

Sobczak, G.J., McClelland, J.E., Remillard, R.A., et al. (2000a), *ApJ* 531, 537{545

Sobczak, G.J., McClelland, J.E., Remillard, R.A., et al. (2000b), *ApJ* 544, 993{1015

Steeghs, D., Miller, J.M., Kaplan, D. and Rupen, M. (2003), *ATEL* 146

Stella, L., Vietri, M. and Morsink, S.M. (1999), *ApJ* 524, L63{L66

Stirling, A.M., Spencer, R.E., de la Force, C.J., et al. (2001), *MNRAS* 327, 1273{1278

Stone, J.M., Pringle, J.E. and Begelman, M.C. (1999), *MNRAS* 310, 1002{1016

Strohmayer, T.E. (2001a), *ApJ* 552, L49{L53

Strohmayer, T.E. (2001b), *ApJ* 554, L169{L172

Sunyaev, R., Churazov, E., Gilfanov, M., et al. (1992), *ApJ* 389, L75{L78

Sunyaev, R., Gilfanov, M., Churazov, E., et al. (1991a), *SvAL* 17, 50{54

Sunyaev, R.A., Kaniovskii, A.S., Efremov, V.V., et al. (1991b), *SvAL* 17, 123{130

Sunyaev, R.A., Lapshov, I.Yu., Rebenev, S.A., et al. (1988), *SvAL* 14, 327{333

Sunyaev, R. and Revnivtsev, M. (2000), *A&A* 358, 617{623

Sutaria, F.K., Kolb, U., Charles, P., et al. (2002), *A&A* 391, 993{997

Swank, J. (1998), in *The Active X-ray Sky: Results from BeppoSAX and RossiXTE*, eds. L. Scarsi et al., Nuclear Physics B Proceedings Supplements (astro-ph/9802188)

Tagger, M. and Pellat, R. (1999), *A&A* 349, 1003{1016

Takahashi, K., Inoue, H. and Dotani, T. (2001), *PASJ* 53, 1171{1177

Tanaka, Y. and Lewin, W.H.G. (1995), in *X-ray Binaries*, eds. W.H.G. Lewin, J. van Paradijs and E.P.J. van den Heuvel, (Cambridge U.Press, Cambridge) 126{174, T1{L95

Tanaka, Y. and Shibasaki, N. (1996), *ARA&A* 34, 607{644, T5{S96

Tanaka, Y., Nandra, K., Fabian, A.C. (1995), *Nature* 375, 659{661

Tananbaum, H., Gursky, H., Kellogg, E., et al. (1972), *ApJ* 177, L5{L10

Timmes, F.X., Woosley, S.E. and Weaver, T.A. (1996), *ApJ* 457, 834{843

Titarchuk, L. and Oshenovich, V. (2000), *ApJ* 542, L111{L114

Tom sick, J.A. and Kaaret, P. (2000), *ApJ* 537, 448{460

Tom sick J.A. and Kaaret, P. (2001), *ApJ* 548, 401{409

Tom sick, J.A., Kaaret, P., Kroeger, R.A. and Remillard, R.A. (1999), *ApJ* 512, 892{900

Trudolyubov, S., Churazov, E., Gilfanov, M., et al. (1999), *A&A* 342, 496{501

Turner, M.J.L., Thomas, H.D., Patchett, B.E., et al. (1989), *PASJ* 41, 345{372

Turner, N.J., Stone, J.M. and Sano, T. (2002), *ApJ* 566, 148{163

Turolla, R., Zane, S. and Titarchuk, L. (2002), *ApJ* 576, 349{356

Ueda, Y., Dotani, T., Ueno, S., et al. (1997), *IAU Circ.* 6627

van den Heuvel, E.P.J. (1992), in *ESA, Environment Observation and Climate Modelling Through International Space Projects* (SEE N 93(23878 08{88)

van der Hooft, F., Kouveliotou, C., van Paradijs, J., et al. (1996), *ApJ* 458, L75{L78

van der Hooft, F., Kouveliotou, C., van Paradijs, J., et al. (1999), *ApJ* 513, 477{490

van der Klis, M. (1994), *ApJS* 92, 511{519

van Dijk, R., Bennett, K., Colmar, W., et al. (1995), *A&A* 296, L33{L36

van der Klis, M. (1995) in *X-ray Binaries*, eds. W.H.G. Lewin, J. van Paradijs and E.P.J. van den Heuvel, (Cambridge U.Press, Cambridge), 252{307

van Paradijs, J. (1995) in *X-ray Binaries*, eds. W.H.G. Lewin, J. van Paradijs and E.P.J. van den Heuvel, (Cambridge U.Press, Cambridge), 536{577

van Paradijs, J. and McClelland, J.E. (1995) in *X-ray Binaries*, eds. W.H.G. Lewin, J. van Paradijs and E.P.J. van den Heuvel, (Cambridge U.Press, Cambridge), 58{125

Vargas, M., Goldwurm, A., Laurent, P., et al. (1997), *ApJ* 476, L23{L26

Vargas, M., Goldwurm, A., Paul, J., et al. (1996), *A&A* 313, 828{832

Vasiliev, L., Trudolyubov, S. and Revnivtsev, M. (2000), *A&A* 362, L53{L56

Vikhlinin, A., Churazov, E., Gilfanov, M., et al. (1994), *ApJ* 424, 395{400

Vikhlinin, A., Finoguenov, A., Shtzikov, A., et al. (1992), *IAU Circ.* 5608

Wagner, R.M., Foltz, C.B., Shahbaz, T., et al. (2001), *ApJ* 556, 42{46

Wagner, R.M., Starrfield, S.G., Hjelming, R.M., et al. (1994), *ApJ* 429, L25{L28

Wagoner, R.V. (1999), *Phys.Rept.* 311, 259{269

Wagoner, R.V., Sibergleit, A.S. and Oregua-Rodriguez, M. (2001), *ApJ* 559, L25{L28

Wardzinski, G., Zdziarski, A.A., Kierlinski, M., et al. (2002), *MNRAS* 337, 829{839

Weaver, K.A., Gelbord, J. and Yaqoob, T. (2001), *ApJ* 550, 261{279

Webster, B.L. and Murdin, P. (1972), *Nature* 235, 37{38

White, N.E. and Marshall, F.E. (1984), *ApJ* 281, 354{359

White, N.E. and van Paradijs, J. (1996), *ApJ* 473, L25{L29

White, N.E., Nagase, F. and Parmar, A.N. (1995) in *X-ray Binaries*, eds. W.H.G. Lewin, J. van Paradijs and E.P.J. van den Heuvel, (Cambridge U. Press, Cambridge) 1{57

White, N.E., Stella, L. and Parmar, A.N. (1988), *ApJ* 324, 363{378

Wijnands, R. and Miller, J.M. (2002), *ApJ* 564, 974{980

Wijnands, R. and van der Klis, M. (2000), *ApJ* 528, L93{L96

Wijnands, R., Homan, J. and van der Klis, M. (1999), *ApJ* 526, L33{L36

Wijnands, R., Mendez, M., Miller, J.M. and Homan, J. (2001), *MNRAS* 328, 451{460

Wijnands, R., Miller, J.M. and van der Klis, M. (2002), *MNRAS* 331, 60{70

Wims, J., Nowak, M.A., Dove, J.B., et al. (1999), *ApJ* 522, 460{475

Wims, J., Nowak, M.A., Pottschmidt, K., et al. (2001a), *MNRAS* 320, 327{340

Wims, J., Reynolds, C.S., Begelman, M.C., et al. (2001b), *MNRAS* 328, L27{L31

Wilson, A.M., Carpenter, G.F., Eyles, C.J., et al. (1977), *ApJ* 215, L111{L115

Wilson, C.K. and Rothschild, R.E. (1983), *ApJ* 274, 717{722

Wood, K.S., Ray, P.S., Bandyopadhyay, R.M., et al. (2000), *ApJ* 544, L45{L48

Woods, P.M., Kouveliotou, C., Finger, M.H., et al. (2002), *IAU Circ.* 7856

Woolsey, S.E., Heger, A. and Weaver, T.A. (2002), *RvMP* 74, 1015{1071

Wu, K., Soria, R., Campbell, D., et al. (2002), *ApJ* 565, 1161{1168

Yaqoob, T., Ebisawa, K. and Mitsuda, K. (1993), *MNRAS* 264, 411{420

Zdziarski, A.A. (2000), in *Highly Energetic Physical Processes, Proceedings IAU Symposium # 195*, eds. C.H.M. Artens, S.T. Sunanta and M.A. Weber, ASP, 153-170, (astro-ph/0001078)

Zdziarski, A.A., Groves, J.E., Poutanen, J., et al. (2001), *ApJ* 554, L45{L48

Zdziarski, A.A., Lubinski, P., Gilfanov, M. and Revnivtsev, M. (2003), *MNRAS* 342, 355{372

Zdziarski, A., Poutanen, J., Paciesas, W.S. and Wen, L. (2002), *ApJ* 578, 357{373

Zhang, S.N., Cui, W. and Chen, W. (1997a), *ApJ* 482, L155{L158

Zhang, S.N., Cui, W., Harmon, B.A., et al. (1997b), *ApJ* 477, L95{L98

Zurita, C., Sanchez-Fernandez, C., Casares, J., et al. (2002), *MNRAS* 334, 999{1008

Zycki, P.T., Done, C. and Smith, D.A. (1999a), *MNRAS* 305, 231{240

Zycki, P.T., Done, C. and Smith, D.A. (1999b), *MNRAS* 309, 561{575